

DEVELOPMENT OF NEW CHIRAL SELECTORS FOR LIQUID  
CHROMATOGRAPHY AND THEIR PERFORMANCE  
RELATIVE TO ESTABLISHED CHIRAL  
STATIONARY PHASES (CSPS)

by

PING SUN

Presented to the Faculty of the Graduate School of  
The University of Texas at Arlington in Partial Fulfillment  
of the Requirements  
for the Degree of

DOCTOR OF PHILOSOPHY

THE UNIVERSITY OF TEXAS AT ARLINGTON

December 2009

Copyright © by Ping Sun 2009

All Rights Reserved

## ACKNOWLEDGEMENTS

My first, and most earnest, acknowledgement must go to my graduate advisor, Dr. Daniel W. Armstrong. I have worked with him for over five years in graduate education, and his unending drive and dedication to science always amaze me. I truly appreciate his mentoring, support, and encouragement. Except for giving scientific advice, he also taught me how to express my ideas, both in oral and writing.

Secondly, I would like to thank my PhD committee members, Dr. Frederick MacDonnell and Dr. Kevin A. Schug. It is my honor to have them serve on my committee. Working with Dr. MacDonnell on Ru projects is really pleasant experience.

I would also like to acknowledge all former and present members in Dr. Armstrong's group. I appreciate their research help and their friendships. Special thanks to Barbara Smith, who is always there, willing to help me.

I am also indebted to the Department of Chemistry and Biochemistry at UT Arlington for financial aid and all department staff members for their kindly help.

Finally, I would like to thank my wonderful parents and sister for unconditional support. Although they know nothing about my research, they always encourage me to pursue my interests. Without their help and support, it would be never possible for me to make a decision to study abroad and pursue PhD. Special thanks to my husband, Rong Jiao, for his encouragement and support through completion of the degree.

November 12, 2009

## ABSTRACT

# DEVELOPMENT OF NEW CHIRAL SELECTORS FOR LIQUID CHROMATOGRAPHY AND THEIR PERFORMANCE RELATIVE TO ESTABLISHED CHIRAL STATIONARY PHASES (CSPS)

Ping Sun, PhD

The University of Texas at Arlington, 2009

Supervising Professor: Dr. Daniel W. Armstrong

HPLC with chiral stationary phases (CSPs) has proven to be the most widely applicable and versatile technique for enantiomeric separations. This dissertation discusses new research in three important areas of enantiomeric separations: HPLC method developments for target chiral analytes using the existing CSPs, mechanistic investigations by NMR, and development of new HPLC CSPs.

Two classes of commercial chiral stationary phases (cyclodextrin-type and macrocyclic glycopeptide-type) were evaluated by separating specific groups of chiral analytes, including  $\beta$ -lactam compounds and ruthenium(II) polypyridyl complexes. The effects of chiral selector structures, mobile phase compositions, and analyte structures have been examined. For Ru(II) complexes, the newly developed Chirobiotic T2 column works more successfully than the other glycopeptide-based stationary phases, while R-naphthylethyl carbamate-functionalized  $\beta$ -cyclodextrin CSP (Cyclobond RN) is the most effective among all tested cyclodextrin-based columns. The exceptional separation capabilities of cyclodextrins (CDs) for Ru complexes

prompted us to conduct NMR mechanistic studies. Enantioselective host-guest complexation between Ru complexes and CDs was investigated and correlated to the separation results (HPLC and CE). It was found that aromatic and anionic derivatizing groups on CDs were beneficial for chiral recognition.

Also, enantiopure Ru complexes and a new class of cyclic oligosaccharides, cyclofructans (CFs), were introduced as bonded chiral stationary phases. Three different chemistries linking the Ru complex to the silica gel were studied. The CSP synthesized by reductive amination of aldehyde-functionalized silica worked best. Extensive liquid chromatographic studies with UV and CD detectors show Ru complex-bonded CSP provide enantioselectivity toward a wide variety of compounds, in particular, compounds with acidic groups. A new class of chiral selectors, cyclofructans, have been bonded to the silica gel for the first time to develop chiral stationary phases. Native CF6 appeared to be a poor chiral selector due to extensive internal hydrogen bonding, which could possibly block the interactions with chiral analytes. Therefore, new CSPs have been designed by derivatizing CF6, in order to disrupt internal hydrogen bonding. Derivatized-CF6 CSPs appeared to separate a very broad range of chiral analytes. Particularly, aliphatic-functionalized CF6 with a low substitution degree baseline separated all tested primary amines. In addition, this class of CSPs has great potential for preparative separations.

## TABLE OF CONTENTS

|  |      |
|--|------|
| ACKNOWLEDGEMENTS .....   | iii  |
| ABSTRACT .....   | iv   |
| LIST OF ILLUSTRATIONS.....   | vii  |
| LIST OF TABLES .....   | xi   |
| Chapter  | Page |
| 1. INTRODUCTION.....   | 1    |
| 2. SEPARATION OF ENANTIOMERS OF $\beta$ -LACTAMS BY HPLC USING<br>CYCLODEXTRIN-BASED CHIRAL STATIONARY PHASES.....   | 10   |
| 3. ENANTIOSEPARATIONS OF CHIRAL RUTHENIUM(II) POLYPYRIDYL<br>COMPLEXES USING HPLC WITH MACROCYCLIC GLYCOPEPTIDE CHIRAL<br>STATIONARY PHASES (CSPS) .....                             | 23   |
| 4. ENANTIOMERIC SEPARATIONS OF RUTHENIUM(II) POLYPYRIDYL<br>COMPLEXES USING HIGH PERFORMANCE LIQUID CHROMATOGRAPHY (HPLC)<br>WITH CYCLODEXTRIN CHIRAL STATIONARY PHASES (CSPS) ..... | 35   |
| 5. ENANTIOSELECTIVE HOST-GUEST COMPLEXATION OF RU(II) TRISDIIMINE<br>COMPLEXES USING NEUTRAL AND ANIONIC DERIVATIZED CYCLODEXTRINS ....  | 60   |
| 6. DEVELOPMENT OF NEW LC CHIRAL STATIONARY PHASES BASED ON<br>RUTHENIUM TRIS(DIIMINE) COMPLEXES .....  | 75   |
| 7. DEVELOPMENT OF NEW HPLC CHIRAL STATIONARY PHASES BASED ON<br>NATIVE AND DERIVATIZED CYCLOFRUCTANS.....  | 97   |
| 8. CONCLUSIONS .....   | 129  |
| APPENDIX   |      |
| A. PUBLICATION INFORMATION OF CHAPTER 2-7 .....  | 132  |
| REFERENCES .....   | 134  |
| BIOGRAPHICAL INFORMATION .....   | 140  |

## LIST OF ILLUSTRATIONS

| Figure   | Page |
|--|------|
| 1.1 Structure of cellulose and amylose derivatives.....  | 3    |
| 1.2 Scheme of the immobilization of the polysaccharide derivatives containing vinyl groups with vinyl monomers .....   | 4    |
| 1.3 Chemical structures of macrocyclic glycopeptides. ....   | 6    |
| 1.4 Schemes of binding chemistries of glycopeptides to silica (A) Carbamate linkage; (B, C) Urea linkage; (D) Ether linkage. ....  | 7    |
| 1.5 Illustrations of two different retention mechanisms.....   | 8    |
| 2.1 Selected chromatograms showing the best (top two), medium (middle two) and worst (bottom two) enantioseparation for the substituted $\beta$ -lactams.....  | 15   |
| 2.2 Performance of different cyclodextrin-based CSPs in different separation modes. (A) Overall Enantioseparation results for 9 CSPs in all separation modes; (B) Different enantioseparation results in three modes on the three aromatic derivatized cyclodextrin CSPs ..... | 17   |
| 2.3 Comparison of separations resulting from the use of different organic modifiers.. ....   | 18   |
| 2.4 Retention times of 13 $\beta$ -lactams on four Cyclodextrin-based CSPs ( $\alpha$ , $\beta$ , $\gamma$ , and DM).....  | 21   |
| 3.1 Mirror image relationship of Ru(II) trisdiimine enantiomers .....  | 24   |
| 3.2 Structure of Ru(II) polypyridyl complexes .....  | 26   |
| 3.3 Separation of [Ru(phen) <sub>3</sub> ]Cl <sub>2</sub> (complex 1) on different Chirobiotic CSPs... ..  | 28   |
| 3.4 Effect of acetonitrile concentration on (a) retention factor, and (b) selectivity and resolution .....   | 30   |
| 3.5 Effect of the salt concentration in the mobile phase on separation. ....   | 32   |
| 3.6 Selected chromatograms in the optimal mobile phase on Chirobiotic T2 column .....  | 34   |

|  |    |
|--|----|
| 4.1 Structure and mirror image relationship of Ru(II) trisdiimine enantiomers. (A) Mononuclear complex (monomer). (B) Dinuclear complex (dimer).....   | 38 |
| 4.2 Structure of the ligands in Ru(II) polypyridyl complexes .....   | 39 |
| 4.3 Comparison of the chromatographic modes on Cyclobond RN CSP .....  | 46 |
| 4.4 Selected chromatograms of Ru(II) polypyridyl complexes in the optimized conditions on Cyclobond RN CSP .....   | 47 |
| 4.5 Chromatogram of $\Lambda$ -[Ru(phen) <sub>2</sub> aminophen]Cl <sub>2</sub> on Cyclobond RN CSP.....   | 47 |
| 4.6 Chromatograms of [Ru <sub>2</sub> (phen) <sub>4</sub> (tpphz)]Cl <sub>4</sub> , <b>9</b> (A1 and A2); and [Ru <sub>2</sub> (phen) <sub>4</sub> (tatpp)]Cl <sub>4</sub> , <b>10</b> (B1 and B2) in the optimized mobile phase on Cyclobond RN CSP ..... | 50 |
| 4.7 Effects of the concentration of NH <sub>4</sub> NO <sub>3</sub> in the mobile phase.....   | 54 |
| 4.8 Effects of acetonitrile concentration.. .....  | 55 |
| 4.9 Resolution procedures for $\Delta$ - and $\Lambda$ -[Ru(phen) <sub>3</sub> ] <sup>2+</sup> cations.....  | 58 |
| 5.1 Schematic structures of native and derivatized cyclodextrins. (A) native cyclodextrin; (B) derivatized cyclodextrin; (C) structure and abbreviation for derivative group .....   | 63 |
| 5.2 Chemical structures of [Ru(phen) <sub>3</sub> ]Cl <sub>2</sub> ( <b>1</b> ) and [Ru(bpy) <sub>3</sub> ]Cl <sub>2</sub> ( <b>2</b> ).....   | 64 |
| 5.3. <sup>1</sup> H NMR spectra of racemic [Ru(phen) <sub>3</sub> ]Cl <sub>2</sub> (2 mM) without and with various cyclodextrins (8 mM) in D <sub>2</sub> O... .....   | 66 |
| 5.4 Job plots of $\Delta$ -[Ru(phen) <sub>3</sub> ]Cl <sub>2</sub> and $\Lambda$ -[Ru(phen) <sub>3</sub> ]Cl <sub>2</sub> in solution with SBE- $\beta$ -CD .....  | 71 |
| 5.5 Scott plots of $\Delta$ -[Ru(phen) <sub>3</sub> ]Cl <sub>2</sub> and $\Lambda$ -[Ru(phen) <sub>3</sub> ]Cl <sub>2</sub> in solution with SBE- $\beta$ -CD.....   | 72 |
| 6.1 Mirror image relationship of Ru(II) <i>tris</i> (diimine) .....  | 76 |
| 6.2 Schemes of three synthetic methods of Ru complex-based CSPs .....  | 79 |
| 6.3 Structures of two Ru <i>tris</i> (diimine) complexes as chiral selectors.....  | 81 |
| 6.4. Comparison between two CSPs using $\Lambda$ -[Ru(phen) <sub>2</sub> (aminophen)] <sup>2+</sup> and $\Lambda$ -[Ru(phen) <sub>2</sub> (phendiamine)] <sup>2+</sup> as the chiral selectors... .....  | 82 |
| 6.5 Comparison between two binding methods .....   | 84 |
| 6.6 Optimized separations in three operation modes. ....   | 86 |

|   |     |
|---|-----|
| 6.7 UV and CD chromatograms of the analyte retained on the Ru-complex column .....  | 89  |
| 6.8 Effect of nature of alcohol on enantioseparations of 6,6'-dibromo-1,1'-bi-2-naphthol in the normal phase mode .....               | 93  |
| 6.9 Effect of concentration of alcohol. The analyte and mobile phase are 6,6'-dibromo-1,1'-bi-2-naphthol.....                         | 94  |
| 6.10 Effect of temperature on enantioresoluion of 6,6'-dibromo-1,1'-bi-2-naphthol... ..   | 95  |
| 7.1 Structure of cyclofructan. (A) Molecular structure of CF6, CF7 and CF8; (B-D) Crystal structure of CF6 .....                      | 99  |
| 7.2 Scheme of chemically-bonded CF6 stationary phase and derivatized-CF6 CSPs and chemical structure of all derivatizing groups ..... | 103 |
| 7.3 Separation of primary amines on derivatized-CF6 stationary phases with different substitution degrees.....                        | 109 |
| 7.4 Edge view of CF6 derivatized with (A) six methyl carbamate groups and (B) eighteen R-naphthylethyl carbamate groups .....         | 110 |
| 7.5 Comparison between aromatic- and aliphatic-derivatized-CF6 CSPs .....   | 112 |
| 7.6 Comparison between native- and aromatic-functionalized CF6 chiral columns .....   | 112 |
| 7.7 Comparison between methyl carbamate- and methyl thiocarbamate-CF6 CSPs.....   | 116 |
| 7.8 Separation of 1,2,2-triphenylethylamine on the IP-CF6 column .....  | 116 |
| 7.9 Selected chromatograms showing enantioseparations of various analytes on different derivatized-CF6 columns.....                   | 121 |
| 7.10 Complimentary character of the aromatic-derivatized CF6 CSPs .....   | 122 |
| 7.11 Separation of 6,6'-dibromo-1,1'-bi-2-naphthol in the normal phase mode and reversed phase mode on the DMP-CF6 column .....       | 124 |
| 7.12 Effect of alcohol modifier on enantioseparation in the normal phase mode on the DMP-CF6 column.....                              | 124 |
| 7.13 Temperature effect on separation of trans-stilbene oxide on the IP-CF6 column... ..  | 126 |
| 7.14 Loading test on the RN-CF6 column.....   | 126 |
| 7.15 SFC chromatogram of althiazide on the RN-CF6 column.....   | 127 |

|  |     |
|--|-----|
| 7.16 Separation of dansyl-norleucine cyclohexylammonium salt<br>on the dimethylphenyl carbamate-CF7 CSP..... | 127 |
|--|-----|

## LIST OF TABLES

| Table   | Page |
|---|------|
| 2.1 Summary of the optimized enantioseparation results .....  | 14   |
| 2.2 Effect of concentration of organic modifier on the separation for compound <b>10</b> .....  | 19   |
| 2.3 Effect of the flow rate of the mobile phase .....   | 20   |
| 3.1 Effect of salt type in the mobile phase on enantioseparation.....   | 31   |
| 3.2 Optimized separation of seven complexes on Chirobiotic T2 CSP .....   | 33   |
| 4.1 Comparison of three aromatic-derivatized Cyclobond CSPs .....   | 46   |
| 4.2 Summary of the optimized results of Ru(II) polypyridyl complexes on Cyclobond RN CSP .....  | 48   |
| 4.3 Effect of the salt type in the mobile phase on enantioseparation .....  | 54   |
| 4.4 Enantiopurity and resolution yield for several monomeric ruthenium(II) polypyridyl complexes (hexafluorophosphate salts) as resolved by Method A and/or B ..... | 58   |
| 5.1 Complexation-induced chemical shifts (CIS) of Ru(II) polypyridyl complexes with various cyclodextrins.....  | 68   |
| 5.2 Differences in CISs (complexation-induced shifts) due to enantiomeric composition of Ru(II) complexes.....  | 69   |
| 6.1 Elemental analysis results of Ru complex-silica products synthesized by three different methods .....   | 83   |
| 6.2 Chromatographic data of enantiomers resolved by the Ru complex-based CSP .....  | 87   |
| 6.3 Enantioselectivity of compounds observed by the circular dichroism (CD) detector .....  | 90   |
| 6.4 Effect of salt type in the mobile phase on enantioseparation.....   | 95   |
| 7.1 Elemental analysis results of three representative CF6-based stationary phases .....  | 104  |

|  |     |
|--|-----|
| 7.2 Physical properties of cyclofructans 6-8.....  | 105 |
| 7.3 Chromatographic data of primary amines separated on<br>derivatized-CF6 CSPs .....  | 115 |
| 7.4 Additive effect of separation of ( $\pm$ ) trans-1-amino-2-indanol<br>(primary amine type) in the polar organic mode on the IP-CF6 column..... | 117 |
| 7.5 Chromatographic data of other compounds separated on<br>six derivatized-CF6 stationary phases in optimized conditions .....                    | 118 |

## CHAPTER 1

### INTRODUCTION

#### 1.1 Chiral Stationary Phases

Enantiomeric separations have become increasingly important in a variety of areas. They are of particular interest to the pharmaceutical industry. It has been recognized that enantiomers of a chiral drug may show remarkable differences in pharmacological activities and pharmacokinetic properties. In 1992, the Food and Drug Administration issued a policy statement concerning the development of new stereoisomeric drugs,<sup>1</sup> which resulted in a great demand for effective enantiomeric separation methods.

Various techniques, including gas chromatography (GC), liquid chromatography (LC), supercritical fluid chromatography (SFC), and capillary electrophoresis (CE), have been utilized to separate enantiomers. Due to good reproducibility, wide selectivity, easy operation, and the capability for both analytical and preparative scale separations, HPLC with chiral stationary phases (CSPs) has become the most successful technique in this field. The chiral stationary phase is prepared by coating or chemically bonding an optically-active molecule (the chiral selector) onto the solid support (usually silica gel). Enantiomeric separations are based on the formation of transient diastereoisomeric complex on the column packing surface.

Currently, over one hundred chiral stationary phases are commercially available. However, only a few types dominate in the field of enantiomeric separations, including polysaccharide stationary phases, macrocyclic glycopeptide stationary phases, and to a lesser extent, cyclodextrin and  $\pi$ -complex stationary phases. Enantiomeric separations using chiral stationary phases by HPLC can be performed in three modes: normal phase, reversed phase, and polar organic modes. A typical normal mobile phase is composed of a nonpolar organic solvent (heptane or hexane) and a polar alcohol modifier (ethanol or isopropanol). The

reversed-phase separation utilizes aqueous mobile phase with an organic modifier. Acetonitrile, methanol, or tetrahydrofuran are commonly used as modifiers. The polar organic mode was first introduced on cyclodextrin stationary phases by Dr. Armstrong.<sup>2</sup> Later, this operation mode was extended to other CSPs. The polar organic mode has been widely applied due to better analyte solubility in the mobile phase, low back-pressure, and short analysis times. In this mode, polar organic solvents (methanol and acetonitrile) are utilized. Small amounts of acid (normally acetic acid) and/or base (triethylamine) are usually added for the analyte containing ionizable groups.

In the following sections, topics related to the separation mechanism, synthesis, and applications of several representative CSPs will be discussed.

### 1.2 Polysaccharide CSPs

Cellulose and amylose are linear polymers, composed of D-(+) glucose units. In the polymeric chain of cellulose, glucose units are linked via  $\beta$ -1,4 linkage, while they are linked via  $\alpha$ -1,4 linkage in amylose. The glucose chains are thought to lie side by side with a helical secondary structure in amylose and in a linear fashion in cellulose (Figure 1.1).<sup>3</sup> Native cellulose and amylose are not useful chiral selectors due to their poor chiral recognition capabilities. However, after derivatization as tricarbamate or triesters and immobilization on the silica support, they become effective chiral stationary phases.<sup>4-12</sup>

Microcrystalline cellulose triacetate was first utilized to synthesize the derivatized-polysaccharide CSP.<sup>13</sup> Later, Okamoto et al prepared a series of triesters or tricarbamates of cellulose and amylose and coated them onto macroporous 3-aminopropylsilica gel.<sup>3, 14</sup> Among them, the 3,5-dimethylphenylcarbamate derivative of cellulose and amylose provided exceptional enantioseparation capabilities, and were commercialized under the trade names Chiralcel OD and Chiralpak AD, respectively. Nowadays more than 20 derivatives of cellulose and amylose, of the coated type, are commercially available. These CSPs are mostly used in the normal phase mode. They have shown enantiomeric selectivity toward a variety of chiral analytes. In addition, they have good column capacity, and are suitable for preparative

separations.

The enantiomeric separation mechanism on these polysaccharide-based CSPs has been studied by various methods, including spectroscopic techniques (such as NMR) and computational modeling methods.<sup>6, 15</sup> Both amylose and cellulose have chiral grooves, which may be important in chiral recognition. The chiral selectors can effectively interact with analytes via hydrogen bonding provided by the electronegative atoms (such as N and O) and dipole-dipole interactions via the carbonyl groups (C=O). Also,  $\pi$ - $\pi$  interaction between the phenyl groups of the CSPs and aromatic analytes can play an important role. In some cases, steric interactions affect enantiomeric separations significantly.

The coated polysaccharide CSPs are prepared by dissolving chiral selectors in certain solvents (such as tetrahydrofuran) and adsorbing them to a suitable support. Therefore, the use of some solvents, which can dissolve the polysaccharide derivative, are prohibited as mobile phases. Cautions need to be taken in the use and maintenance of these columns.

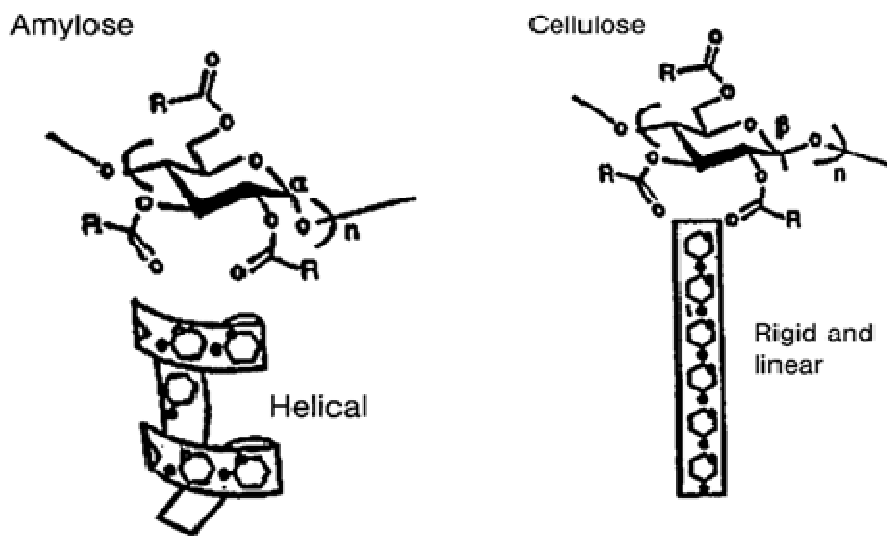


Figure 1.1 Structure of cellulose and amylose derivatives. Reprint with permission from Ref. 3

In order to improve the column durability, researchers continued searching for effective chemical binding approaches to immobilize polysaccharides to the silica gel. Several methods have been examined and the scheme of one method is shown in Figure 1.2.<sup>16</sup> The immobilization is carried out by a radical photo-polymerization reaction. An amylose-derivative polymer [amylose 2,3-bis(3,5-dimethylphenylcarbamate)-6-3,5-dimethylphenylcarbamate)/(2-methacryloyloxyethylcarbamate) which contained a 30% 2-methacryloyloxyethylcarbamate residue at the 6-position, was prepared. Then, it was coated on the amino-functionalized silica gel. Next, the copolymerization reaction was carried out in a toluene solution containing azobisisobutyronitrile (AIBN) and 2,3-dimethylbutadiene. Since 2004, three polysaccharide stationary phases of the immobilized version (Chiralpak<sup>®</sup> IA, IB, IC) have become commercially available and they appear to be stable in the presence of a wide variety of solvents. However, it has been observed that the bonded polysaccharide stationary phase produces lower enantioselectivity than the coated analog.

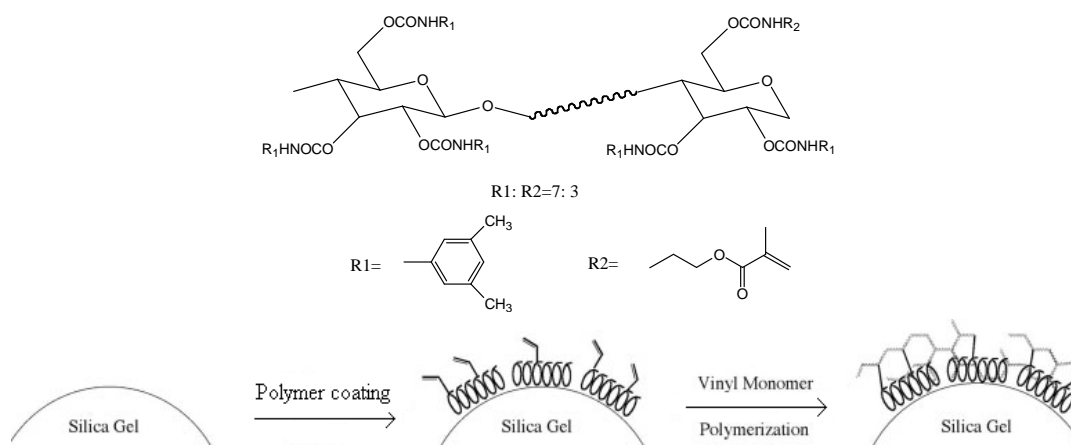


Figure 1.2 Scheme of the immobilization of the polysaccharide derivatives containing vinyl groups with vinyl monomers. Reprint with permission from Ref. 16

### 1.3 Macrocyclic Glycopeptide CSPs

Macrocyclic glycopeptides as chiral selectors for HPLC stationary phase were introduced by Armstrong in 1994.<sup>17-27</sup> To date, there are six commercial CSPs: vancomycin (Chirobiotic V and V2), teicoplanin (Chirobiotic T and T2), teicoplanin aglycone (Chirobiotic TAG), and ristocetin A (Chirobiotic R). Except for the teicoplanin aglycone, which is produced by removing the sugar moieties from teicoplanin, the others are produced by fermentation. They have somewhat similar structures and possess a characteristic aglycon “basket”, which consist of three or four fused macrocyclic rings (Figure 1.3). These four glycopeptides differ in the openness of the aglycon basket. Vancomycin has the most open basket, while teicoplanin and teicoplanin aglycon have the most closed baskets. All the glycopeptides contain abundant functional groups, such as carboxylic acid groups, amino groups, hydroxyl groups, amide linkages, and aromatic moieties. The ionizable groups on the chiral selectors may play a crucial role when associating with the enantiomers containing ionizable groups. The variety of their functionality provides broad capabilities for chiral recognition. It is found that chiral amino acids have been separated most successfully on the glycopeptide CSPs.

One unique feature of the macrocyclic glycopeptides-based CSPs is their complementary selectivity. For example, if a partial separation is obtained on one glycopeptide CSP, an increase in resolution (i.e., baseline separation) is often observed on a different, but related, Chirobiotic CSP using the same or similar mobile phase.

There are various methods for chemically binding macrocyclic glycopeptides to the silica support. These glycopeptides possess abundant functional groups (such as the amine group, the carboxylic group, and the hydroxyl group), which can react with binding reagents. The reagents may be organosilanes which contain isocyanate groups, epoxy groups, or amine groups. Consequently, the linkage between the glycopeptides and the silica support may be a carbamate, urea, or ether.<sup>17</sup> Figure 1.4 A and B illustrate the carbamate and urea linkages respectively. 3-Isocyanatopropyltriethoxysilane was used as the binding agent in the

approaches shown in Figure 1.4 A and B. In Figure 1.4 C, an alkyl diisocyanate reagent was used.

These CSPs appear to be multimodal stationary phases in that they can work effectively in all three operation modes and each mode has a different mechanism of chiral recognition. The systematic method development using these columns has been discussed. Generally, if an analyte contains more than one polar functional groups, the polar organic mode should be tested first.

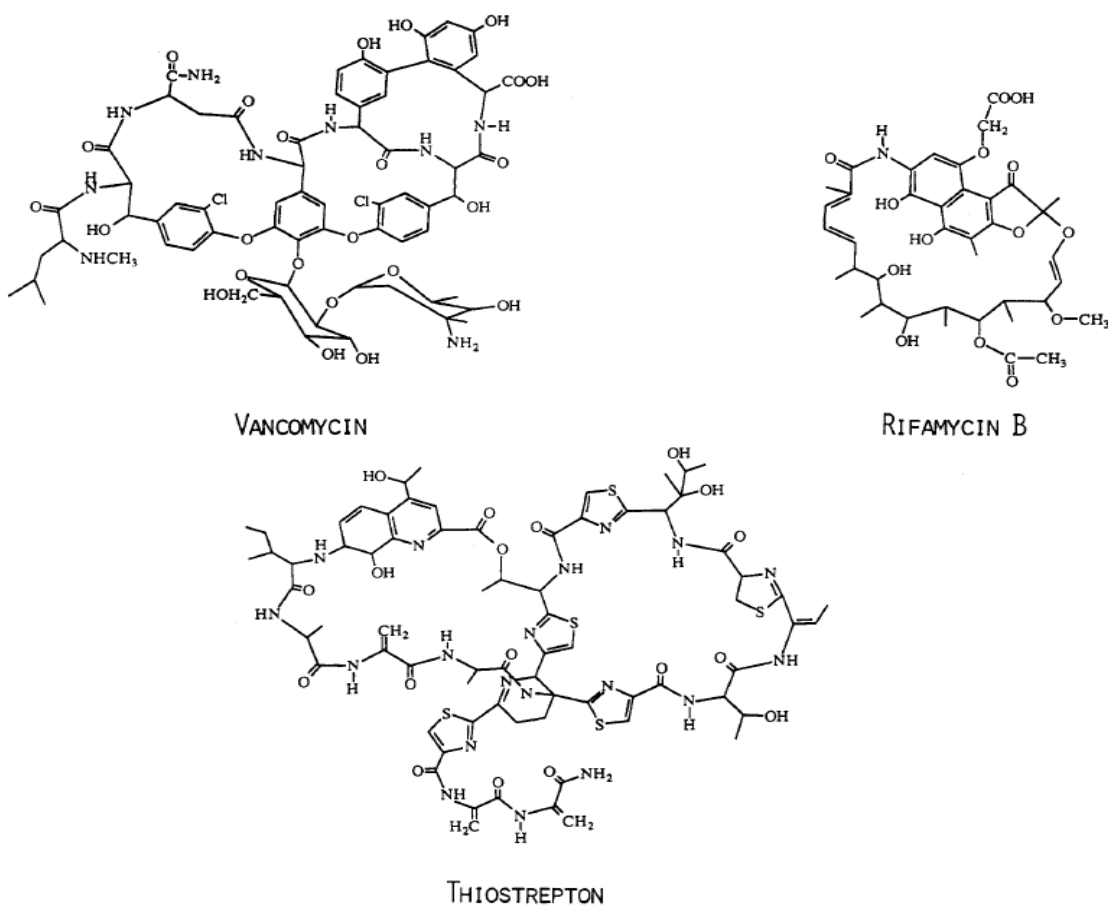


Figure 1.3 Chemical structures of macrocyclic glycopeptides. Reprint with permission from Ref.17

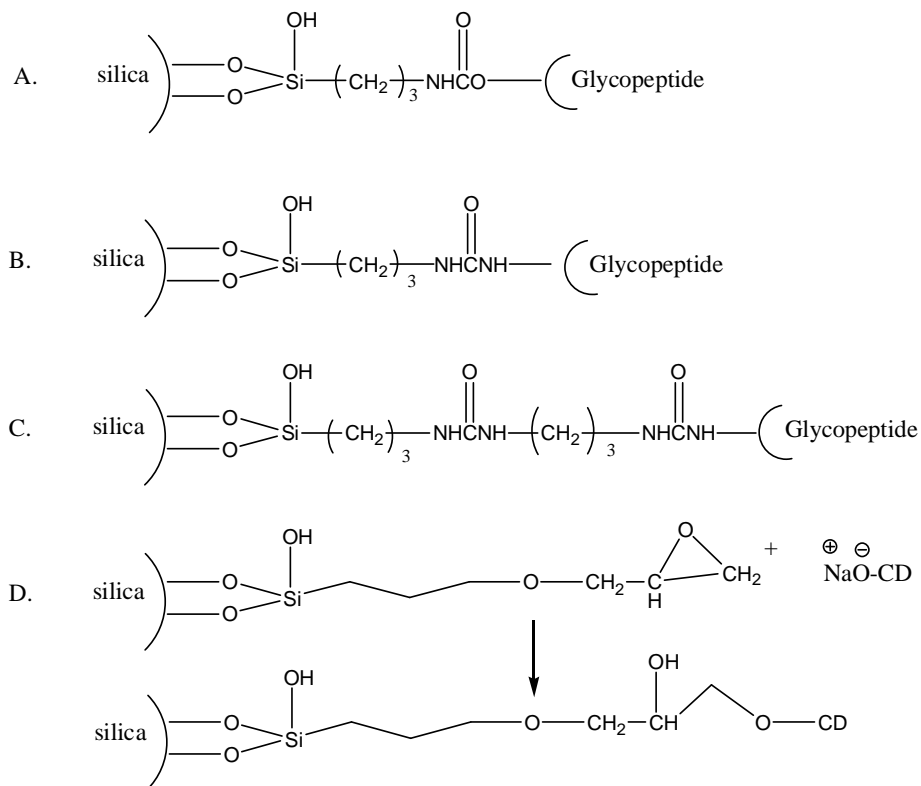


Figure 1.4 Schemes of binding chemistries of glycopeptides to silica. (A) Carbamate linkage; (B, C) Urea linkage; (D) Ether linkage.

#### 1.4 Cyclodextrin CSPs

Cyclodextrins (CDs) are cyclic oligomers of  $\alpha$ -(1,4)-linked glucose, and cyclodextrins containing 6, 7 and 8 (named  $\alpha$ ,  $\beta$ ,  $\gamma$ -CD) glucose units are the most common ones. The first stable-bonded  $\beta$ -cyclodextrin CSP was developed in early 1980's.<sup>28, 29</sup> Since then, other cyclodextrins, including native  $\alpha$ -cyclodextrin,  $\gamma$ -cyclodextrin, and various derivatives of  $\beta$ -cyclodextrin, have been utilized to produce chiral stationary phases.<sup>30-34</sup> The shape of cyclodextrins is like a "cup". The cavity size of CDs increases with more glucose units. The cavity diameters of  $\alpha$ ,  $\beta$ ,  $\gamma$ -CD are 0.57 nm, 0.78 nm, and 0.95 nm, respectively.<sup>28, 29</sup> Secondary 2- and 3-hydroxyl groups are positioned on one rim of the cyclodextrin torus, while 6-hydroxyl groups are on the other rim. The inside cavity of CDs is hydrophobic in nature due to the

methylene hydrogens.

Cyclodextrins can also be chemically bonded to the silica gel via the methods shown in Figure 1.4 A and C, in which an isocyanate or diisocyanate reagent is used. However, most commercially available cyclodextrin CSPs utilize the ether linkage, which is free of nitrogen atoms (Figure 1.4 D).<sup>28, 29</sup>

Like glycopeptide CSPs, the cyclodextrin stationary phases are considered to be multimodal columns and there are significant differences of the separation mechanism in different modes.<sup>28, 29, 34</sup> Under reversed phase conditions (Figure 1.5), inclusion complexation between the hydrophobic portion of analytes and the CD cavity is the primary interaction which results in chiral recognition. Other interactions, such as hydrogen bonding and steric interactions may also contribute to chiral recognition. In the polar organic mode, the CD cavity is mainly occupied by the cavity play an important role in chiral recognition. Aromatic derivative groups (i.e., dimethylphenyl, naphthylethyl) of CDs play an important role when used in the normal phase mode.

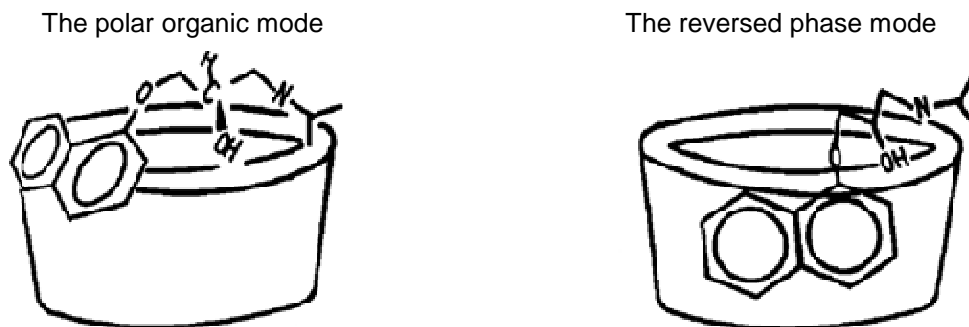


Figure 1.5 Illustrations of two different retention mechanisms. Reprint with permission from Ref. 34

### 1.5 $\pi$ -complex CSPs

The  $\pi$ -complex CSPs were first developed by Mikes and co-workers in the 1970's.<sup>35</sup> Later Pirkle et al developed analogous CSPs and commercialized some of them. Therefore, this type of CSP is sometimes referred to as a Pirkle-type CSP.<sup>36-42</sup> They have been produced by chemically binding either a chiral  $\pi$ -acidic or  $\pi$ -basic moiety to the silica gel. The newest versions of  $\pi$ -complex CSPs contain both moieties, which broaden the application range of this type of CSP. Basically,  $\pi$ - $\pi$  acceptor-donor interactions are essential for enantiomeric separations on these stationary phases. The CSPs, containing  $\pi$ -acidic groups, are mostly used to separate the analytes with  $\pi$ -basic moieties and vice versa. Other interactions, such as hydrogen bonding, dipole-dipole, and steric interactions, also contribute to chiral recognition. The  $\pi$ -complex CSPs are most often used in the normal phase mode, because  $\pi$ - $\pi$  interaction and hydrogen bonding interaction are more pronounced in nonpolar solvents.

### 1.6 Summary

Choosing the correct column from such a large pool of CSPs is challenging. Understanding chiral recognition mechanisms can help the selection of potential columns and appropriate mobile phases. Some practical factors should also be considered, including the solubility of analyte in the mobile phase, analysis time, column cost, column robustness, and column capacity.

### 1.7 Dissertation Organization

The following chapters present new research in three areas related to enantiomeric separations: (1) HPLC method development for specific groups of chiral analytes using established commercial chiral stationary phases (chapter 2-4); (2) the investigation of enantiomeric separation mechanisms by NMR spectroscopy (chapter 5); and (3) syntheses and evaluations of new chiral stationary phases (chapter 6-7).

## CHAPTER 2

### SEPARATION OF ENANTIOMERS OF $\beta$ -LACTAMS BY HPLC USING CYCLODEXTRIN-BASED CHIRAL STATIONARY PHASES

The enantiomeric separation of 12  $\beta$ -lactam compounds on 3 native cyclodextrin and 6 derivatized  $\beta$ -cyclodextrin stationary phases was evaluated using high performance liquid chromatography (HPLC). The dimethylphenyl carbamate functionalized chiral stationary phase (CSP) (Cyclobond I 2000 DMP) separated 11 of the 12  $\beta$ -lactams in the reversed phase mode. The dimethylated  $\beta$ -cyclodextrin column (Cyclobond I 2000 DM) was the second most effective CSP and it separated 8 of the 12 compounds. The reversed phase separation mode was the most effective approach. The effects of the composition and the flow rate on enantioseparations were studied. The effect of the structure of the substituents on the  $\beta$ -lactams was examined.

#### 2.1 Introduction

$\beta$ -Lactams, including penicillins and cephalosporins, are one of the most widely used types of antibiotics. Their antibacterial function results from the four-membered  $\beta$ -lactam ring inhibiting the formation of bacterial cell walls.<sup>43-46</sup> Many synthetic methods have been developed to construct  $\beta$ -lactams with functional groups and defined stereochemistry.<sup>47, 48</sup> In addition,  $\beta$ -lactams have been used as important building blocks in the synthesis of other compounds of biological importance, such as amino acid, peptides, and heterocyclic molecules.<sup>49-51</sup>

Stereochemistry greatly affects the synthetic approach, as well as the biological activity of these compounds, so there is a great need for obtaining enantiomerically pure  $\beta$ -lactams. Due to its flexibility, broad selectivity and high efficiency, liquid chromatography with chiral stationary phases (CSPs) has been widely used for enantioseparations.<sup>35, 38, 52-55</sup> Some enantiomers of  $\beta$ -lactams with aromatic substituents in the 3- or 4-position were separated on an amino acid-derived CSP ((S)-N-3,5-dinitrobenzoylleucine).<sup>38</sup> It was reported that a C3, C4-

substituted  $\beta$ -lactamic cholesterol absorption inhibitor was separated on an amylose-based chiral stationary phases (Chiralpak AD and AS).<sup>54</sup> The enantiomers of 12  $\beta$ -lactams were separated on two types of CSPs, one of which was a cellulose-tris-3,5-dimethylphenyl carbamate, and the other of which was a macrocyclic glycopeptide antibiotic teicoplanin or teicoplanin aglycone CSP.<sup>55</sup>

Cyclodextrin-based CSPs have been widely used to separate chiral compounds,<sup>28, 29, 56-59</sup> especially those with aromatic moieties. This class of chiral stationary phases has not been used for separating bicyclic and tricyclic  $\beta$ -lactams to our knowledge. In this work, the enantioseparation of 12 chiral  $\beta$ -lactams is evaluated by comparing 3 native and 6 derivatized cyclodextrin based CSPs in different chromatographic modes. The effects of the composition of the mobile phase and flow rate on enantioseparation are studied. The effects of the structure of the analytes on retention and selectivity also are discussed.

## 2.2 Experimental Section

### *2.2.1. Materials*

2-Azetidinone was purchased from Aldrich (Milwaukee, WI, USA). The racemic  $\beta$ -lactams cis-6-azabicyclo[3.2.0]heptan-7-one (1), cis-7-azabicyclo[4.2.0]octan-8-one (2), cis-7-azabicyclo[4.2.0]oct-3-en-8-one (3), cis-7-azabicyclo[4.2.0]oct-4-en-8-one (4), cis-8-azabicyclo[5.2.0]nonan-9-one (5), cis-9-azabicyclo[6.2.0]decan-10-one (6), cis-9-azabicyclo[6.2.0]dec-4-en-10-one (7), cis-3,4-benzo-6-azabicyclo[3.2.0]heptan-7-one (8), cis-4,5-benzo-7-azabicyclo[4.2.0]octan-8-one (9), cis-5,6-benzo-8-azabicyclo[5.2.0]nonan-9-one (10), exo-3-azatricyclo[4.2.1.0<sup>2.5</sup>] nonan-4-one (11) and exo-3-azatricyclo[4.2.1.0<sup>2.5</sup>] non-7-en-4-one (12) were prepared by cycloaddition of chlorosulfonyl isocyanate to the corresponding cycloalkenes and cycloalkadienes.<sup>55</sup> They are dissolved in either ethanol or acetonitrile. Ethanol (200 proof) was obtained from Aaper Alcohol and Chemical Company (Shelbyville, KY, USA). Acetonitrile, methanol, tetrahydrofuran (THF), isopropanol and heptane of HPLC grade were purchased from Fisher Scientific (Fairlawn, NJ, USA). Water was deionized and filtered through

active charcoal and a 5- $\mu$ m filter. Cyclobond I ( $\beta$ -cyclodextrin), II ( $\gamma$ -cyclodextrin), III ( $\alpha$ -cyclodextrin), AC (acetylated  $\beta$ -cyclodextrin), DM (dimethylated  $\beta$ -cyclodextrin), RSP (hydroxypropyl ether  $\beta$ -cyclodextrin), DMP (dimethylphenyl carbamate  $\beta$ -cyclodextrin), RN and SN (naphthylethyl carbamate) CSPs were obtained from Advanced Separation Technologies (Whippany, NJ, USA).

### *2.2.2 Equipment*

Chromatographic separations were carried out in three HPLC systems. The first system was a HP (Agilent Technologies, Palo Alto, CA, USA) 1050 system with a UV VWD detector, an autosampler, a quaternary pump and Chemstation software. The second system consisted of a UV detector (SPD-6A, Shimadzu, Kyoto, Japan), a pump (LC-6A, Shimadzu), a system controller (SCL-10A, Shimadzu) and a chromatographic integrator (SPD-6A, Shimadzu). The third one included a pump (LC-10A, Shimadzu), a UV detector (SPD-10A, Shimadzu) and an integrator (SPD-6A, Shimadzu). In these systems, the samples were injected via a six-port injection valve with a 10 $\mu$ L sample loop (Rheodyne, Cotati, CA, USA). Mobile phase was degassed by ultrasonication under vacuum for 5 min. All compounds are detected at 210 nm.

### *2.2.3 Column evaluation*

All CSPs were evaluated in the reversed phase mode using acetonitrile-water, methanol-water, and tetrahydrofuran-water. Except DM, all CSPs were also evaluated in the polar organic mode using acetonitrile/methanol. Aromatic derivatized CSPs (DMP, SN and RN) were evaluated in the normal phase mode with isopropanol-heptane mobile phase. All separations were carried out at room temperature with the mobile phase flow rate of 1.0 mL/min.

### *2.2.4 Calculations*

The retention factor ( $k$ ) was calculated using the equation  $k = (t_r - t_0)/t_r$ , where  $t_r$  is the retention time, and  $t_0$  is the dead time which is determined by the peak of the refractive index change due to the sample solvent. Selectivity ( $\alpha$ ) was calculated by  $\alpha = k_2/k_1$ , where  $k_1$  and  $k_2$  are

the retention factors of the first and second eluted enantiomers, respectively. The resolution ( $R_s$ ) was determined using  $R_s = 2 \times (t_{r2} - t_{r1}) / (w_1 + w_2)$ , where  $w$  is the base peak width. The efficiency (the number of theoretical plates,  $N$ ) was calculated by  $N = 16 \times (t_r / w_b)^2$ .

## 2.3 Results And Discussion

### *2.3.1 Evaluation*

In this work, nine cyclodextrin-based CSPs were evaluated for their ability to separate 12 chiral bicyclic or tricyclic  $\beta$ -lactam compounds in the reversed phase mode. Because these  $\beta$ -lactams have no ionizable groups, the pH of the mobile phase does not greatly affect the enantioseparation. Three types of organic modifier were used: methanol, acetonitrile, and tetrahydrofuran. Except for the Cyclobond I 2000 DM CSP, the other eight columns were evaluated in the polar organic mode with acetonitrile/methanol as the mobile phase. In the normal phase mode, the main attractive interactions between analytes and the chiral stationary phase are of the  $\pi$ - $\pi$  and dipolar types, so only the aromatic derivatized cyclodextrin-based CSPs (DMP, RN, and SN) were used in the normal phase mode with heptane /2-propanol as the mobile phase.

In the reversed phase mode, enantioselectivity ( $\alpha \geq 1.02$ ) was observed for all the 12  $\beta$ -lactams. Table 2.1 shows the compound structure and the separation results (including  $k_1'$ ,  $\alpha$ ,  $R_s$ , and the mobile phase composition) under optimized conditions. If the chiral analytes are partially separated ( $0.3 < R_s < 1.5$ ), the condition with the largest  $R_s$  was selected. When baseline separation occurred ( $R_s \geq 1.5$ ), the conditions that produced the smallest  $k'$  are given. The results show that seven  $\beta$ -lactams (Compounds **4**, **5**, **6**, **7**, **8**, **9**, and **10**) are baseline separated and five (Compounds **1**, **2**, **3**, **11**, and **12**) are partially separated. Decreasing the flow rate from 1.0 mL/min to 0.5 mL/min improved all the enantioseparations. At the lower flow rate compounds **4**, **5**, and **7** were baseline separated, while at higher flow rates, they were not.

Table 2.1 Summary of the optimized enantioseparation results

| Number          | Structure | CSP <sup>a</sup> | k <sub>1</sub> | α    | Rs <sup>b</sup> | Rs* <sup>c</sup> | Mobile Phase (v/v)            |
|-----------------|-----------|------------------|----------------|------|-----------------|------------------|-------------------------------|
| 1               |           | DMP              | 3.14           | 1.06 | 0.8             | 0.9              | ACN/H <sub>2</sub> O=1/99     |
| 2               |           | DMP              | 7.85           | 1.07 | 0.9             | 0.9              | ACN/H <sub>2</sub> O=1/99     |
| 3               |           | DMP              | 3.88           | 1.08 | 0.9             | 1.0              | ACN/H <sub>2</sub> O=1/99     |
| 4               |           | DMP              | 4.70           | 1.11 | 1.3             | 1.5              | ACN/H <sub>2</sub> O=1/99     |
| 5               |           | DMP              | 3.96           | 1.10 | 1.2             | 1.5              | MeOH/H <sub>2</sub> O=30/70   |
| 6               |           | DMP              | 7.40           | 1.08 | 1.5             | 1.6              | ACN/H <sub>2</sub> O=15/85    |
| 7               |           | DM               | 2.68           | 1.14 | 1.4             | 1.5              | THF/H <sub>2</sub> O=0.1/100  |
| 8               |           | DMP              | 4.20           | 1.10 | 1.5             | 1.9              | ACN/H <sub>2</sub> O=15/85    |
| 9               |           | DMP              | 5.20           | 1.13 | 1.9             | 2.4              | ACN/H <sub>2</sub> O=15/85    |
| 10              |           | DM               | 2.13           | 1.20 | 1.6             | 2.0              | ACN/H <sub>2</sub> O=5/95     |
| 11              |           | SN               | 7.34           | 1.07 | 1.2             | 1.2              | ACN/H <sub>2</sub> O=5/95     |
| 12              |           | DM               | 1.24           | 1.11 | 1.2             | 1.3              | THF/H <sub>2</sub> O=0.1/99.9 |
| 13 <sup>d</sup> |           | II               | 0.91           |      |                 |                  | MeOH/ACN=1/99                 |

<sup>a</sup>for the CSP designated by the abbreviations, see 2.2; <sup>b</sup>obtained at 1.0 mL/min; <sup>c</sup>obtained at 0.5 mL/min; <sup>d</sup>k' on α, β, DMP, DM, RSP, RN, SN, and AC in the reversed phase (acetonitrile/water =1/99) and polar organic mode (acetonitrile/methanol=99/1) are 0.19 and 0.47, 0.07 and 0.41, 0.23 and 0.57, 0.09, 0.17 and 0.44, 0.22 and 0.42, 0.20 and 0.52, 0.13 and 0.42, respectively.

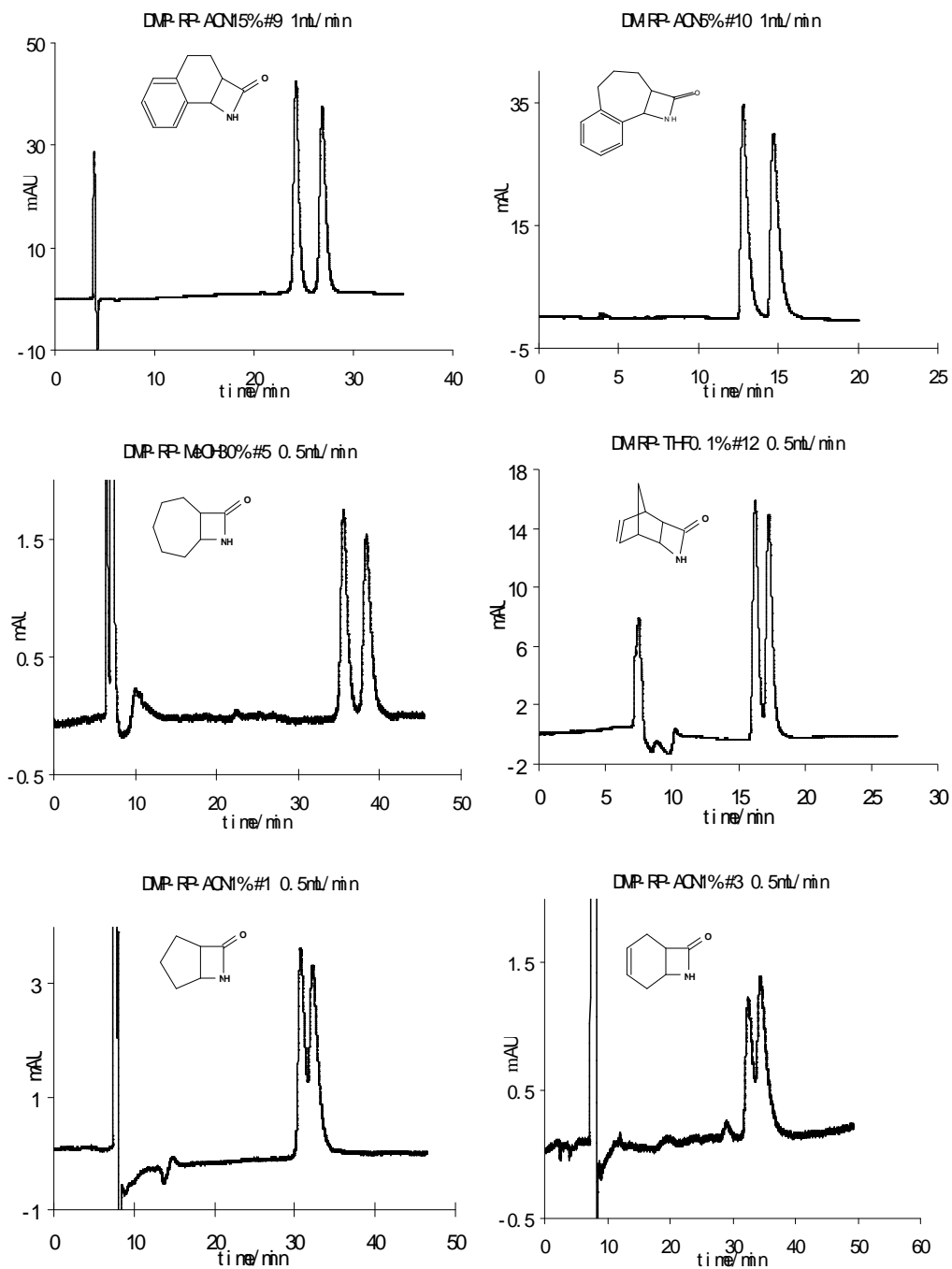


Figure 2.1 Selected chromatograms showing the best (top two), medium (middle two) and worst (bottom two) enantioseparation for the substituted  $\beta$ -lactams

In order to illustrate the effect of the analyte structure on the enantioseparation, Table 2.1 also includes the chromatographic retention data of compound **13** (2-azetidinone, a nonchiral compound). This compound has greater retention in the polar organic mode (methanol/acetonitrile=1/99) than in the reversed phase mode (acetonitrile/water =1/99). It is most strongly retained on the  $\gamma$ -cyclodextrin CSP, with a  $k'$ =0.91, shown in Table 2.1. Enantioresolution varied for different  $\beta$ -lactams and Figure 2.1 shows selected chromatograms for the best (compounds **9** and **10**), moderate (compounds **5** and **12**), and the worst resolutions (compounds **1** and **3**).

Different columns have different selectivities for these  $\beta$ -lactams. Figure 2.2a shows the performance of nine CSPs. The dimethylphenyl functionalized  $\beta$ -cyclodextrin (Cyclobond I 2000 DMP) is the most effective column for separating these  $\beta$ -lactam enantiomers. It showed enantioselectivity for eleven of the  $\beta$ -lactams (all except compound **12**), including five baseline separations and six partial separations. The dimethylated  $\beta$ -cyclodextrin (Cyclobond I 2000 DM) is the second effective column with two baseline and six partial separations. For the native cyclodextrin CSPs, only  $\gamma$ -cyclodextrin showed any enantioselectivity for these compounds (e.g. for two of the chiral  $\beta$ -lactam compounds). It is apparent that the different functional groups of the derivatized cyclodextrin CSPs provide enhanced enantioselectivity and expand the usefulness of CSPs based on cyclodextrin.

Only the aromatic derivatized cyclodextrin CSPs (DMP, SN and RN) can be used to separate enantiomers in all three chromatographic modes (shown in Figure 2.2b). Eleven compounds are separated in the reversed phase mode on the Cyclobond DMP compared to four on the RN and three on the SN column. In the normal phase mode, the DMP, RN, and SN columns can separate one, one, and two compounds, respectively. In the polar organic mode, only compound **10** was separated on the DMP and SN columns, while the RN column did not achieve any enantioseparations. The separation efficiencies in the reversed phase mode are significantly greater than in the other two modes. Comparing the resolution ( $R_s$ ) achieved in

different modes for the same compound, the reversed phase separations consistently produced larger  $R_s$  values for these compounds. The separation of compound **10** on the Cyclobond I-2000 SN is a good example. With acetonitrile/water (20/80), the  $R_s$  is 2.0, while in 100% acetonitrile and 2-propanol/heptane (5/95) the values are 0.5 and 1.0 respectively. The change in enantioresolution in different chromatographic modes depends on the retention mechanism. In the reversed phase mode, inclusion complexation is the dominant retentive interaction while CSPs form dipolar and  $\pi$ -complexes in the normal phase mode. The hydrogen bonding interactions are the most important in the polar organic mode.

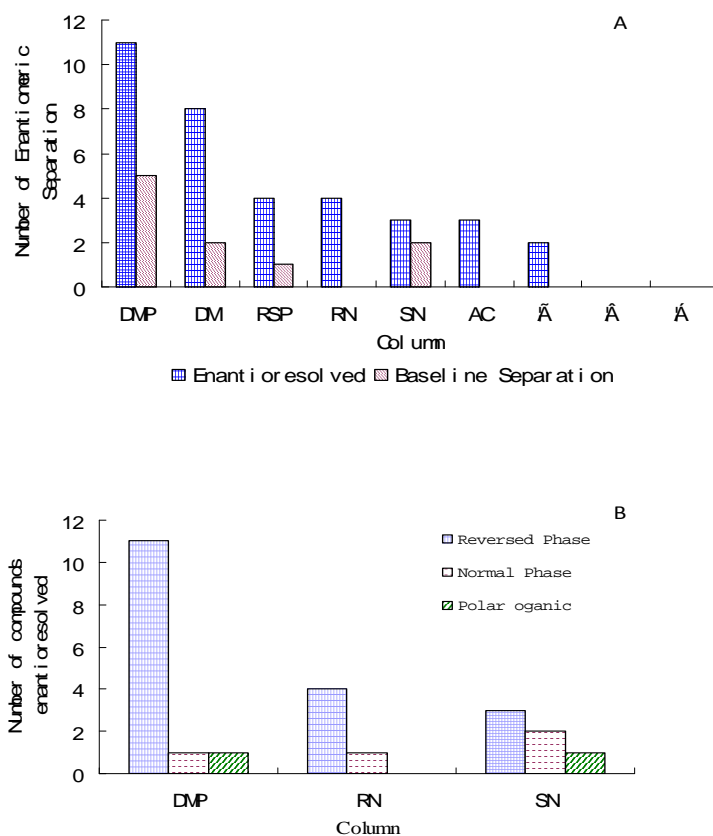


Figure 2.2 Performance of different cyclodextrin-based CSPs in different separation modes. (A) Overall Enantioseparation results for 9 CSPs in all separation modes; (B) Different enantioseparation results in three separation modes on the three aromatic derivatized cyclodextrin CSPs

### 2.3.2 Effect of mobile phase on enantioseparation

#### 2.3.2.1 Type of organic modifier

In the reversed phase mode on Cyclobond CSPs, acetonitrile and methanol are more commonly used than tetrahydrofuran as organic modifiers. The optimized separations for ten of twelve compounds were achieved with acetonitrile or methanol and water as the mobile phase (Table 2.1). The best separations for compounds **7** and **12** were achieved with tetrahydrofuran (THF)-water mobile phases. Comparing acetonitrile and methanol as organic modifiers, acetonitrile is more successful mainly due to the higher chromatographic efficiencies produced the selectivity was similar for most compounds. In some specific cases, changing from acetonitrile to methanol has a notable effect on enantioselectivity. For example, using acetonitrile/water as the mobile phase, no selectivity for compound **10** was seen on the Cyclobond I 2000 DMP column, while it was partially separated with a methanol-water mobile phase, as shown in Figure 2.3.

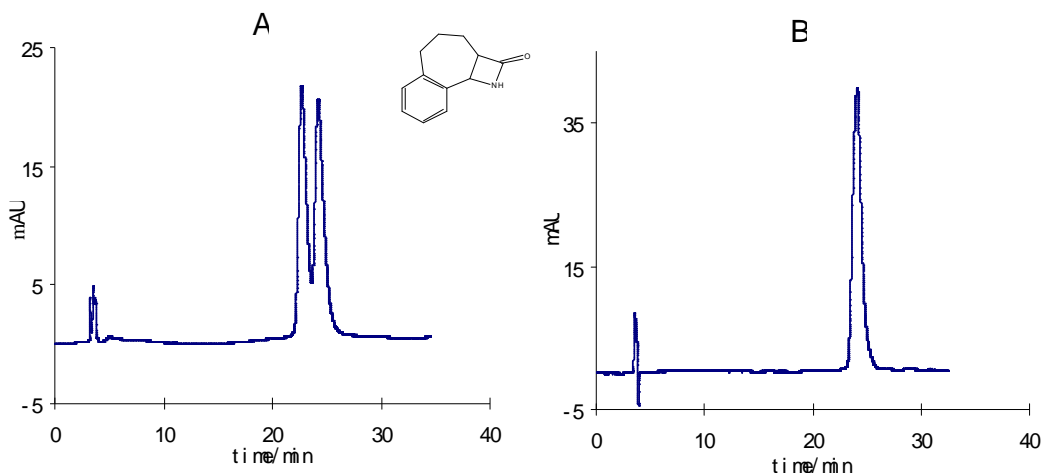


Figure 2.3 Comparison of separations resulting from the use of different organic modifiers. Compound 10 was separated on the Cyclobond I 2000 DMP column using the following mobile phases: A) 70/30 water/methanol and B) 85/15 water/acetonitrile

### 2.3.2.2 Concentration of organic modifier

When operating in the reversed phase mode, an important interaction between the CSPs and analytes is the hydrophobic inclusion complex. Organic solvents compete with the analytes for the nonpolar cavity of the cyclodextrin, so the analytes are more strongly retained when the concentration of the organic modifier is decreased. Changing the concentration of organic modifier changes the retention, selectivity and resolution. Table 2.2 lists the separation results for compound **10** as separated on the Cyclobond I 2000 SN column.

Table 2.2 Effect of concentration of organic modifier on the separation for compound **10**<sup>a</sup>

| Percent of Acetonitrile | $k_1$ | $\alpha$ | $R_s$ |
|-------------------------|-------|----------|-------|
| 0                       | 20.78 | 1.39     | 3.4   |
| 5                       | 7.40  | 1.27     | 2.2   |
| 10                      | 5.04  | 1.25     | 2.1   |
| 15                      | 3.33  | 1.19     | 1.8   |
| 20                      | 2.23  | 1.15     | 1.4   |
| 30                      | 0.92  | 1.10     | 1.1   |
| 40                      | 0.73  | 1.05     | 0.6   |
| 50                      | 0.59  | 1.00     | 0     |
| 60                      | 0.46  | 1.00     | 0     |
| 70                      | 0.23  | 1.00     | 0     |
| 80                      | 0.18  | 1.00     | 0     |
| 90                      | 0.25  | 1.00     | 0     |
| 100                     | 0.63  | 1.08     | 0.6   |

<sup>a</sup>The results for compound **10** were obtained on the Cyclobond I 2000 SN column.

When the percentage of acetonitrile is below 80%, decreasing the concentration of acetonitrile increases the retention, enantioselectivity, and resolution of the analytes. However, when the percentage of acetonitrile is above 80%, the reverse trend is obtained. In pure acetonitrile (the polar organic mode), a partial separation ( $R_s=0.6$ ,  $\alpha=1.08$ ) was obtained.

### 2.3.2.3 Flow rate of the mobile phase

Changing the flow rate of the mobile phase affects the efficiency of liquid chromatography. The effect of flow rate for the separation was investigated for compound **12** on the Cyclobond I 2000 SN column with a THF/water (1/99) mobile phase (shown in Table 2.3). When decreasing the flow rate from 1.0 ml/min to 0.2 ml/min, the selectivity (in the range of

1.128-1.130) and the retention factor (0.64) are the same within experimental error. The main factor contributing the change of resolution is efficiency ( $N_1$ , the number of theoretical plates of the first peak). Decreasing the flow rate from 1.0 to 0.2 mL/min improved the efficiency ( $N$  increased from 7040 to 8200) and resolution slightly ( $R_s$  changed from 0.99 to 1.14). In some cases, the flow rate shows larger effect on chromatographic separation. In Table 2.1, decreasing the flow rate from 1.0 mL/min to 0.5 mL/min improve the resolution of compound **9** from 1.9 to 2.4.

Table 2.3 Effect of the flow rate of the mobile phase<sup>a</sup>

| Fow rate (mL/min) | $k_1$ | $\alpha$ | $R_s$ | $N$  |
|-------------------|-------|----------|-------|------|
| 1.0               | 0.64  | 1.13     | 0.99  | 7040 |
| 0.9               | 0.64  | 1.13     | 1.06  | 7530 |
| 0.8               | 0.64  | 1.13     | 1.09  | 7620 |
| 0.7               | 0.64  | 1.13     | 1.10  | 7940 |
| 0.6               | 0.64  | 1.13     | 1.12  | 8080 |
| 0.5               | 0.64  | 1.13     | 1.13  | 8110 |
| 0.4               | 0.64  | 1.13     | 1.13  | 8160 |
| 0.3               | 0.64  | 1.13     | 1.13  | 8140 |
| 0.2               | 0.64  | 1.13     | 1.14  | 8170 |

<sup>a</sup>the results of compound **12** were obtained on SN column using tetrahydrofuran/water (1/99) as mobile phase.

### 2.3.3 Effect of analyte structure

It was found that the simple, unsubstituted lactam (compound **13**) has very little retention on any column and under any of the mobile phase conditions (Table 2.1). Clearly the hydrophobicity provided by the cyclic or bicyclic hydrocarbon substituent is essential for retention in the reversed phase mode and this substituent structure affects enantioselectivity as well.

In the reversed phase mode, solute retention results from an inclusion complex formation with the cyclodextrin cavity, and this is affected by the hydrophobicity of the solutes. Figure 2.4 indicates that the size of the substituent ring of the  $\beta$ -lactams affects the retention greatly. An examination of the retention results of compounds **1**, **2**, **5**, and **6** on the Cyclobond

DM column reveals that the size increase from a five-membered to eight-membered ring enhances the retention due to higher hydrophobicity.

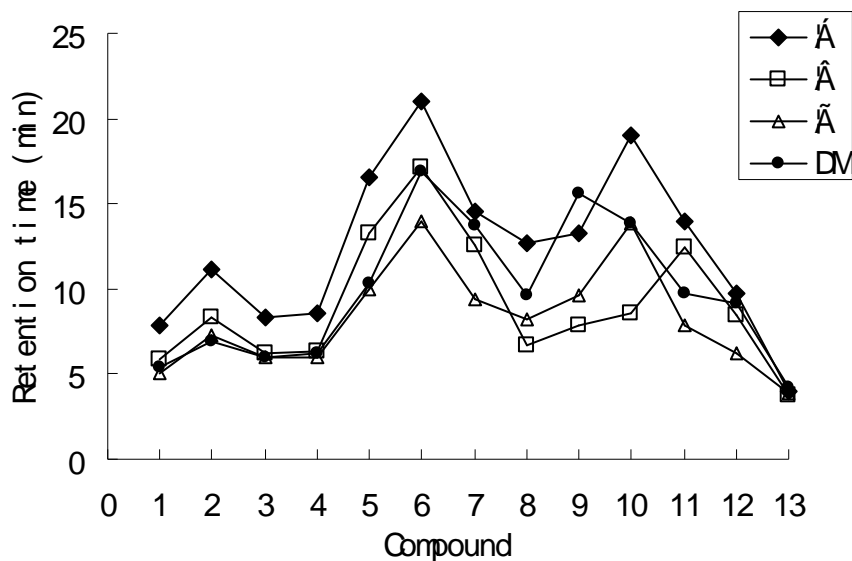


Figure 2.4 Retention times of 13  $\beta$ -lactams on four Cyclodextrin-based CSPs ( $\alpha$ ,  $\beta$ ,  $\gamma$ , and DM). The mobile phase for  $\alpha$ ,  $\beta$ ,  $\gamma$ -cyclodextrin CSPs is acetonitrile-water (1/99), while it is acetonitrile-water (5/95) for Cyclobond I-2000 DM CSP.

The presence of an aromatic ring is beneficial to chiral recognition on Cyclobond-based CSP as well. Comparison of compounds **1** and **8**, **2** and **9** on the Cyclobond I 2000 DMP column (shown in Table 2.1) shows the effect of addition of an aromatic ring. The Cyclobond DMP CSP shows baseline resolution for compounds **8** ( $R_s=1.9$ ) and **9** ( $R_s=2.4$ ), but not for **1** ( $R_s=0.9$ ) and **2** ( $R_s=0.9$ ) under optimized conditions.

The presence of double-bond also shows a beneficial effect on enantioseparation. Comparison of the chromatographic results of compounds **2**, **3** and **4** on the Cyclobond DM column is a good example. Compared to **2**, compounds **3** and **4** have a double-bond, which are positioned differently in the ring. It was observed that adding a double-bond decreased the retention (shown in Figure 2.4) while enhancing selectivity. Cyclobond DM CSP shows enantioselectivity for compound **4**, but not for compounds **2** and **3**.

## 2.4 Conclusions

Enantioseparation of 12  $\beta$ -lactams was achieved on nine cyclodextrin-based CSPs. Baseline separation was observed for seven compounds. The Cyclobond DMP column was the most effective stationary phase in that it separated 11 of 12 substituted  $\beta$ -lactams. Cyclobond DM also is effective and separated 8 of 12  $\beta$ -lactams. Cyclobond RSP, RN, SN, AC, and  $\gamma$  cyclodextrin CSPs show enantioselectivity for a few  $\beta$ -lactams, while the native  $\alpha$  and  $\beta$ -cyclodextrin CSPs do not show any enantioselectivity for these analytes. The reversed phase mode was the most effective approach and only two separations were observed in the normal phase and polar organic modes. The composition of organic modifier and the flow rate affect all enantioseparations. The substituents on the  $\beta$ -lactams contribute much to retention and enantioselectivity. In particular more rigid aromatic and tricyclic compounds produced the greatest separation factors and resolutions.

## CHAPTER 3

### ENANTIOSEPARATIONS OF CHIRAL RUTHENIUM(II) POLYPYRIDYL COMPLEXES USING HPLC WITH MACROCYCLIC GLYCOPEPTIDE CHIRAL STATIONARY PHASES (CSPS)

A high-performance liquid chromatographic method using macrocyclic glycopeptide chiral stationary phases (CSPs) was used to separate enantiomers of seven ruthenium(II) polypyridyl complexes. Among the five different CSPs, the Chirobiotic T2 was most effective and baseline separated all complexes. All complexes show the same elution order with the  $\Delta$ -enantiomer being retained longer than the  $\Lambda$ -enantiomer. The mobile phase composition, including organic modifier type, organic modifier percent, salt type, and salt concentration, produced significant effects on the enantioresolution.

#### 3.1 Introduction

The chirality of octahedral transition metal complexes bound by three bidentate ligands has received a considerable amount of attention for several decades. Right- and left-handed configurations of metal complexes are referred to as  $\Delta$ - and  $\Lambda$ -enantiomers, respectively (Figure 3.1). Ru(II) polypyridyl complexes have attracted growing interest due to their robust nature and unique photophysical characteristics.<sup>60</sup> These complexes are widely used as catalysts for asymmetric synthesis,<sup>61, 62</sup> and to construct various supramolecular assemblies.<sup>63, 64</sup> Enantiomers of Ru(II) complexes have shown specific interactions with DNA.<sup>65-67</sup> Because many applications require stereochemically pure compounds, there is a great need for preparative methods by which pure single enantiomers can be obtained and analytical methods by which their enantiomeric excess can be determined.

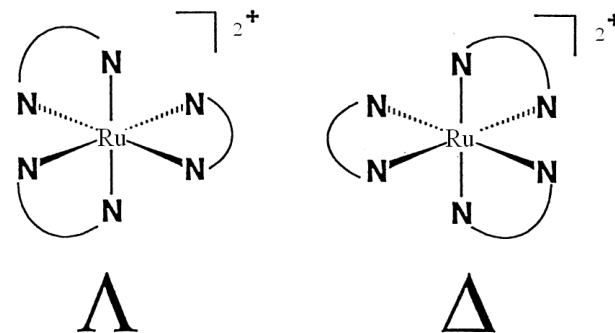


Figure 3.1 Mirror image relationship of Ru(II) trisdiimine enantiomers

There are different methods available for enantiomeric resolution of Ru complexes. Capillary electrophoresis (CE) has been successfully applied to separate Ru complex enantiomers.<sup>68-70</sup> Enantiomers of sixteen metal complexes, with different metal centers ( $\text{Ru}^{2+}$ ,  $\text{Ni}^{2+}$ ,  $\text{Cr}^{3+}$ , and  $\text{Co}^{3+}$ ), have been separated by capillary zone electrophoresis (CZE) using tartrate salt as the chiral selector in the running buffer.<sup>68</sup> CZE with double-stranded DNA as the chiral selector was used to separate enantiomers of  $[\text{Ru}(\text{phen})_3]^{2+}$  and  $[\text{Ru}(\text{bpy})_3]^{2+}$ .<sup>69</sup> However, CE is only an analytical method and not suitable for preparative-scale separations. The chromatographic method using chiral selector as an additive in the mobile phase was also reported with limited success.<sup>71</sup> Due to high efficiency, wide selectivity, and easy operation, HPLC with chiral stationary phases (CSPs) has attracted attention for the enantioseparations of organometallic compounds. Cellulose- and amylose-based CSPs have been used to separate enantiomers of novel chiral metal tetrahedrane-type clusters.<sup>72, 73</sup> Cyclodextrin-based CSPs have been reported to separate enantiomers of metallocene<sup>56</sup> and Ru(II) polypyridyl complexes.<sup>74</sup> Enantiomers of Ni, Co, Cu, and Cr extended metal atom chain complexes have been separated on a Vancomycin CSP.<sup>75</sup> A Teicoplanin CSP was used to separate a series of chiral Ru(II) complexes, including  $\text{RuL}_3^{2+}$  ( $\text{L} = 2,2'$ -bipyridine(bpy), 1,10-phenanthroline(phen), and 4,7-diphenyl-1,10-phenanthroline(dpphen)) and some mixed ligand complexes.<sup>76</sup> However, the retention time is unsatisfiably long and the enantioselectivity is not high enough in some cases.

Macrocyclic glycopeptides as chiral selectors for HPLC stationary phase were introduced in 1994.<sup>57</sup> To date, four different macrocyclic glycopeptides have been commercialized to produce CSPs: vancomycin, teicoplanin, teicoplanin aglycone, and ristocetin A. They have somewhat similar structures and consist of an aglycon portion of fused macrocyclic rings that form a characteristic “basket” shape. The unique structure of the macrocyclic glycopeptides and their wide variety of functional groups (e.g. aromatic, hydroxyl, amine, carboxylic acid, and hydrophobic pockets, etc.) give them broad selectivity for a wide variety of compounds.<sup>26, 57, 77-82</sup>

In this study, direct high-performance liquid chromatographic methods using the macrocyclic glycopeptide CSPs were developed for the separation of enantiomers of Ru(II) polypyridyl complexes. Baseline resolution was obtained for all seven complexes. Five of them ( $[\text{Ru}(\text{phen})_2\text{nitrophen}]^{2+}$ ,  $[\text{Ru}(\text{phen})_2\text{aminophen}]^{2+}$ ,  $[\text{Ru}(\text{phen})_2\text{phendiamine}]^{2+}$ ,  $[\text{Ru}(\text{phen})_2(\text{py})_2]^{2+}$ , and  $[\text{Ru}(\text{dppz})_3]^{2+}$ ) have never been separated on the macrocyclic glycopeptide CSPs. The analysis times for  $[\text{Ru}(\text{phen})_3]^{2+}$  and  $[\text{Ru}(\text{bpy})_3]^{2+}$  obtained in this study were greatly reduced compared to previously reported results using a teicoplanin CSP.<sup>76</sup> In addition, the effects of the mobile phase composition on the separations were investigated.

### 3.2 Experimental Section

#### *3.2.1 Materials*

Racemates of seven Ru(II) polypyridyl complexes used in this study are:  $[\text{Ru}(\text{phen})_3]\text{Cl}_2$  (1) (phen=1,10-phenanthroline),  $[\text{Ru}(\text{phen})_2\text{nitrophen}]\text{Cl}_2$  (2) (nitrophen=5-nitro-1,10-phenanthroline),  $[\text{Ru}(\text{phen})_2\text{aminophen}]\text{Cl}_2$  (3) (aminophen=5-amino-1,10-phenanthroline),  $[\text{Ru}(\text{phen})_2\text{phendiamine}]\text{Cl}_2$  (4) (phendiamine=5,6-diamino-1,10-phenanthroline),  $[\text{Ru}(\text{phen})_2(\text{py})_2]\text{Cl}_2$  (5) (py=pyridine),  $[\text{Ru}(\text{dppz})_3]\text{Cl}_2$  (6) (dppz=dipyrido[3,2-a: 2',3'-c]phenazine),  $[\text{Ru}(\text{bpy})_3]\text{Cl}_2$  (7) (bpy=2,2'-bipyridine). At least one single enantiomer ( $\Delta$  or  $\Lambda$ ) for each complex was available for determining elution order. The structure of all complexes is shown in Figure 3.2. Chirobiotic T (Teicoplanin), TAG (Teicoplanin aglycone), T2 (Teicoplanin),

V (Vancomycin), and R (Ristocetin A) CSPs were obtained from Advanced Separation Technologies (Whippany, NJ, USA). All the columns are 250X46 mm.

Acetonitrile and methanol of HPLC grade were purchased from EMD (Gillbstown, NJ, USA). Water was obtained from Millpore (Billerica, MA). Tetramethylammonium nitrate (TMAN),

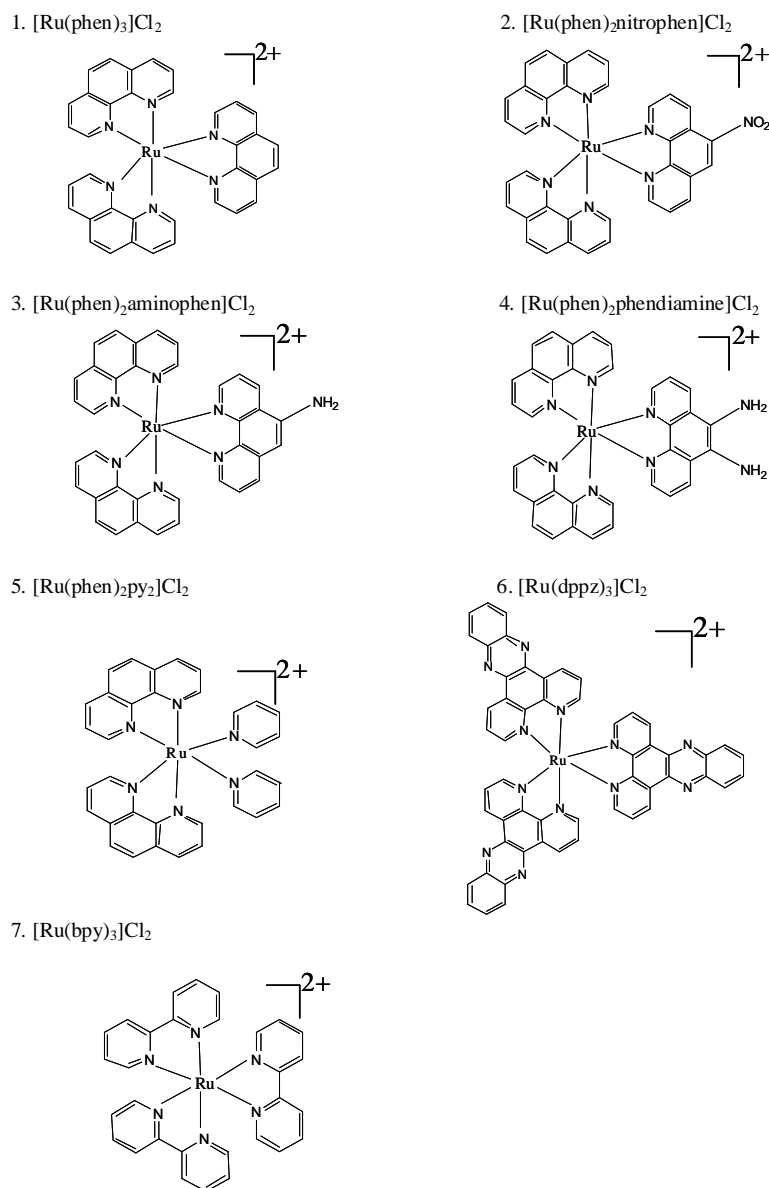


Figure 3.2 Structure of Ru(II) polypyridyl complexes

ammonium trifluoroacetate, ammonium nitrate, and ammonium acetate were purchased from Sigma-Aldrich (St. Louis, MO).

### 3.2.2 LC analysis

The chromatographic system is an HP (Agilent Technologies, Palo Alto, CA, USA) 1050 system, which consists of a UV VWD detector, an autosampler, a quaternary pump and Chemstation software. For the LC analysis, the injection volume, the flow rate, and the detection wavelength is 5  $\mu$ L, 1 mL/min, and 254 nm, respectively. Separations were carried out at room temperature ( $\sim 22$   $^{\circ}$ C). The mobile phase was degassed by ultrasonication under vacuum for 5 min. Each sample was analyzed in duplicate. The chloride ( $\text{Cl}^-$ ) salts and hexafluorophosphate ( $\text{PF}_6^-$ ) salts of Ru(II) complexes were dissolved in methanol and acetonitrile, respectively. Samples were dissolved at 1.0 mg/ml concentration and subsequently diluted with methanol or acetonitrile for LC injection.

### 3.2.3 Calculations

The retention factor ( $k'$ ) was calculated using the equation  $k' = (t_r - t_0)/t_r$ , where  $t_r$  is the retention time, and  $t_0$  is the dead time which is determined by the peak of the refractive index change due to the sample solvent. Selectivity ( $\alpha$ ) was calculated by  $\alpha = k_2'/k_1'$ , where  $k_1'$  and  $k_2'$  are the retention factors of the first and second eluted enantiomers, respectively. The resolution ( $R_s$ ) was determined using  $R_s = 2 \times (t_{r2} - t_{r1}) / (w_1 + w_2)$ , where  $w$  is the base peak width.

## 3.3 Results And Discussion

### 3.3.1 Performance of Chirobiotic CSPs

The Ru(II) complexes in this study contain two or three diimine ligands (phen, bpy, or dppz). The simplest of these is  $[\text{Ru}(\text{phen})_3]\text{Cl}_2$  (complex 1), which is used as a model compound. The performance of five Chirobiotic CSPs (T, TAG, T2, V, and R), was tested by analyzing  $[\text{Ru}(\text{phen})_3]\text{Cl}_2$  under similar mobile phase compositions (acetonitrile/methanol/water/ $\text{NH}_4\text{NO}_3$ ). The chromatograms obtained using four CSPs are shown in Figure 3.3.  $[\text{Ru}(\text{phen})_3]\text{Cl}_2$  enantiomers were partially separated on the Chirobiotic R column (Figure 3.3). The mobile

phase was changed to increase retention and possibly resolution, however, no obvious improvement in the enantioseparation was observed. The analyte was not retained on the Chirobiotic V column, when using the same mobile phase as for the Chirobiotic R. A weaker mobile phase (lower acetonitrile and salt concentration) was used and a broad peak was obtained (Figure 3.3).

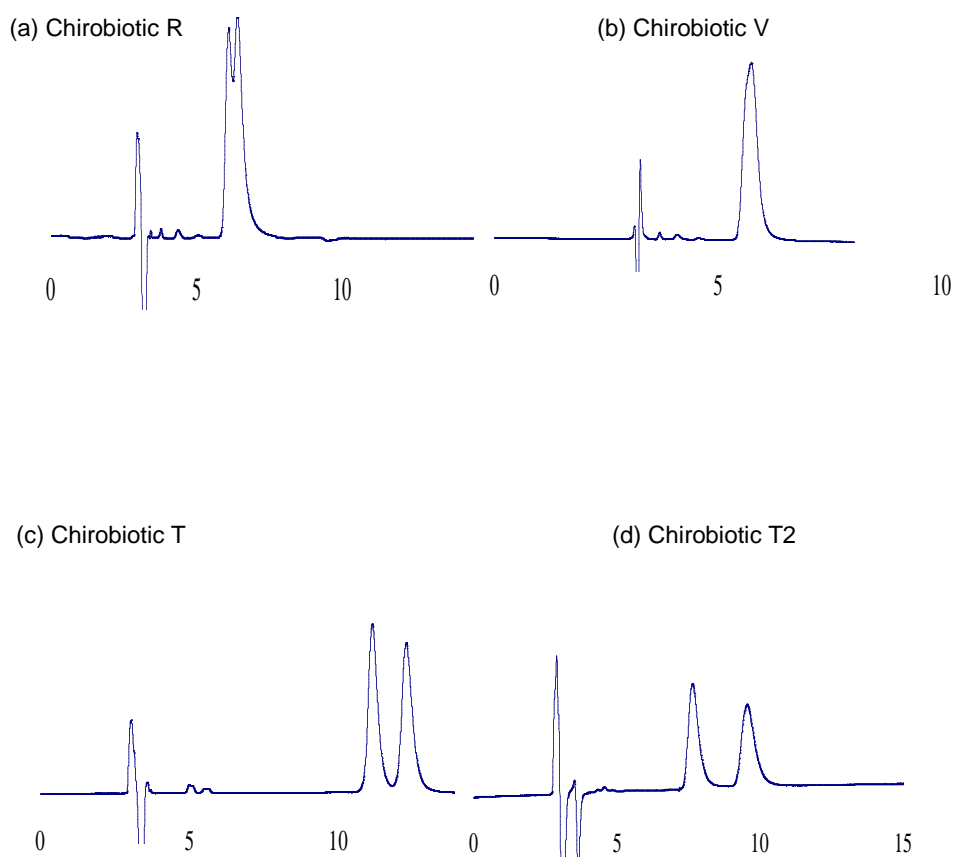


Figure 3.3 Separation of  $[\text{Ru}(\text{phen})_3]\text{Cl}_2$  (complex 1) on different Chirobiotic CSPs. The mobile phase composition is: (a) 40%methanol/40%acetonitrile/20%water/0.08M  $\text{NH}_4\text{NO}_3$ ; (b) 60%methanol/20%acetonitrile/20%water/0.04M  $\text{NH}_4\text{NO}_3$ ; (c) 20%methanol/60%acetonitrile/20%water/0.08M  $\text{NH}_4\text{NO}_3$ ; (d) 20%methanol/60%acetonitrile/20%water/0.08M  $\text{NH}_4\text{NO}_3$ .

In contrast to the vancomycin column, the teicoplanin series of CSPs (T, TAG, and T2) showed much greater retention for  $[\text{Ru}(\text{phen})_3]\text{Cl}_2$  and stronger mobile phases were required for elution. As shown in Fig. 3.3, the Chirobiotic T and T2 columns provided baseline separations of complex 1, while the analyte was not eluted on the Chirobiotic TAG column (data not shown). Shorter retention and much greater selectivity were obtained on the Chirobiotic T2 column.

The comparison of the performances of five macrocyclic glycopeptides stationary phases revealed that the retention strength order from strongest to weakest was TAG > T > T2 > R > V. These five CSPs exhibit distinctly different selectivities toward  $[\text{Ru}(\text{phen})_3]\text{Cl}_2$ . Of the macrocyclic glycopeptide CSPs tested, the teicoplanin-based CSPs appear to have superior enantioselectivity. The Chirobiotic T2 column is synthesized using a different linkage chemistry and silica gel. It has been reported that T2 exhibits better selectivity than T<sup>81</sup> and has a higher loading capacity. Our results also indicate that the Chirobiotic T2 should offer improved selectivity and resolution for the chiral ruthenium complexes.

### *3.3.2 Effect of the mobile phase composition on enantioseparation using teicoplanin (T2) column*

The influence of the mobile phase on the enantioseparation of  $[\text{Ru}(\text{phen})_3]\text{Cl}_2$  was studied since interactions between stationary phases and analytes can be greatly affected by the mobile phase used. In order to evaluate the effect of organic modifier concentration, the percentage of acetonitrile was decreased from 100% to 0% while maintaining a constant salt concentration (0.08 M tetramethylammonium nitrate). Figure 3.4 shows the effect of organic modifier concentration on retention, enantioselectivity, and resolution.

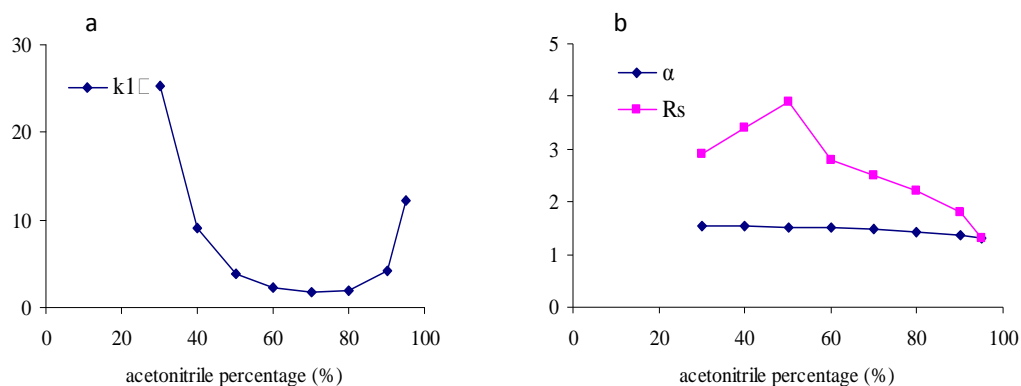


Figure 3.4 Effect of acetonitrile concentration on (a) retention factor, and (b) selectivity and resolution. The analyte and CSP are  $[\text{Ru}(\text{phen})_3]\text{Cl}_2$  (1), the Chirobiotic T2, respectively. The mobile phase is acetonitrile/water/0.08M tetramethylammonium nitrate.

A typical U-shaped curve (Fig. 3.4a) was obtained when plotting retention vs. the acetonitrile percentage. When the acetonitrile percentage is above 70%, increasing the concentration of acetonitrile increases the retention. When acetonitrile is below 70%, the reversed trend is observed. This U-shaped behavior is usually observed on the macrocyclic glycopeptide CSPs.<sup>57, 77</sup> Hydrophobic interactions between the analyte and the stationary phase contribute significantly to retention at higher concentrations of aqueous buffer, while other interactions (e.g. hydrogen bonding) become dominant at higher concentrations of organic modifier.<sup>77</sup> Fig. 3.4b indicates that the selectivity ( $\alpha$ ) exhibits a slight increase with reduced acetonitrile concentration. The effect of the organic modifier concentration on resolution is more complex since retention, selectivity, and efficiency all contribute to resolution. In this case study, maximal resolution was obtained at 50% acetonitrile/ 50% water/0.08 M TMAN.

Separations can also be affected by the nature of the organic modifiers. Acetonitrile and methanol are commonly used as organic modifiers with the Chirobiotic columns. Methanol/water/0.08 M TMAN was tested as the mobile phase for comparison with acetonitrile.  $K_1'$ ,  $\alpha$ , and  $R_s$  of complex 1 are 12.0, 1.68, and 2.5, respectively, when using 70%

methanol/30% water/0.08 M TMAN as the mobile phase. Compared with acetonitrile (data shown in Table 3.2, the optimized results of 1,  $[\text{Ru}(\text{phen})_3]\text{Cl}_2$ ), higher selectivity and longer retention time were observed using methanol as organic modifier. Methanol has a lower elution strength than acetonitrile because it is more polar, however the reason for the beneficial effect of methanol on enantioselectivity is unknown. It has been reported that methanol produces higher enantioselectivity on the teicoplanin-based CSPs.<sup>26, 77</sup> In order to combine the good efficiency of acetonitrile and the high enantioselectivity of methanol, optimization can be carried out using the two organic modifiers simultaneously. This dual modifier system proved to be successful and necessary for the separation of  $[\text{Ru}(\text{dppz})_3]\text{Cl}_2$  (complex 6). It cannot be baseline separated using acetonitrile-aqueous or methanol-aqueous mobile phases, but baseline resolution was obtained using 60% acetonitrile/20% methanol/20% water/0.08M TMAN.

In our study, salt additive was necessary for the elution of ruthenium(II) complexes. Different salts (ammonium nitrate, tetramethylammonium nitrate, ammonium trifluoroacetate, and ammonium acetate) were used as the additive in 70% acetonitrile/30% water at identical concentrations (0.08 M), since the minimum retention was observed with this mobile phase composition. The empirical results (Table 3.1) reveal that different salts do affect retention and selectivity. Since tetramethylammonium nitrate (TMAN) as an additive produced the highest selectivity and resolution, it was applied to optimize separations of the other Ru(II) complexes. Furthermore, an increase in salt concentration was found to decrease retention and resolution (Figure 3.5). This may be due to increased competition of salt for the interaction sites of the stationary phase (e.g. ionic interaction sites).<sup>83</sup>

Table 3.1 Effect of salt type in the mobile phase on enantioseparation

| Salt type                            | $k_1'$ | $\alpha$ | $R_s$ |
|--------------------------------------|--------|----------|-------|
| $\text{NH}_4\text{NO}_3$             | 0.97   | 1.42     | 1.7   |
| $\text{N}(\text{CH}_3)_4\text{NO}_3$ | 1.81   | 1.48     | 2.5   |
| $\text{NH}_4\text{COOCF}_3$          | 0.62   | 1.44     | 1.5   |
| $\text{NH}_4\text{COOCH}_3$          | 6.54   | 1.39     | 2.0   |

Note:  $[\text{Ru}(\text{phen})_3]\text{Cl}_2$  (complex 1) is separated on Chirobiotic T2 column. The mobile phase is 70%acetonitrile/30%water/0.08M salt.

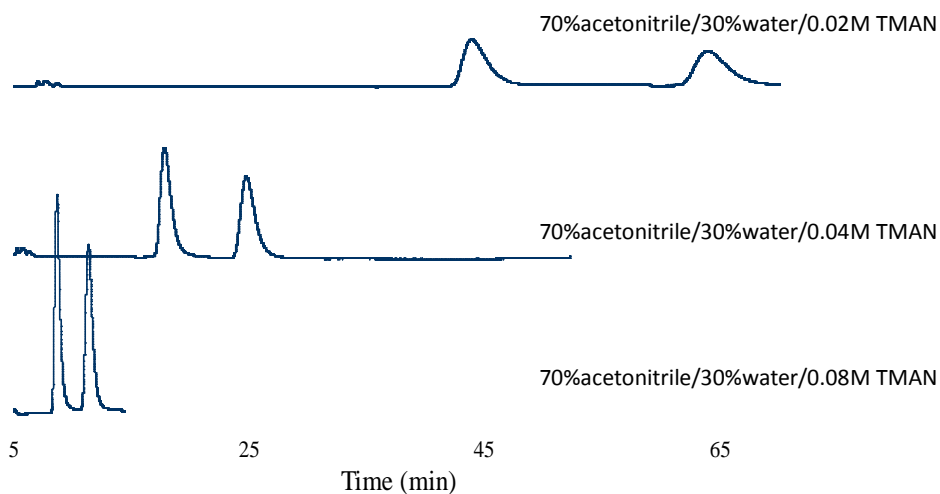


Figure 3.5 Effect of the salt concentration in the mobile phase on separation. The analyte and CSP are  $[\text{Ru}(\text{phen})_3]\text{Cl}_2$  (1), the Chirobiotic T2, respectively.

### 3.3.3 Enantioseparation of Ru(II) complexes

Based on its high enantioselectivity for complex 1, the separation and optimization of all seven Ru(II) polypyridyl compounds were carried out on the Chirobiotic T2 column. Various mobilephases composed of acetonitrile/water/TMAN were tested. If resolution was not adequate, a small amount of methanol was added in order to improve selectivity. Baseline enantioseparation of six of seven compounds was achieved with only acetonitrile as the organic modifier, while complex 6 was only baseline separated using acetonitrile/methanol/water/TMAN. The chromatographic results at optimal separation conditions are shown in Table 3.2. For Ru(II) polypyridyl complexes, the Chirobiotic T2 CSP provided good enantioselectivity (in the range of 1.16–1.48) and all seven compounds were baseline separated ( $R_s > 1.5$ ). Selected chromatograms are shown in Figure 3.6. The separation results demonstrate that this method is applicable for the accurate determination of enantiomeric excess (ee).

Table 3.2 Optimized separation of seven complexes on Chirobiotic T2 CSP

| Number | Name  | $k_1'$ | $\alpha$ | $R_s$ | Elution order     | Mobile phase |
|--------|---|--------|----------|-------|-------------------|--------------|
| 1      | [Ru(phen) <sub>3</sub> ]Cl <sub>2</sub>                 | 1.81   | 1.48     | 2.5   | $\Lambda, \Delta$ | A            |
| 2      | [Ru(phen) <sub>2</sub> nitrophen]Cl <sub>2</sub>        | 3.01   | 1.27     | 1.6   | $\Lambda, \Delta$ | B            |
| 3      | [Ru(phen) <sub>2</sub> aminophen]Cl <sub>2</sub>        | 2.36   | 1.43     | 2.2   | $\Lambda, \Delta$ | A            |
| 4      | [Ru(phen) <sub>2</sub> phen diamine]Cl <sub>2</sub>     | 3.26   | 1.43     | 2.4   | $\Lambda, \Delta$ | A            |
| 5      | [Ru(phen) <sub>2</sub> py <sub>2</sub> ]Cl <sub>2</sub> | 2.36   | 1.22     | 1.5   | $\Lambda, \Delta$ | B            |
| 6      | [Ru(dppz) <sub>3</sub> ]Cl <sub>2</sub>                 | 7.97   | 1.23     | 1.5   | $\Lambda, \Delta$ | C            |
| 7      | [Ru(bpy) <sub>3</sub> ]Cl <sub>2</sub>                  | 3.33   | 1.16     | 1.5   | $\Lambda, \Delta$ | D            |

Note: the mobile phase compositions are: A: 70%acetonitrile/30%water/0.08M TMAN; B: 60%acetonitrile/40%water/0.08M TMAN; C: 60%acetonitrile/20%methanol/20%water/0.08M TMAN; D: 50%acetonitrile/50%water/0.08M TMAN.

The enantiomeric elution order indicated in Table 3.2 was established by injecting a single enantiomer under the same experimental conditions. The elution order of Ru(II) polypyridyl complexes was very consistent: the  $\Lambda$ -enantiomer eluted first. This indicates that the  $\Delta$ -enantiomer shows greater affinity for the chiral stationary phase. Interestingly, a study with cyclodextrin-based CSP's showed the opposite elution order for these complexes.<sup>74</sup> The fact that all seven complexes show the same elution order could be explained by their similar ligands, which may interact with the stationary phase in similar ways. The consistency of elution order using the teicoplanin CSP, while not absolute proof of the absolute configuration of the Ru polypyridyl complexes, provides some circumstantial evidence at the point in time.

The effect of the counteranions of the Ru(II) complexes on the separation was investigated. Six analytes with the same chiral cation ([Ru(phen)<sub>3</sub>]<sup>2+</sup>) and different anions (Cl<sup>-</sup>, Br<sup>-</sup>, F<sup>-</sup>, BF<sub>4</sub><sup>-</sup>, PF<sub>6</sub><sup>-</sup>, and CF<sub>3</sub>SO<sub>3</sub><sup>-</sup>) were injected on the T2 CSP using the same mobile phase (70%acetonitrile/30%water/0.08M TMAN). The various anions showed no effect on the retention time, selectivity, and efficiency. It is likely that the mobile-phase nitrate anion exchanges rapidly with the initial counter-ions, and this new ion-pair undergoes the chiral recognition process.

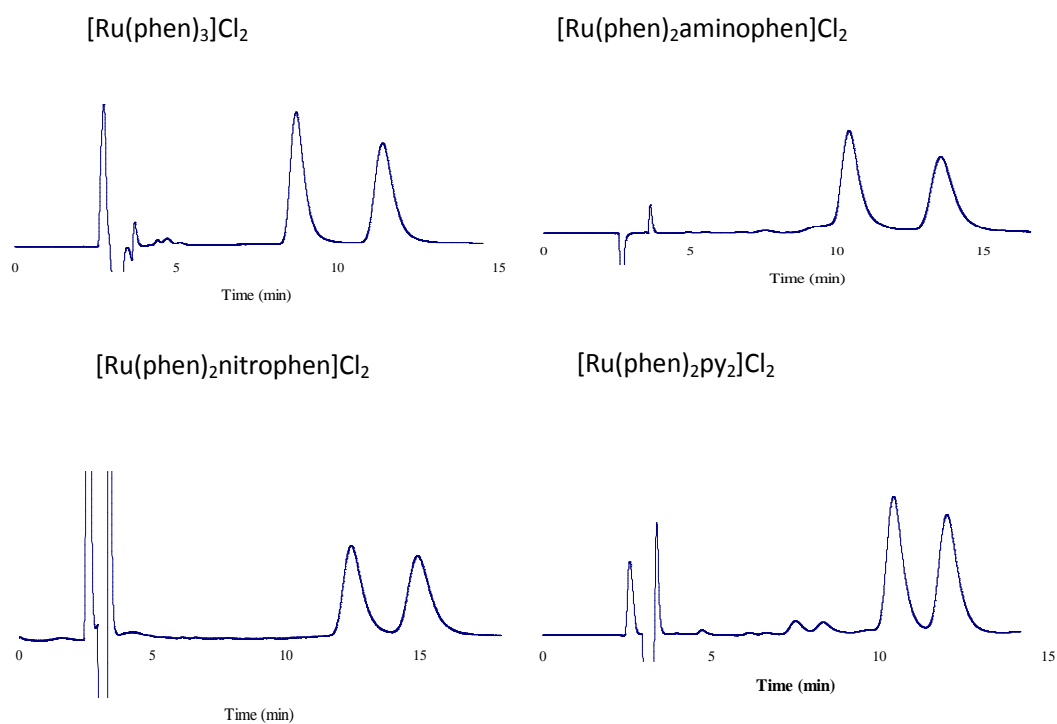


Figure 3.6 Selected chromatograms in the optimal mobile phase on Chirobiotic T2 column. The mobile phase compositions of each complex are shown in Table 3.2.

### 3.4 Conclusion

This study has demonstrated that the teicoplanin-based CSPs are the best macrocyclic glycopeptide columns for the enantioseparation of Ru(II) polypyridyl complexes. The newly developed Chirobiotic T2 column works more successfully than the Chirobiotic T. Enantioseparation was optimized by variation of the mobile phase composition. As a result, baseline separation was achieved for all seven complexes. This method was highly suitable for monitoring enantiomeric excess. In all cases tested, the  $\Lambda$ -enantiomer eluted first.

## CHAPTER 4

### ENANTIOMERIC SEPARATIONS OF RUTHENIUM(II) POLYPYRIDYL COMPLEXES USING HIGH PERFORMANCE LIQUID CHROMATOGRAPHY (HPLC) WITH CYCLODEXTRIN CHIRAL STATIONARY PHASES (CSPS)

Rapid, highly efficient, analytical resolution of the enantiomers of eight different monomeric ruthenium(II) polypyridyl complexes has been achieved using HPLC with cyclodextrin chiral stationary phases. This technique also proved capable of separating both of the diastereomers and the enantiomers of one dinuclear complex in a single run, whereas similar efforts with another dinuclear complex gave only one stereoisomer cleanly. Factors such as the stereochemistry of the chiral selectors, solvent polarity, and salt effects can be altered to provide precise control of the enantioselective interactions. The ability to quickly and quantitatively determine the enantiopurity of a given ruthenium complex allowed facile reexamination and optimization of the commonly used bulk resolution procedures based on diastereomeric coprecipitation with sodium arsenyl (+)-tartrate or sodium arsenyl (-)-tartrate salts.

#### 4.1 Introduction

The helical chirality inherent in octahedral transition-metal complexes bound by three bidentate ligands has fascinated chemists for over a century.<sup>84</sup> The right- and left-handed configurations of these metal complexes are referred to as  $\Delta$  and  $\Lambda$  enantiomers, respectively (part a of Figure 4.1). Derivatives of  $[\text{Ru}(\text{bpy})_3]^{2+}$  and  $[\text{Ru}(\text{phen})_3]^{2+}$  (bpy=2,2' bipyridine and phen=1,10-phenanthroline) have enjoyed a unique amount of attention, owing to the robust nature of the complexes and the favorable electrochemical and photophysical properties.<sup>60, 85</sup> In addition, the skeletal rigidity and variable functionality of such ruthenium(II) complexes has led to their application as catalysts for asymmetric synthesis.<sup>61, 62, 86</sup> They have shown potential as DNA probes or cleavage agents, in part, because of their stereoselective interactions with

DNA.<sup>65-67, 87-91</sup> They can also be used as building blocks in the synthesis of a variety of higher nuclearity, supermolecular assemblies.<sup>63, 64, 92-101</sup> As seen in part b of Figure 4.1, having only two such metal centers quickly increases the stereochemical complexity. Many of these applications require stereochemically pure compounds or, at least, a knowledge of the stereochemical composition.

Keene and co-workers developed the first general chromatographic method for the separation of the geometric isomers, diastereomers, and enantiomers of metal-polypyridyl complexes containing up to three chiral centers.<sup>100, 100-104</sup> Their method relies on cation exchange and ion pairing chromatography, in which the nature of the anionic additive to the mobile phase is typically the determining factor. Diastereomers can be separated on cation-exchange resins by the addition of nonchiral anionic additives (e.g., benzenesulfonate, toluene-4-sulfonate), whereas the resolution of enantiomers requires anionic chiral selectors such as (+)- and (-)-O,O'-dibenzoyl-tartrate or (+)- and (-)-O,O'-di-*p*-toluoyl-tartrate. The biggest disadvantage of this method is the relatively long times that are sometimes required to complete a separation. More recently, they have shown that DNA-based columns can be useful for the resolution of chiral ruthenium complexes.<sup>105</sup>

Lacour and co-workers<sup>71, 106</sup> and more recently Gruselle et al.<sup>107</sup> have shown that ruthenium complexes can be resolved on silica using  $\Delta$ - or  $\Lambda$ -[tris(tetrachlorocatecholato)P(V)] as a chiral ion-pairing agent. Resolutions of ruthenium complexes were also reported using capillary electrophoresis (CE).<sup>68-70, 108-111</sup> Kane-Maguire et al. used capillary zone electrophoresis (CZE) with enantiopure tartrate salt as the chiral selector in the running buffer to separate enantiomers of 16 transition-metal complexes,<sup>68</sup> which have different metal centers (Ru<sup>2+</sup>, Ni<sup>2+</sup>, Cr<sup>3+</sup>, and Co<sup>3+</sup>) and bidentate ligands (bipyridine, phenanthroline, and oxalate). Chiral discrimination of [Ru(phen)<sub>3</sub>]<sup>2+</sup> and [Ru(bpy)<sub>3</sub>]<sup>2+</sup> was also achieved using CZE with double-stranded DNA dissolved in the run buffer.<sup>69</sup> The DNA was shown to have different

binding affinities to the enantiomers. Unfortunately, the CE technique often has reproducibility problems, and it is incapable of working as a preparative method.

Because of its flexibility, broad selectivity, and high efficiency, HPLC with chiral stationary phases (CSPs) is the dominant method for enantiomeric separations and analyses. It is widely used both as an analytical method and as a preparative tool. Vos and co-workers were among the first to explore HPLC as a method to resolve ruthenium(II) polypyridyl complexes.<sup>76, 112</sup> They used a teicoplanin chiral stationary phase to resolve a series of chiral monomeric ruthenium(II) complexes, including  $[\text{Ru}(\text{L})_3]^{2+}$  ( $\text{L} = 2,2'$ -bipyridine (bpy), 1,10-phenanthroline (phen), and 4,7-diphenyl-1,10-phenanthroline (dpphen)) and some mixed-ligand complexes. They also separated the diastereomers and enantiomers of one dinuclear complex at both the analytical and semi-preparative scale using this technique.

Since bonded cyclodextrin stationary phases developed in our laboratory were first commercialized in 1983, they have proven to be successful for separating enantiomers.<sup>28, 29, 56, 58, 59, 113, 114</sup> Among them, the aromatic-derivatized cyclodextrin CSPs are multimodal and capable of working in three operational modes, which extends the range of enantiomers resolved. Although they have been widely applied to resolve many different classes of compounds, this class of stationary phases has not been applied to the transition-metal polypyridyl complex enantiomers, to our knowledge.

In this work, we explore the use of enantioselective cyclodextrin-based HPLC as an analytical method to resolve eight chiral ruthenium(II) monomer complexes and to analyze the enantiomeric excess (ee) of these enantiomers obtained by other resolution procedures. Furthermore, these HPLC methods are shown to be applicable for the separation and resolution of the diastereomers and enantiomers of dinuclear complexes, such as those represented in part b of Figure 4.1. Finally, the development of HPLC methods for quantifying the ee of such complexes gives us a rapid and more-accurate assessment of the enantiomeric composition of

the ruthenium complexes than the commonly applied circular dichroism (CD) and high-field NMR (with chiral-shift reagents) methods.<sup>88, 106, 115-117</sup>

In particular, we report that the *R*-naphthylethyl-carbamatederivatized  $\beta$ -cyclodextrin stationary phase shows high enantioselectivity for this entire class of compounds. Other factors including the composition of the polar-organic mobile phase and the ligand structure were shown to have profound effects on the resolution efficiency. Using this method, we can also quickly and quantitatively evaluate the efficiency of resolution methods for such cationic complexes, including the commonly used method of diastereoselective coprecipitation with the chiral dianions,  $[\text{As}_2((+)\text{-tartrate})_2]^{2-}$  and  $[\text{As}_2((-)\text{-tartrate})_2]^{2-}$ .

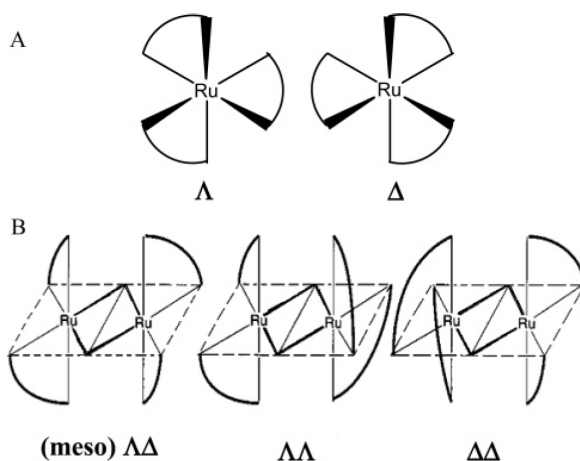


Figure 4.1. Structure and mirror image relationship of Ru(II) trisdiimine enantiomers. (A) Mononuclear complex (monomer). (B) Dinuclear complex (dimer)

## 4.2 Experimental section

### 4.2.1 Materials

The compounds arsenic(III)oxide, L(+)- and D(-)-tartaric acid, tetra-*n*-butylammonium chloride hydrate, hydrazine monohydrate, palladium on carbon (Pd/C, 10%), acetic acid (HOAc), triethylamine (TEA), sodium chloride, potassium nitrate, ammonium chloride, ammonium trifluoroacetate, and ammonium nitrate were purchased from Alfa Aesar (Ward Hill, MA) or

Aldrich Chemical (St. Louis, MO) and used without further purification. Ammonium hexafluorophosphate was purchased from Oakwood Products (West Columbia, SC). Acetonitrile (ACN) and methanol (MeOH) of HPLC grade were purchased from EMD (Gillbstown, NJ). Water was obtained from Millipore (Billerica, MA).

The compounds: 5-nitro-1,10-phenanthroline,<sup>118</sup>  $\text{Ru}(\text{phen})_2\text{Cl}_2$ ,<sup>119, 120</sup>  $[\text{Ru}(\text{phen})_3]\text{Cl}_2$  (**1**),<sup>121</sup>  $[\text{Ru}(\text{phen})_2\text{phendione}]\text{Cl}_2$  (**4**),<sup>65, 122</sup> (phendion=1,10-phenanthroline-5,6-dione),  $[\text{Ru}(\text{phen})_2\text{tatpp}](\text{PF}_6)_2$  (**5**),  $[\text{Ru}(\text{phen})_2(\text{py})_2]\text{Cl}_2$  (**6**)<sup>123</sup> (py=pyridine),  $[\text{Ru}(\text{dppz})_3]\text{Cl}_2$  (**7**),<sup>117</sup>  $[\text{Ru}(\text{bpy})_3]\text{Cl}_2$  (**8**),<sup>124</sup>  $[\text{Ru}_2(\text{phen})_4(\text{tpphz})]\text{Cl}_2$  (**9**),<sup>93</sup> and  $[\text{Ru}_2(\text{phen})_4(\text{tatpp})]\text{Cl}_4$  (**10**),<sup>125</sup> were prepared according to literature procedures. The structures of the dppz, tpphz, and tatpp ligands are shown in Figure 4.2.

Cyclobond I ( $\beta$ -cyclodextrin), II ( $\alpha$ -cyclodextrin), III ( $\gamma$ -cyclodextrin), AC (acetylated  $\beta$ -cyclodextrin), DM (dimethylated  $\beta$ -cyclodextrin), RSP (hydroxypropyl ether  $\beta$ -cyclodextrin), DMP (dimethylphenyl carbamate  $\beta$ -cyclodextrin), RN, and SN (i.e., *R* or *S*-naphthylethyl carbamate derivatives of  $\beta$ -cyclodextrins) CSPs were obtained from Advanced Separation Technologies (Whippany, NJ, USA). All of the columns are 250  $\times$  4.6 mm (i.d.).

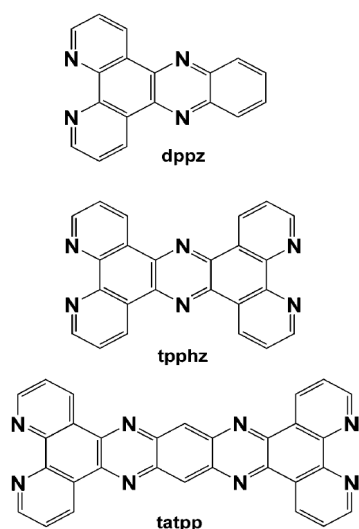


Figure 4.2 Structure of the ligands in Ru(II) polypyridyl complexes

#### 4.2.2 Equipment

The chromatographic system was a HP (Agilent Technologies, Palo Alto, CA, USA) 1050 system with a UV VWD detector, an autosampler, a quaternary pump and Chemstation software. The injection volume is 5  $\mu$ L. The circular dichroism detector is Jasco CD-2095 (JASCO Corporation, Tokyo, Japan).  $^1\text{H}$  NMR spectra were obtained on a Bruker JEOL Eclipse Plus 500 MHz spectrometer, using  $\text{CD}_3\text{CN}$  as the solvent. Chemical shifts are given in ppm and referenced to TMS.

#### 4.2.3 Synthesis of sodium arsenyl (+) or (-) tartrate

These salt compounds were prepared using slight modifications of the literature procedures.<sup>126, 127</sup> L(+)-tartaric acid (20 g, 0.133 mol) and NaOH (5.33 g, 0.133 mol) were dissolved in water (150 mL), and the solution was heated to reflux.  $\text{As}_2\text{O}_3$  (13.1 g, 0.066 mol) was added, and the resulting slurry refluxed for 45 min, during which the solution became clear. The solution was filtered while hot, and 300 mL ethanol was added to the filtrate, which resulted in some precipitation. The resulting mixture was cooled to 4 ° C for 12 h, upon which a large mass of white crystals formed. The crystals were isolated by filtration, washed with cold ethanol, and air-dried. Yield 29 g (90%). In an analogous manner,  $\text{Na}_2[\text{As}_2((-)\text{-tartrate})_2]\cdot 3\text{H}_2\text{O}$  could be prepared in a similar yield from D(-)-tartaric acid. Both salts were identical to those reported by Marcovich and Tapscott in all respects.<sup>126</sup>

#### 4.2.4 Resolution procedure for $[\text{Ru}(\text{phen})_3]\text{Cl}_2$ .

The following resolution procedure was widely applicable for most monomeric ruthenium complexes. Metatheses were conducted as follows: hexafluorophosphate salts of the complexes were converted to chloride salts by dissolving the complex in a minimal volume of dry acetone and dropwise addition of a saturated solution of tetra-*n*-butylammonium chloride hydrate in acetone. The chloride salt of the complex precipitates immediately and is collected by filtration, rinsed with acetone and diethyl ether, and dried in vacuo at 60 ° C for 2 h. Arsenyltartrate salts were decomposed by dissolution in hot 2 M  $\text{HNO}_3$ , and the resulting

solution was treated with a saturated solution of aqueous  $\text{NH}_4\text{PF}_6$  to precipitate the hexafluorophosphate salts. These precipitates are isolated by filtration, washed with cold water, and dried in vacuo at  $60^\circ\text{C}$  for 2 h.

Racemic  $[\text{Ru}(\text{phen})_3]\text{Cl}_2$  (1.0 g) was dissolved in 25 mL hot water ( $80^\circ\text{C}$ ). A solution of  $\text{Na}_2[\text{As}_2((+)\text{-tart})_2]\cdot 3\text{H}_2\text{O}$  (2.25 g in 30 mL hot water) was added into the racemic solution while stirring vigorously. The solution was chilled at  $4^\circ\text{C}$  overnight. The solution was filtered, and the precipitate was treated by method A and the filtrate by method B.

**Method A.** The precipitate of enantioenriched  $\Lambda$ - $[\text{Ru}(\text{phen})_3][\text{As}_2((+)\text{-tart})_2]$  was converted to the hexafluorophosphate salt and then chloride salt as described above. Yield 0.41 g (62% ee). The chloride salt was then dissolved in 15 mL water and warmed to  $80^\circ\text{C}$  and treated with  $\text{Na}_2[\text{As}_2((+)\text{-tart})_2]\cdot 3\text{H}_2\text{O}$  (1.25 g in 15 mL hot water) and chilled to  $4^\circ\text{C}$  overnight. The precipitate was isolated by filtration and washing with cold water and ethanol. The precipitate was converted to the hexafluorophosphate salt as described above. Yield 0.42 g  $\Lambda$ - $[\text{Ru}(\text{phen})_3][\text{PF}_6]_2$  (64%; 99.8% ee).

**Method B.** The filtrate was warmed to  $80^\circ\text{C}$ , and a solution of  $\text{Na}_2[\text{As}_2((-)\text{-tart})_2]\cdot 3\text{H}_2\text{O}$  (1.25 g in 15 mL hot water) was added while stirring. The solution was chilled overnight, and the precipitate isolated by filtration and washing with cold water and ethanol. The precipitate was converted to the hexafluorophosphate salt as described above. Yield 0.53 g  $\Delta$ - $[\text{Ru}(\text{phen})_3][\text{PF}_6]_2$  (82%; 99.5% ee).

#### 4.2.5 Preparation of $[\text{Ru}(\text{phen})_2\text{nitrophen}](\text{PF}_6)_2$ (**2**)

$\text{Ru}(\text{phen})_2\text{Cl}_2$  (1.05 g, 1.97 mmol) was dissolved in 50 mL of a 1:1 mixture of water and ethanol and heated to reflux under  $\text{N}_2$  atmosphere. Once refluxing, 5-nitro-1,10-phenanthroline (0.525 g, 2.3 mmol) was added in portions, and the mixture was refluxed for 12 h. After cooling, the solution was filtered, and the product was precipitated as a hexafluorophosphate salt upon the addition of aqueous  $\text{NH}_4\text{PF}_6$ . The product was isolated by filtration, washed with water, and

oven dried at 60 ° C. Yield 1.2 g *rac*-**2** (70%). Anal. Calcd for  $\text{RuC}_{36}\text{H}_{23}\text{N}_7\text{O}_2\text{P}_2\text{F}_{12} \cdot \text{H}_2\text{O}$ : C, 43.47; H, 2.53; N, 9.85. Found: C, 43.65; H, 2.35; N, 10.11.  $^1\text{H}$  NMR (500 MHz,  $\text{CD}_3\text{CN}$ ): 9.15 (1H, s), 9.06 (1H, d,  $^3J=7.8$  Hz), 8.76 (1H, d,  $^3J=7.3$  Hz), 8.59-8.63 (3H, m), 8.26 (2H, s), 8.25 (2H, s), 8.20 (1H, d,  $^3J=6.5$  Hz), 8.15 (1H, d,  $^3J=5.05$  Hz), 8.04-8.06 (2H, m), 7.98-8.0 (2H, m), 7.71-7.76 (2H, m), 7.60-7.66 (4H, m). UV-vis: MeCN [ $\lambda_{\text{max}}$ , nm ( $\epsilon$   $\text{M}^{-1}\text{cm}^{-1}$ )]: 445 (18200).

The complex was resolved as described in method B for  $[\text{Ru}(\text{phen})_3]\text{Cl}_2$ . The  $\Delta$  enantiomer was obtained in 70% yield (94.5% ee). CD for  $\Delta$ - $[\text{Ru}(\text{phen})_2(\text{nitrophen})](\text{PF}_6)_2$  ( $\Delta$ -**2**) [ $\text{CH}_3\text{CN}$ ,  $\lambda_{\text{max}}$ , nm ( $\Delta\epsilon$   $\text{M}^{-1}\text{cm}^{-1}$ )]: 415 (+15.6), 464 (-15.3). The  $\Lambda$  complex was also obtained by method B by reversing the order of arsenyl tartrate addition (first the (-) salt, then the (+) salt). Yield 72% (95.6% ee). CD for  $\Lambda$ - $[\text{Ru}(\text{phen})_2(\text{nitrophen})](\text{PF}_6)_2$  ( $\Lambda$ -**2**) [ $\text{CH}_3\text{CN}$ ,  $\lambda_{\text{max}}$ , nm ( $\Delta\epsilon$   $\text{M}^{-1}\text{cm}^{-1}$ )]: 415 (-15.6), 464 (+15.4).

#### 4.2.6 Preparation of $\Delta$ - or $\Lambda$ - $[\text{Ru}(\text{phen})_2(\text{aminophen})](\text{PF}_6)_2$ ( $\Delta$ -**3** or $\Lambda$ -**3**)

A solution containing  $\Delta$ - or  $\Lambda$ - $[\text{Ru}(\text{phen})_2(\text{nitrophen})]\text{Cl}_2$  (0.4 g, 0.53 mmol) and 10% Pd/C catalyst (0.5 g) in 50 mL ethanol was purged with  $\text{N}_2$  gas for 15 min. The reaction mixture was heated to 68-75 ° C. To this mixture, 6 mL  $\text{N}_2\text{H}_4 \cdot \text{H}_2\text{O}$  in 20 mL ethanol was added dropwise over a period of 1 h while refluxing the solution. The reflux was continued for another 6 to 8 h. The solution was cooled overnight and filtered over Celite, washing with additional ethanol. The sample was concentrated by removing excess ethanol via rotary evaporation and was treated with an aqueous solution of  $\text{NH}_4\text{PF}_6$ . The reddish-orange precipitate was filtered and oven dried at 60 ° C. Yield 80%. Anal. Calcd for  $\text{RuC}_{36}\text{H}_{25}\text{N}_7\text{P}_2\text{F}_{12}$ : C, 44.82; H, 2.82; N, 10.16. Found: C, 45.16; H, 2.63; N, 10.24.  $^1\text{H}$  NMR (500 MHz,  $\text{CD}_3\text{CN}$ ): 8.56-8.60 (5H, m), 8.25 (2H, s), 8.24 (2H, s), 8.21 (1H, d,  $^3J=8.5$  Hz), 8.06 (1H, d,  $^3J=5.05$  Hz), 8.02 (2H, apparent triplet,  $^3J=5.5$ ), 7.98 (2H, apparent triplet,  $^3J=5.1$ , 4.1), 7.56-7.66 (6H, m), 7.39 (1H, dd,  $^3J=8.5$  Hz,  $^4J=5.9$ Hz), 7.19 (1H, s), 5.57 (2H, br. s).

#### 4.2.7 LC analysis

For the LC analysis, the flow rate and the detection wavelength were 1 mL/min and 254 nm, respectively. All of the analytical separations utilized an injection volume of 5  $\mu$ L of solution containing 1 mg/mL of the ruthenium complex of interest in methanol or acetonitrile. The mobile phase was degassed by ultrasonication under vacuum for 5 min. All of the experiments were repeated three times at room temperature. The chloride (Cl<sup>-</sup>) salts and hexafluorophosphate (PF<sub>6</sub><sup>-</sup>) salts of ruthenium(II) complexes were dissolved in methanol and acetonitrile, respectively. Three parameters, retention factor ( $k'$ ), selectivity ( $\alpha$ ), and resolution (Rs), were assayed to analyze and optimize the separations. The retention factor was calculated using the equation  $k' = (t_r - t_0)/t_r$ , where  $t_r$  is the retention time and  $t_0$  is the dead time which, is determined by the peak of the refractive index change due to the sample solvent. Selectivity was calculated by  $\alpha = k_2'/k_1'$ , where  $k_1'$  and  $k_2'$  are the retention factors of the first and second eluted enantiomers, respectively. The resolution (Rs) was determined using  $Rs = 2(t_{r2} - t_{r1})/(w_1 + w_2)$ , where  $w$  is the base-peak width. For baseline separations, Rs values must be equal to or greater than 1.5. For the complexes, which could not be baseline separated ( $Rs < 1.5$ ), the flow rate was decreased to 0.5 mL/min, to achieve better efficiency. Once the resolution was satisfactory, efforts were made to minimize the retention time (factor).

### 4.3 Results And Discussion

#### 4.3.1 Performance of cyclodextrin-based CSPs

Most studies reporting chromatographic enantiomeric separations of tris(diimine) ruthenium(II) complexes are limited to mononuclear species,<sup>68-71, 100, 109, 110</sup> with the notable exception of Keene and co-workers, who have reported the column chromatographic resolution of numerous dimeric and even trimeric complexes.<sup>104, 105</sup> It should be noted that these resolutions typically first require the separation of diastereomers. Our purpose was to develop a broadly effective HPLC technique for the facile separation of enantiomers not only of mononuclear complexes but also for diastereomers and enantiomers that are found in dinuclear

species of ruthenium polypyridyl complexes. The ruthenium(II) complexes (eight mononuclear and two dinuclear ones) in this study include both homoleptic and heteroleptic diimine complexes that have diverse ligand structures (Figure 4.2). Among them,  $[\text{Ru}(\text{phen})_3]\text{Cl}_2$  (**1**) was used as a model compound to screen CSPs and operational modes.

Three native cyclodextrin and six derivatized  $\beta$ -cyclodextrin stationary phases were evaluated for their ability to separate  $[\text{Ru}(\text{phen})_3]\text{Cl}_2$ . Three of them (Cyclobond RN, SN, and DMP) showed enantioselectivity. It is particularly noteworthy that only Cyclobond RN, SN, and DMP are aromatic-derivatized among these nine CSPs. The ruthenium complex enantiomers are separated by aromatic-derivatized but not by nonaromatic-derivatized cyclodextrin, which suggests that the  $\pi$ -stacking interaction provided by the aromatic group of CSPs plays an important role and is necessary in chiral recognition. In addition to providing  $\pi$ -stacking interaction, the derivatized functional groups of CSPs have the effect of extending the mouth, which could allow the accommodation of larger analytes. Because of the different structure of these aromatic functional groups, Cyclobond RN, SN, and DMP showed different enantioselectivities. Table 4.1 shows the optimized enantioseparation results for  $[\text{Ru}(\text{phen})_3]\text{Cl}_2$  on these three CSPs. Among the three columns, R-naphthylethyl carbamate  $\beta$ -cyclodextrin (Cyclobond RN) CSP is the best stationary phase for  $[\text{Ru}(\text{phen})_3]\text{Cl}_2$ . The capability of cyclodextrin in discriminating ruthenium(II) complex enantiomers was also reported by Kano's group, using NMR.<sup>115</sup> The conclusion that "cyclodextrin has an asymmetrically twisted cavity in which a guest having a helix configuration is well fit" is in accord with our results that cyclodextrin CSPs are capable of well discriminating enantiomers of helical ruthenium(II) polypyridyl complexes.

Three chromatographic modes were studied, and enantioseparations were observed in the polar organic and the reversed phase modes. Figure 4.3 shows the chromatograms for the separation of  $[\text{Ru}(\text{phen})_3]\text{Cl}_2$  in these two modes in the optimized conditions. In the reversed phase mode,  $k_1'$ ,  $\alpha$ , and  $R_s$  in the optimized condition are 1.182, 1.64, 1.5, respectively. In the

polar organic mode, the separation is faster ( $k_1' = 0.467$ ) and more selective ( $\alpha = 1.97$ ). The longer retention time in the reversed phase mode may be due to the formation of a strong inclusion complex between phenanthroline aromatic ring and the derivatized cyclodextrin. Comparing these two modes, the polar organic mode gives better enantioseparations due to shorter separation times and better selectivities.

#### 4.3.2 Chromatographic resolution of mononuclear ruthenium(II) complexes

Analogous HPLC studies on the Cyclobond RN column in the polar-organic mode were carried out for all 10 of the ruthenium(II) complexes. The optimized enantioseparation results (including  $k_1'$ ,  $\alpha$ ,  $R_s$ , and the mobile-phase composition) for the 8 monomeric complexes are given in Table 4.2, and selected chromatograms are shown in Figure 4.4. Enantioselectivity values range between 1.23 and 2.95. Good enantioselectivity and chromatographic efficiencies provided complete baseline enantiomeric separations within minutes for all 8 complexes. These baseline resolution results demonstrate that accurate measurements of enantiomeric excess (ee) can be achieved with this method using HPLC and the Cyclobond RN CSP. For example, the ee of  $\Lambda$ -[Ru(phen)<sub>2</sub>aminophen]Cl<sub>2</sub> was determined to be 98.9% from its chromatogram (Figure 4.5). Comparable sensitivities and short analysis times are generally difficult or impossible with direct analysis via polarimetry, circular dichroism, or NMR with chiral shift reagents.

All of the above resolutions were conducted on relatively small samples (~5  $\mu$ g) using a typical analytical column (25cm $\times$ 0.46 cm, i.d.). To test the preparative capabilities of this chiral stationary phase (CSP), 2mg of [Ru(phen)<sub>2</sub>nitrophen]Cl<sub>2</sub> was dissolved in 100  $\mu$ L methanol and injected onto the analytical column. The two enantiomers were readily separated in a single run in approximately 12 min. Using typical assumptions on the scalability of HPLC separations, conservative estimates show that separations of 100 mg racemate on a standard semiprep column (25 $\times$ 5.08 cm, i.d.) of the same type could be made in a single run. Vos and co-workers

have shown that HPLC separations on the order of 30 mg racemate are possible with semi-prep columns (25×1 cm, i.d.) using the Teicoplanin CSP.<sup>112</sup>

Table 4.1 Comparison of three aromatic-derivatized Cyclobond CSPs

| Name of CSP   | $k_1'$ | $\alpha$ | $R_s$ | Mobile Phase (v/v)                               |
|---------------|--------|----------|-------|--|
| Cyclobond RN  | 0.47   | 1.97     | 2.4   | 80MEOH/20ACN/0.2 NH <sub>4</sub> NO <sub>3</sub> |
| Cyclobond SN  | 4.82   | 1.07     | 0.7   | 100MEOH/0.4HOAC/0.8TEA                           |
| Cyclobond DMP | 12.04  | 1.13     | 1.0   | 100MEOH/0.4HOAC/1.2TEA                           |

Note: MEOH: methanol; ACN: acetonitrile; HOAC: acetic acid; TEA: triethylamine.

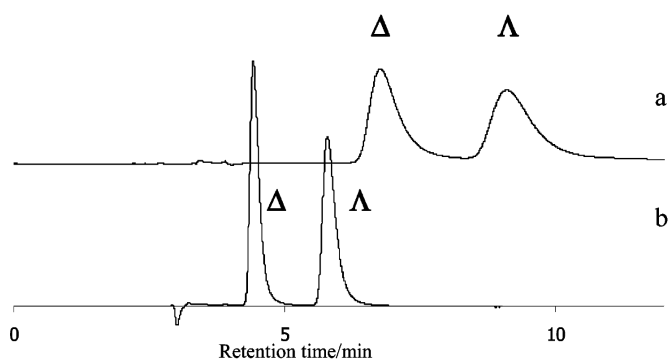


Figure 4.3 Comparison of the chromatographic modes on Cyclobond RN CSP. (a) The reversed phase mode: the mobile phase is 20%acetonitrile/80%buffer (Buffer: 0.1%triethylammonium acetate in water, pH=4.1). The polar organic mode: the mobile phase is 80methanol%/20%acetonitrile/0.2%NH<sub>4</sub>NO<sub>3</sub>.

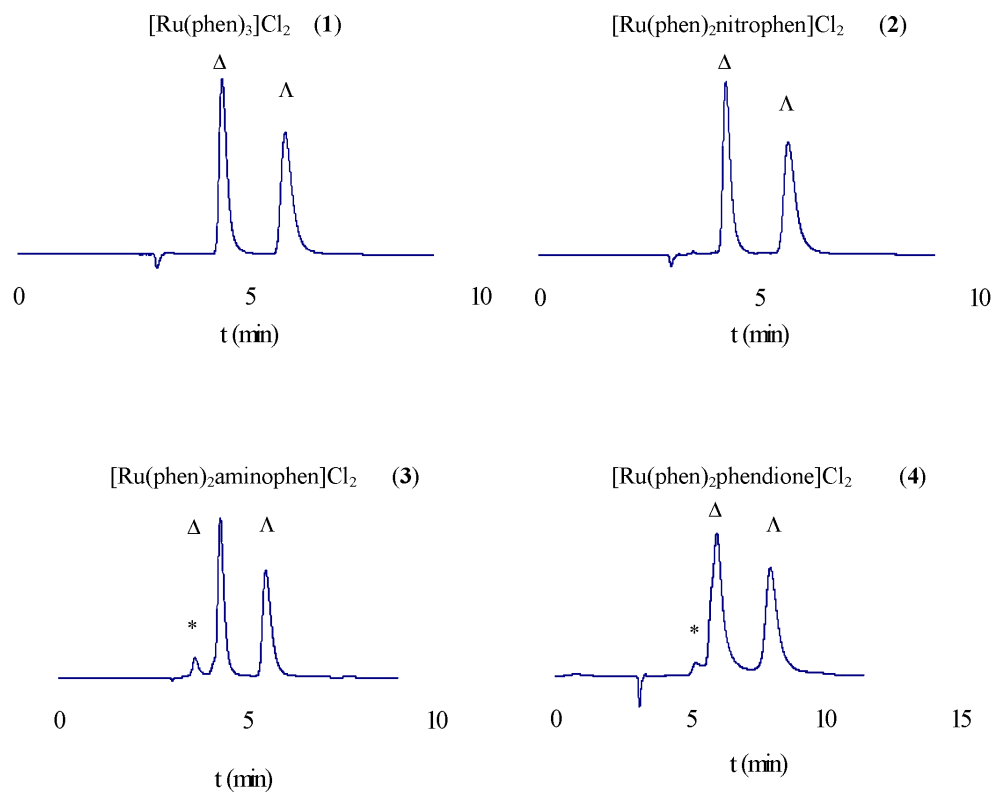


Figure 4.4 Selected chromatograms of Ru(II) polypyridyl complexes in the optimized conditions on Cyclobond RN CSP. The mobile phase composition for each compound is shown in Table 4.2, respectively. The (\*) denotes impurities in the samples.

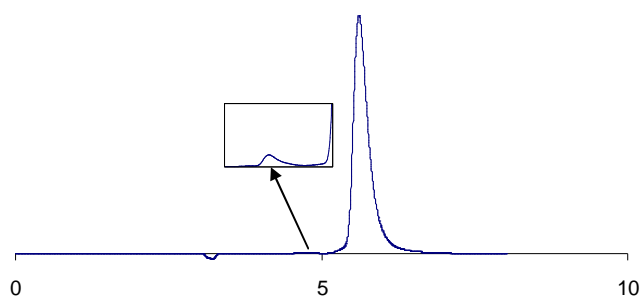


Figure 4.5 Chromatogram of  $\Lambda$ -[Ru(phen)<sub>2</sub>aminophen]Cl<sub>2</sub> on Cyclobond RN CSP. The enlarged chromatogram is the  $\Delta$ -enantiomer impurity. The mobile phase is 80methanol%/20%acetonitrile/0.2%NH<sub>4</sub>NO<sub>3</sub>.

Table 4.2 Summary of the optimized results of Ru(II) polypyridyl complexes on Cyclobond RN CSP

Note:

| Number          | Name  | $k_1'$ | $\alpha$ | $R_s$ | Mobile Phase (v/v)                               | Elution order |
|-----------------|---|--------|----------|-------|--|---------------|
| 1               | [Ru(phen) <sub>3</sub> ](Cl <sub>2</sub> )                      | 0.47   | 1.97     | 2.4   | 80MEOH/20ACN/0.2 NH <sub>4</sub> NO <sub>3</sub> | Δ, Λ          |
| 2               | [Ru(phen) <sub>2</sub> nitrophen](Cl <sub>2</sub> )             | 0.41   | 2.14     | 2.2   | 80MEOH/20ACN/0.2 NH <sub>4</sub> NO <sub>3</sub> | Δ, Λ          |
| 3               | [Ru(phen) <sub>2</sub> aminophen](Cl <sub>2</sub> )             | 0.42   | 1.94     | 2.2   | 80MEOH/20ACN/0.2 NH <sub>4</sub> NO <sub>3</sub> | Δ, Λ          |
| 4               | [Ru(phen) <sub>2</sub> phendione](Cl <sub>2</sub> )             | 0.91   | 1.69     | 1.7   | 95MEOH/5ACN/0.4NH <sub>4</sub> NO <sub>3</sub>   | Δ, Λ          |
| 5 <sup>a</sup>  | [Ru(phen) <sub>2</sub> tatpp](PF <sub>6</sub> ) <sub>2</sub>    | 1.56   | 1.40     | 1.5   | 100MEOH/0.4NH <sub>4</sub> NO <sub>3</sub>       | Δ, Λ          |
| 6               | [Ru(phen) <sub>2</sub> py <sub>2</sub> ](Cl <sub>2</sub> )      | 1.91   | 1.23     | 1.5   | 100MEOH/0.4 NH <sub>4</sub> NO <sub>4</sub>      | Δ, Λ          |
| 7               | [Ru(dppz) <sub>3</sub> ](Cl <sub>2</sub> )                      | 1.07   | 2.74     | 3.9   | 70MEOH/30ACN/0.2NH <sub>4</sub> NO <sub>3</sub>  | Δ, Λ          |
| 8 <sup>a</sup>  | [Ru(bpy) <sub>3</sub> ](Cl <sub>2</sub> )                       | 1.10   | 1.27     | 1.5   | 95MEOH/5ACN/0.4NH <sub>4</sub> NO <sub>3</sub>   | Δ, Λ          |
| 9 <sup>b</sup>  | [Ru <sub>2</sub> (phen) <sub>4</sub> (tpphz)](Cl <sub>4</sub> ) | 0.86   | 2.95     | 3.5   | 60MEOH/40ACN/0.3NH <sub>4</sub> NO <sub>3</sub>  | ΔΔ, ΔΛ, ΛΛ    |
| 10 <sup>b</sup> | [Ru <sub>2</sub> (phen) <sub>4</sub> (tatpp)](Cl <sub>4</sub> ) | 2.51   | 2.16     | 2.8   | 70MEOH/30ACN/0.4NH <sub>4</sub> NO <sub>3</sub>  | ΔΔ, ΔΛ, ΛΛ    |

Note: The flow rate is 0.5 mL/min. In other conditions, the flow rate is 1.0 mL/min. For the dimer, the results were calculated for one pair of enantiomers.

#### 4.3.3 Chromatographic separation of diastereomers and enantiomers in dinuclear ruthenium(II) complexes

Dinuclear complexes, such as **9** and **10**, contain two chiral centers, and therefore they are often prepared as a mixture of both diastereomers (e.g.,  $\Delta\Delta$  and  $\Lambda\Lambda$  vs  $\Delta\Lambda$  and  $\Lambda\Delta$ ) and enantiomers; making the separation problem considerably more challenging. For **9** and **10**, the problem is simplified somewhat in that the  $\Delta\Lambda$  complex is a meso structure, and thus only three stereoisomers ( $\Delta\Delta$ ,  $\Lambda\Lambda$ , and  $\Delta\Lambda$ ) need be separated. Figure 4.6 shows selected chromatograms of  $[\text{Ru}_2(\text{phen})_4(\text{tpphz})]\text{Cl}_4$  (**9**, panels A1 and A2) and  $[\text{Ru}_2(\text{phen})_4(\text{tatpp})]\text{Cl}_4$  (**10**, panels B1 and B2). Both CD and UV detectors were employed, and thus UV absorption and CD chromatograms were obtained simultaneously. For dimer **9**, three peaks are clearly seen in the UV chromatogram (panel A2), and the relative peak areas are consistent with statistical expectations. Figure 4.6 (panel A1) shows two of the three peaks to be chiroptic, and the assignment of these as  $\Delta\Delta$ -**9** and then  $\Lambda\Lambda$ -**9** are based on the sign of the CD and by injection of enantiopure samples. The meso structure,  $\Delta\Lambda$ -**9**, can be assigned as the middle peak in the UV trace because its CD signal is expected to be nil, thus it was possible to separate all three stereoisomers in one chromatographic run in this case. However, the separations with **10** were less successful, as seen in Figure 4.6 (panel B2), in which two overlapping peaks are seen at the end of the chromatogram. From the CD data, we can assign the first large peak to the  $\Delta\Delta$  enantiomer and the two overlapping UV peaks as first the  $\Delta\Lambda$  complex and then the  $\Lambda\Lambda$  stereoisomer because only the latter peak is chiroptic (as seen by the dotted lines relating the UV to CD data). As with **9**, the meso complex comes between the two enantiomers; however, here only one pure enantiomer is obtained ( $\Delta\Delta$ ) because  $\Delta\Lambda$  and  $\Lambda\Lambda$  are only partially separated in this one-run experiment. The elution order ( $\Delta\Delta$ ,  $\Delta\Lambda$ ,  $\Lambda\Lambda$ ) is the same for both dimers as determined by the injection of enantiopure samples. Note that the signs of the CD signals are reversed for **9** (panel A1) and **10** (panel B1), which seems odd but is simply due to different null points in the CD spectra of these two complexes at this wavelength (254 nm). The appearance of several impurity peaks early in chromatogram of **10** are to the instability of this

complex toward normalphase chromatography.<sup>125</sup> Prior attempts to purify crude isolates of **10** by column chromatography on silica or alumina (typically with MeCN eluent) are known to cause some decomposition to an uncharacterized side-product(s),<sup>125</sup> and are likely to be occurring to a lesser extent here.

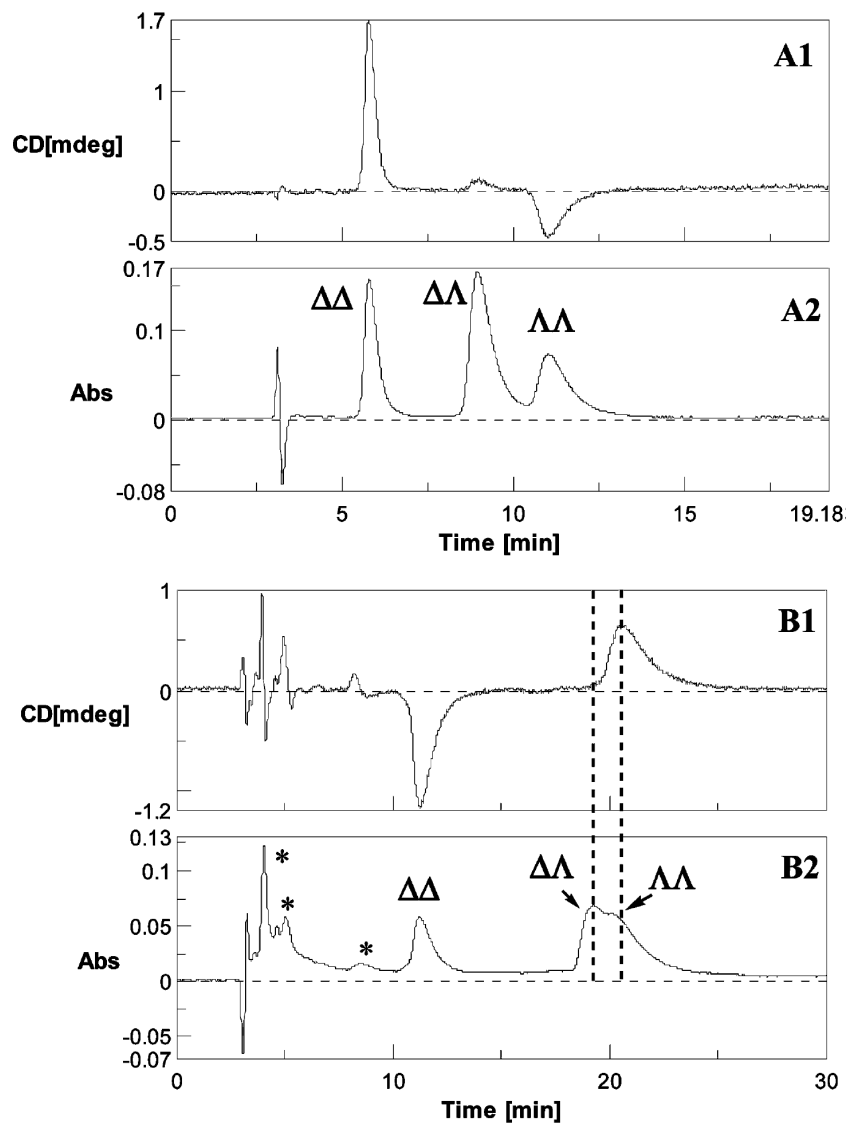


Figure 4.6 Chromatograms of  $[\text{Ru}_2(\text{phen})_4(\text{tpphz})]\text{Cl}_4$ , **9** (A1 and A2); and  $[\text{Ru}_2(\text{phen})_4(\text{tatpp})]\text{Cl}_4$ , **10** (B1 and B2) in the optimized mobile phase on Cyclobond RN CSP.

#### 4.3.4 Effects of the ligand structure, complex charge, and counterion

The enantiomeric elution order indicated in Table 4.2 was established by injecting a single enantiomer standard under the same experiment conditions as well as the CD measurements. All of the mononuclear ruthenium(II) complexes show the same elution order, that is, the  $\Delta$  isomer eluted first. This means that the  $\Lambda$  enantiomer binds to derivatized  $\beta$ -cyclodextrin with greater affinity. The fact that **1-8** have the same elution order indicates that this method may be useful for determining the absolute configuration of related metal complexes with analogous ligands. **2-6** are mixed ligand complexes and contain two phenanthroline ligands. The dppz in  $[\text{Ru}(\text{dppz})_3]\text{Cl}_2$  (**7**) and the bpy ligand in  $[\text{Ru}(\text{bpy})_3]\text{Cl}_2$  (**8**) are also diimine ligands, similar to the phenanthroline ligand. The fact that such complexes often show similar LC enantioselectivity also was reported previously. On the silica-bonded teicoplanin LC stationary phase,  $[\text{Ru}(\text{bpy})_3]^{2+}$ ,  $[\text{Ru}(\text{phen})_3]^{2+}$ , and  $[\text{Ru}(\text{dpphen})_3]^{2+}$  showed the same elution order, with the  $\Delta$  isomer being retained more strongly.<sup>76</sup> In a CE,  $[\text{Ru}(\text{bpy})_3]^{2+}$  and  $[\text{Ru}(\text{phen})_3]^{2+}$  also showed similar enantioselectivity.<sup>68, 109</sup> For the dinuclear complexes (**9** and **10**), the same elution order (i.e.,  $\Delta\Delta$  eluted before  $\Lambda\Lambda$ ) was obtained. The meso ( $\Delta\Lambda$ ) stereoisomer was eluted between  $\Delta\Delta$  and  $\Lambda\Lambda$  forms, which means that the meso form has intermediate binding strength for the cyclodextrin-based stationary phase (Figure 4.6 (B2)).

The elution order also was determined on the *S*-naphthylethyl carbamate  $\beta$ -cyclodextrin (Cyclobond RN) CSP. The configuration of the naphthylethyl carbamate moieties is opposite on the RN and SN  $\beta$ -cyclodextrin stationary phases. The elution order for all except  $[\text{Ru}(\text{dppz})_3]^{2+}$  (**7**) reversed, which means the  $\Delta$  enantiomer shows a greater affinity for this chiral stationary phase. This indicates that the stereogenic configuration of the naphthylethyl carbamate group is a major factor for chiral recognition, and the cyclodextrin plays a secondary role. In the polar-organic mode, chiral recognition is mainly through external interaction (outer sphere) between the analyte and derivatized cyclodextrin. In fact, it has been shown that both the attached chiral naphthylethyl carbamate moiety and the chiral base-cyclodextrin molecule contribute to chiral

recognition.<sup>128, 129</sup> Furthermore, they can do so in a synergistic or antagonistic fashion.<sup>128, 129</sup> Clearly, in the case of all of the ruthenium(II) complexes, the *R*-naphthylethyl carbamate groups and the underlying  $\beta$ -cyclodextrin act synergistically to produce enhanced enantiomeric separations. If the cyclodextrins played no role in the enantiomeric selectivity for these complexes, then the *S*-naphthylethyl carbamate- $\beta$ -cyclodextrin CSP would produce equivalent enantiomeric separations but of the opposite retention order. This, however, is not the case.

The cyclodextrin-based stationary phase binds ruthenium(II) complexes with a marked dependence upon the ligand structure, as seen from the data in Table 4.2. As these data were obtained with varying mobile-phase compositions, it is difficult to make specific structure-binding correlations; however, with an 80% methanol/20% acetonitrile/0.2%  $\text{NH}_4\text{NO}_3$  mobile phase, the  $k_1'$  of **1**, **2**, **3**, **4**, and **5** are 0.467, 0.412, 0.422, 0.225, 0.185, respectively. **2**, **3**, and **4** are retained less than **1**, which is likely due to their stronger hydrogen-bonding interactions with the methanol mobile phase. **5** was much less retained than **1**, possibly due to steric effect from the bulky (tatpp) ligand.

As seen from the results in Table 4.2, the retention is greatly affected by the overall charge of the complex cations. The retention for the quadruple-charged dinuclear complexes, **9** ( $k_1'=0.865$ ) and **10** ( $k_1'=2.32$ ), is considerably stronger than of the doubly charged mononuclear complexes, **1** ( $k_1'=0.267$ ) and **2** ( $k_1'=0.191$ ), when chromatographed using the same mobile phase (60% methanol/40% acetonitrile/0.3%  $\text{NH}_4\text{NO}_3$ ). We presume that this is primarily due to the stronger electrostatic interaction with the commonly formed nitrate-cyclodextrin inclusion complex in the CSP. The role of the initial counteranion in the complex salt is apparently unimportant in the separation process. When the anion with  $[\text{Ru}(\text{phen})_3]^{2+}$  was changed intentionally to  $\text{Br}^-$ ,  $\text{F}^-$ ,  $\text{BF}_4^-$ ,  $\text{PF}_6^-$ , and  $\text{CF}_3\text{SO}_3^-$ , the same retention times and enantioselectivity (within experimental error) were obtained under the same experimental conditions. It seems likely that the mobile-phase nitrate anion rapidly exchanges with these counterions, and it is this ion-pair that dictates the chiral recognition process. Keene has showed that the anion present in

the mobile phase is critical for effective separations in ion-pairing chromatography on cation exchange resins. showed that the anion present in the mobile phase is critical for effective separations in ion-pairing chromatography on cation exchange resins.

Effects of the mobile phase were investigated by changing salt type, salt concentration, and modifier solvent concentration. Different salts (potassium nitrate, ammonium trifluoroacetate, ammonium nitrate, sodium chloride, triethylammonium acetate, and ammonium chloride) were used as the additive in 100% methanol, at identical concentration (0.0125M). Enantioseparation of  $[\text{Ru}(\text{phen})_3]\text{Cl}_2$  was obtained with all of these additives. However, the mobile phases, that utilized different salt additives show different retention and selectivity (Table 4.3). Among them, ammonium nitrate ( $\text{NH}_4\text{NO}_3$ ) produced the highest selectivity and excellent resolution values. Furthermore, increasing the salt concentration was found to increase the enantioselectivity and retention (Figure 4.7).

In addition, adding an organic modifier solvent, such as acetonitrile, affects separation greatly. To study the effect of acetonitrile concentration, the percentage of acetonitrile was increased from 0 to 100% (Figure 4.8). Because ammonium nitrate will precipitate at high percentages of acetonitrile, an acetic acid/triethylamine salt, which is commonly used in the polar-organic mode, was used at the concentration of 1.0% acetic acid/1.0% triethylamine. The retention factor curve shows a U shape. When the percentage of acetonitrile is below 30%, increasing the concentration of acetonitrile decreases the retention. When the percentage of acetonitrile is above 30%, the reverse trend is obtained; and also, the selectivity decreases slightly from 1.341 to 1.146 with increasing acetonitrile concentration. Generally, in the polar-organic mode on cyclodextrin CSPs, the retention time can be decreased by increasing the methanol concentration because methanol competes with analytes for hydrogen-bonding sites in the stationary phase.<sup>30</sup> This can explain the phenomenon in the range of 30 to 100% acetonitrile. However, the mechanism by which a small amount of acetonitrile reduces retention is still not clear. Nonetheless, adding an appropriate amount of acetonitrile can decrease the

retention, while maintaining good selectivity. On the basis of the salt and acetonitrile concentration studies, enantioseparation could be optimized by controlling acetonitrile and ammonium nitrate concentrations to achieve the shortest retention time, good selectivities, and baseline resolutions.

Table 4.3 Effect of the salt type in the mobile phase on enantioseparation

| Salt type                 | $k_1'$ | $\alpha$ | $R_s$ |
|---------------------------|--------|----------|-------|
| potassium nitrate         | 5.84   | 1.48     | 1.5   |
| ammonium trifluoroacetate | 1.48   | 1.62     | 1.5   |
| ammonium nitrate          | 2.45   | 1.67     | 2.0   |
| sodium chloride           | 3.11   | 1.54     | 1.5   |
| triethylammonium acetate  | 9.70   | 1.34     | 1.0   |
| ammonium chloride         | 2.47   | 1.56     | 1.6   |

Note: The mobile phase is 0.0125 M salt in methanol. All the results were obtained on Cyclobond RN CSP and the analyte is  $[\text{Ru}(\text{phen})_3]\text{Cl}_2$ .

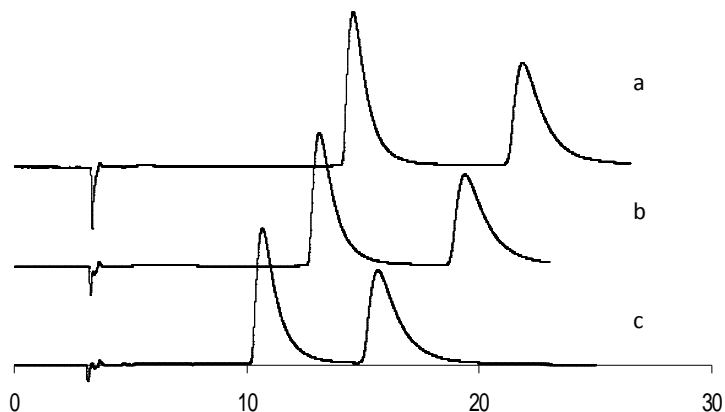


Figure 4.7 Effects of the concentration of  $\text{NH}_4\text{NO}_3$  in the mobile phase. The analyte, the CSP, and the mobile phase are  $[\text{Ru}(\text{phen})_3]\text{Cl}_2$ , Cyclobond RN and 100%methanol/ammonium nitrate, respectively. (a) 0.0500M; (b) 0.0250M; (c) 0.0125M.

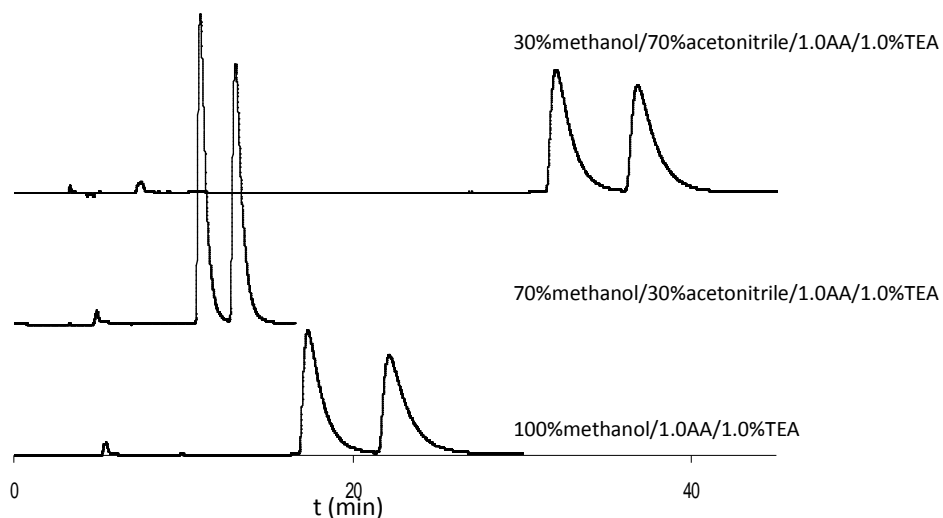


Figure 4.8 Effects of acetonitrile concentration. The analyte, and the CSP are  $[\text{Ru}(\text{phen})_3]\text{Cl}_2$  and Cyclobond RN, respectively. AA: acetic acid; TEA: triethylamine

#### 4.3.5 Large scale resolution of ruthenium(II) diimine complexes

Whereas it is possible to use preparative-scale HPLC to isolate enantiopure complexes, large-scale resolution (1-0.5 g) for many trisdiimine metal complexes can often be achieved via diastereoselective precipitation with chiral anions, such as  $[\text{As}_2((+)\text{-tart})_2]^{2-}$ ,  $[\text{Sb}_2((+)\text{-tart})_2]^{2-}$ ,  $[(-)\text{-O,O'}\text{-dibenzoyl-L-tartrate}]^{2-}$ ,<sup>94, 130</sup> and  $\Delta$  and  $\Lambda$ - $[\text{P}^{\text{V}}\text{-(tetrachlorocatecholate)}_3]$ . In particular, sodium arsenyl-(+)-tartrate and potassium antimonyl-(+)-tartrate have been frequently employed with good success.<sup>65, 84, 123, 131-134</sup> The resolution procedures vary in detail but follow the same general procedures outlined in Figure 4.9. In this section, we reexamine this general procedure, using chiral HPLC to evaluate the enantiopurity of the complex at each step. First, however, some comments on the tartrate salts are appropriate.

Both the arsenyl and antimonyl tartrate salts contain a dimeric dianion with arsenic or antimony atoms at the axial positions of a twisted ( $C_2$  symmetric), flattened spheroid.<sup>135</sup> A crystal structure of  $\Lambda$ - $[\text{Fe}(\text{phen})_3][\text{Sb}_2((+)\text{-tart})_2]$  is known and reveals how the left-handed twist

of the dianion allows closer ion pairing with the  $\Lambda$  dication than with the  $\Delta$  dication.<sup>136</sup> The closer ion pairing leads to selective precipitation of the  $\Lambda$  complex when L-(+)-tartrate salts are used and the  $\Delta$  complex with D-(-)-tartrate salts. The absolute structure of the  $\Lambda$ -configuration of **1** (PF<sub>6</sub> salt) has also been determined by crystallography and correlated with its CD spectrum.<sup>137</sup>

The tartrate salts are readily prepared from the metal oxide (As<sub>2</sub>O<sub>3</sub> or Sb<sub>2</sub>O<sub>3</sub>) and the appropriate tartaric acid (+ or -). For example, sodium arsenyl (+)-tartrate was first reported in 1895 by Henderson<sup>127</sup> and later in 1980, and the (+)- and (-)-tartrate salts were synthesized by Marcovich and Tapscott.<sup>126</sup> Neither report gave yields, and the reaction conditions varied from heating from 15 min to several days. We find that the Henderson procedure,<sup>127</sup> with minor modifications, reliably gives the arsenyl salts, Na<sub>2</sub>[As<sub>2</sub>((+)-tart)<sub>2</sub>] $\cdot$ 3H<sub>2</sub>O and Na<sub>2</sub>[As<sub>2</sub>((-)-tart)<sub>2</sub>] $\cdot$ 3H<sub>2</sub>O in ~90% yield. The details of this procedure are reported in the experimental section.

Most resolution procedures for [Ru(phen)<sub>3</sub>]Cl<sub>2</sub> and related complexes are based on the procedures first developed by Dwyer and Gyrfas in 1949.<sup>131-133</sup> This procedure is depicted in Figure 4.9 (Method A) and essentially involves two diastereoselective precipitations of the cationic complex with the same chiral anion. For example, treatment of [Ru(phen)<sub>3</sub>]Cl<sub>2</sub> with Na<sub>2</sub>[As<sub>2</sub>((+)-tart)<sub>2</sub>] $\cdot$ 3H<sub>2</sub>O gives an initial precipitate of  $\Lambda$ -[Ru(phen)<sub>3</sub>][As<sub>2</sub>((+)-tart)<sub>2</sub>], which we find to be approximately 62% ee. This salt can be metathesized to the water-soluble chloride salt and retreated with Na<sub>2</sub>[As<sub>2</sub>((+)-tart)<sub>2</sub>] $\cdot$ 3H<sub>2</sub>O to give  $\Lambda$ -[Ru(phen)<sub>3</sub>][PF<sub>6</sub>]<sub>2</sub> (after metathesis), which is 99% ee by chiral HPLC. The overall yield of the  $\Lambda$  complex is 64% (0.42 g based on 1.3 g racemate). Similar results are obtained for the  $\Delta$  complex if Na<sub>2</sub>[As<sub>2</sub>((-)-tart)<sub>2</sub>] $\cdot$ 3H<sub>2</sub>O is used instead.

Figure 4.9 also shows a modification to this procedure (method B) that gives the chiral product in greater yield with considerably less manipulation of the intermediates (mainly the metathesis reactions). Method B is based on the observation by Hiort and co-workers,<sup>65</sup> who noted that the  $\Delta$  enantiomer of the cationic complex can be isolated from the initial filtrate (assuming the initial solution was treated with Na<sub>2</sub>[As<sub>2</sub>((+)-tart)<sub>2</sub>] $\cdot$ 3H<sub>2</sub>O) by precipitation with

hexafluorophosphate anion, metathesis to the chloride salt, and treatment of this solution with  $\text{Na}_2[\text{As}_2((-)\text{-tart})_2]\cdot 3\text{H}_2\text{O}$ . We have found that this procedure can be further streamlined, in that, the initial filtrate can be treated directly with  $\text{Na}_2[\text{As}_2((-)\text{-tart})_2]\cdot 3\text{H}_2\text{O}$ , without bothering to isolate and metathesize the complex. The precipitate of  $\Delta\text{-}[\text{Ru}(\text{phen})_3][\text{As}_2((-)\text{-tart})_2]$  can then be converted to the  $\text{PF}_6^-$  salt, giving  $\Delta\text{-}[\text{Ru}(\text{phen})_3][\text{PF}_6]_2$  in >99% ee and 80% yield (0.53 g based on 1.3 g racemate). Of course, the two methods can be used together to obtain reasonable amounts of enantiopure  $\Delta\text{-}$  and  $\Lambda\text{-}[\text{Ru}(\text{phen})_3]\text{Cl}_2$  and the waste products can be recycled to improve the yield even further.

We examined the enantiopurity of a number of ruthenium complexes after resolution by both methods A and B (Table 4.4) and find that typically method B works better, faster, and gives higher recovery (yield) than method A. Interestingly, whereas both method A and B resolve most of the trischelate complexes tested, we were unable to significantly resolve  $[\text{Ru}(\text{bpy})_3]^{2+}$  using either method A (9.4% ee) or method B (4.5% ee).

As has been shown by ourselves<sup>117, 138</sup> and others,<sup>131-133, 139</sup> the stereochemistry at these ruthenium centers is very robust and difficult to racemize. Dwyer showed that oxidation to the Ru(III) analogue and reduction back to the ruthenium(II) center leaves the stereochemistry unaltered.<sup>132</sup> Photolysis appears to be the only efficient manner to racemize a particular enantiomer in this class of ruthenium(II) complexes.<sup>140-142</sup> Such stability suggests these complexes may have utility as chiral selectors in their own right, and we are beginning to explore this possibility.

Table 4.4 Enantiopurity and resolution yield for several monomeric ruthenium(II) polypyridyl complexes (hexafluorophosphate salts) as resolved by Method **A** and/or **B**

| Compound             | ee (%) | Yield | Notes                      |
|----------------------|--------|-------|----------------------------|
| $\Lambda$ -1 (Run 1) | 98.9   | 64    | Method A                   |
| $\Lambda$ -1 (Run 2) | 99.8   | 64    | Method A                   |
| $\Delta$ -1 (Run 1)  | 99.5   | 78    | Method B                   |
| $\Delta$ -1 (Run 2)  | 99.8   | 82    | Method B                   |
| $\Delta$ -2          | 94.5   | 70    | Method B                   |
| $\Lambda$ -2         | 95.6   | 72    | Method B                   |
| $\Delta$ -3          | 99.4   | n.a.  | prepared from $\Delta$ -2  |
| $\Lambda$ -3         | 95.2   | n.a.  | prepared from $\Lambda$ -2 |
| $\Delta$ -4          | 96.1   | 60    | Method B                   |
| $\Lambda$ -4         | 97.9   | 65    | Method B                   |
| $\Lambda$ -7         | 99.9   |       | Method B <sup>a</sup>      |
| $\Lambda$ -8         | 9.4    | n.r.  | Method A                   |
| $\Delta$ -8          | 4.5    | n.r.  | Method B                   |

Note: n.a. = not applicable; n.r. = not resolved. <sup>a</sup>Prepared as described in Torres, A. S.; Maloney, D. J.; Tate, D.; MacDonnell, F. M. *Inorg. Chim. Acta.* **1999**, 293, 37-43.

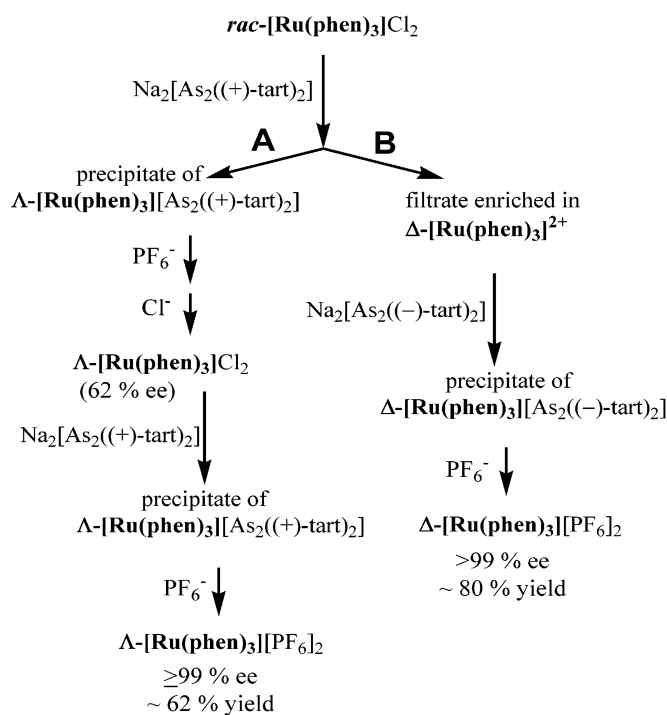


Figure 4.9 Resolution procedures for  $\Delta$ - and  $\Lambda$ -[Ru(phen)<sub>3</sub>]<sup>2+</sup>

#### 4.4 Conclusion

The stability and interesting photonic properties of ruthenium trisdiimine complexes have led to an extensive body of work on the preparation of monomeric, oligomeric, and polymeric molecules containing this structural unit. The chirality of the trisdiimine complex inevitably leads to situations in which the absolute stereochemistry needs to be controlled and the optical purity assessed. The chiral HPLC method developed in this work shows that this class of complexes can be reliably separated and examined for optical purity. The factors that affect the separation efficiency have been parametrized such that the stereochemical makeup of most monomeric and many dimeric complexes can be quantitatively examined. We used this tool to reexamine and improve on the most-common resolution procedures and can now report on their efficiency with high accuracy.

## CHAPTER 5

### ENANTIOSELECTIVE HOST-GUEST COMPLEXATION OF RU(II) TRISDIIMINE COMPLEXES USING NEUTRAL AND ANIONIC DERIVATIZED CYCLODEXTRINS

Enantioselective host-guest complexation between five racemic Ru(II) trisdiimine complexes and eight derivatized cyclodextrins (CDs) has been examined by NMR techniques. The appearance of non-equivalent complexation-induced shifts of between the  $\Delta$  and  $\Lambda$ -enantiomers of the Ru(II) trisdiimine complexes and derivatized CDs is readily observed by NMR. In particular, sulfobutyl ether- $\beta$ -cyclodextrin sodium salt (SBE- $\beta$ -CD), R-naphtylethyl carbamate  $\beta$ -cyclodextrin (RN- $\beta$ -CD), and S-naphtylethyl carbamate  $\beta$ -cyclodextrin (SN- $\beta$ -CD) showed good enantiodiscrimination for all five Ru complexes examined, which indicates that aromatic and anionic derivatizing groups are beneficial for chiral recognition. The complexation stoichiometry between SBE- $\beta$ -CD and  $[\text{Ru}(\text{phen})_3]^{2+}$  was found to be 1: 1 and binding constants reveal that  $\Lambda$ - $[\text{Ru}(\text{phen})_3]^{2+}$  binds more strongly to SBE- $\beta$ -CD than the  $\Delta$ -enantiomer. Correlations between this NMR method and separative techniques based on CDs as chiral discriminating agents (i.e., selectors) are discussed in detail.

#### 5.1 Introduction

Octahedral, tris-chelate metal complexes, such as ruthenium(II) tris(diimine) complexes, have often been used as probes of DNA and other biological structures.<sup>65, 87, 90, 105, 143, 144</sup> These complexes are chiral and two enantiomers are  $\Delta$  and  $\Lambda$ . Ruthenium (II) trisdiimine complexes are substitutionally inert and generally easy to resolve into enantiomers which are robust and not easily racemized even under harsh conditions.<sup>117, 145, 146</sup> These Ru(II) trisdiimine complexes can be prepared in heteroleptic form<sup>147</sup> and can be modified by a variety of ligand transformations without disturbing the stereochemistry about the metal center.<sup>63, 64, 94, 97</sup> Several groups, including ourselves, have used these complexes as chiral synthons or building blocks

for a variety of supramolecular assemblies<sup>94, 97, 98, 111, 148</sup> or as chiral probes in biological systems.<sup>65, 87, 90, 105, 143, 144</sup>

In these situations, it is often necessary to work with enantiopure complexes and thus the determination of optical purity becomes an important issue. Circular dichroism and optical rotary dispersion are two commonly used methods, however, these data do not give the absolute optical purity of the product. Absolute measures of enantiopurity require separation based-techniques such as chiral HPLC, capillary electrophoresis (CE), and other column-based separation methods<sup>100, 107, 148</sup> or spectroscopic methods such as NMR in the presence of chiral-shift reagents.<sup>88, 117</sup> All of these techniques rely, to a significant extent, on the formation of diastereomeric, non-covalent complexes (e.g. host-guest complexes) between the metal-trisdiimine coordination complex and the chiral-selector (in chromatography or electrophoresis) or chiral-shift reagent (in NMR).

Cyclodextrins are well-known host molecules with large ring-like structures composed of  $\alpha$ -(1,4)-linked D-(+)-gluco-pyranose units with  $\alpha$ -,  $\beta$ -, and  $\gamma$ -cyclodextrins being the most commonly used, containing six, seven, and eight gluco-pyranose units, respectively. They are chiral and non-racemic and are known to exhibit different complexation with chiral guests.<sup>29, 149</sup> Derivatization of the CD's with methyl-, acetyl-, ionic- and aromatic functional groups has been shown to improve both binding and chiral recognition ability in many cases.<sup>74, 113, 115, 150-165</sup> We have reported on the success of cyclodextrin-based HPLC columns and cyclodextrin-based chiral selectors in CE for efficient separation of ruthenium(II) trisdiimine complexes,<sup>74, 150</sup> presumably via differential host-guest complexation. Owens et. al. have shown that the detection of diastereomeric host-guest complexes using CD's as the hosts by NMR can be a screening method for the selection of chiral selectors and separation conditions in CE and LC.<sup>156</sup> Other comparative CE and NMR studies of the chiral recognition of racemic guests with cyclodextrin hosts are also known.<sup>115, 157, 160</sup>

In this work, we report on the host-guest complexation of a number of homoleptic and heteroleptic ruthenium(II) trisdiimine complexes with three particular types of CDs, which are found to have the best resolving efficiencies in LC and CE studies.<sup>74, 150</sup> These are the anionic sulfated, anionic sulfoalkylated, and neutral aromatic modified CDs. The formation and detection of diastereomeric host-guest complexes between  $M(\text{phen})_3^{n+}$  complexes ( $M=\text{Ru(II)}$ ,  $\text{Rh(III)}$ ,  $\text{Fe(II)}$ ,  $\text{Co(II)}$ , and  $\text{Zn(II)}$ ) and native  $\alpha$ -,  $\beta$ -,  $\gamma$ -cyclodextrins (CDs) as well as carboxymethyl derivatized CD's has been previously reported using NMR techniques.<sup>115</sup> To our knowledge, however, the interactions between Ru(II) trisdiimine complexes and these three classes of cyclodextrins (anionic sulfated, anionic sulfoalkylated, and neutral aromatic derivitized) have never been studied using NMR. The aim of this work is to examine these CD's for their enantioselectivity upon complexation with racemic ruthenium trisdiimine complexes using  $^1\text{H}$  NMR spectroscopy. Binding constants and stoichiometry are determined in one case and correlations between the NMR findings and LC and CE data are presented.

## 5.2 Experimental Section

### *5.2.1 Chemicals*

Sulfated- $\alpha$ -cyclodextrin sodium salt (S- $\alpha$ -CD, the average degree of substitution, DS=5), sulfated- $\beta$ -cyclodextrin sodium salt (S- $\beta$ -CD, DS=5), carboxymethyl- $\beta$ -cyclodextrin sodium salt (CM- $\beta$ -CD, DS=3) were obtained from Aldrich. Trappsol<sup>®</sup> sulfated- $\gamma$ -cyclodextrin sodium salt (S- $\gamma$ -CD, DS=13) was purchased from CTD, Inc. Sulfobutyl ether- $\beta$ -cyclodextrin sodium salt (SBE- $\beta$ -CD, DS=5.5) was from CyDex, Inc. 3,5-Dimethylphenyl  $\beta$ -cyclodextrin (DMP- $\beta$ -CD, DS=3), R-naphtylethyl carbamate  $\beta$ -cyclodextrin (RN- $\beta$ -CD, DS=2), and S-naphtylethyl carbamate  $\beta$ -cyclodextrin (SN- $\beta$ -CD, DS=2) were from Astec (Whippany, NJ). All derivitized groups are randomly positioned. The structures of cyclodextrins are shown in Figure 5.1. Deuterium oxide ( $\text{D}_2\text{O}$ ) was purchased from Aldrich.

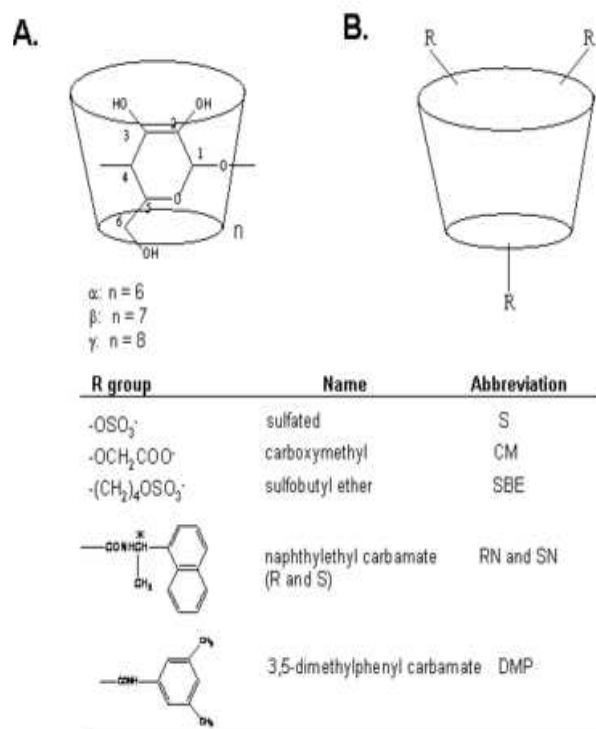


Figure 5.1 Schematic structures of native and derivatized cyclodextrins. (A) native cyclodextrin; (B) derivatized cyclodextrin; (C) structure and abbreviation for derivative group.

Racemates of the following complexes:  $[\text{Ru}(\text{phen})_3]\text{Cl}_2$  (**1**) (phen=1,10-phenanthroline),  $[\text{Ru}(\text{bpy})_3]\text{Cl}_2$  (**2**) (bpy=2,2'-bipyridine),  $[\text{Ru}(\text{phen})_2\text{nitrophen}]\text{Cl}_2$  (**3**) (nitrophen=5-nitro-1,10-phenanthroline),  $[\text{Ru}(\text{phen})_2\text{aminophen}]\text{Cl}_2$  (**4**) (aminophen=5-amino-1,10-phenanthroline),  $[\text{Ru}(\text{phen})_2\text{phendiamine}]\text{Cl}_2$  (**5**) (phendiamine=5,6-diamino-1,10-phenanthroline) were prepared as described in the literature.<sup>74, 118-122, 124</sup> The chemical structures of complexes **1** and **2** are shown in Figure 5.2.

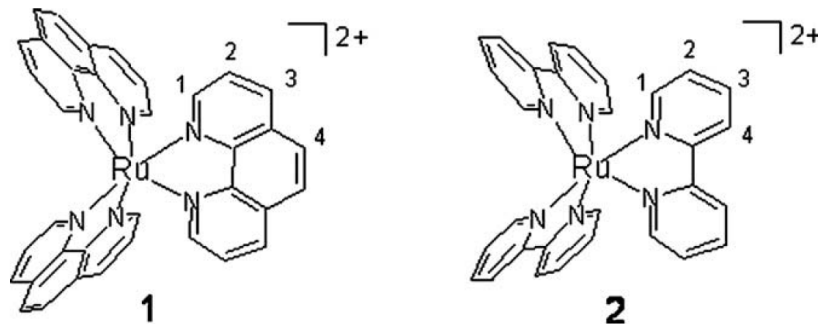


Figure 5.2 Chemical structures of [Ru(phen)<sub>3</sub>]Cl<sub>2</sub> (**1**) and [Ru(bpy)<sub>3</sub>]Cl<sub>2</sub> (**2**). Note: The numbers denote the positions of chemically distinct protons and are used to assign peaks in the proton NMR spectra.

### 5.2.2 NMR measurements

<sup>1</sup>H NMR spectra (500 MHz) were recorded on a JEOL JNM-A500 NMR spectrometer at 25 °C. All spectra were referenced to the internal HOD signal at 4.65 parts per million (ppm). Unless specified, spectra were recorded with 1mM guest (Ru complex) and 4 mM host (cyclodextrin) in D<sub>2</sub>O. The Ru complex and CD were dissolved separately in D<sub>2</sub>O and then mixed. The precipitate was observed when Ru complex mixed with sulfated-CDs and the supernatant was taken for NMR analysis (See Discussion).

Stoichiometry of [Ru(phen)<sub>3</sub>]Cl<sub>2</sub> and SBE-β-CD was determined by Job's method.<sup>157, 160, 161</sup> The molar fraction of guest was varied in the range of 0.15-0.80 while maintaining a total concentration of 5 mM. Apparent binding constants of Δ- and Λ-[Ru(phen)<sub>3</sub>]Cl<sub>2</sub> with SBE-β-CD were calculated according to Scott's method.<sup>157, 160, 161</sup> The concentration of CD was increased from 2 mM to 10 mM while the guest concentration remained unchanged (1 mM). The Scott equation expresses the relationship between the apparent binding constant (*K<sub>a</sub>*), the complexation-induced shift (CIS) at saturation ( $\Delta\delta_s$ ), the host concentrations, and observed CIS ( $\Delta\delta_{obs}$ ):

$$\frac{[selector]}{\Delta\delta_{obs}} = \frac{[selector]}{\Delta\delta_s} + \frac{1}{K_a\Delta\delta_s} \quad (1)$$

[selector] is the host concentration. In this work, the selector is the cyclodextrin host and the [selector] and  $\Delta\delta_{\text{obs}}$  are directly obtained from the experiments.  $K_a$  and  $\Delta\delta_s$  could be determined by Scott plot [selector]/  $\Delta\delta_{\text{obs}}$  against [selector]. The slope equals  $1/\Delta\delta_s$  and the intercept with y axis is  $1/K_a\Delta\delta_s$ .

### 5.3 Results

#### *5.3.1 Chiral discrimination of $[\text{Ru}(\text{phen})_3]^{2+}$ by different derivatized cyclodextrins*

In order to study the effect of derivatized cyclodextrins on the chiral recognition of Ru(II) complexes, eight derivatized (neutral and negatively charged) CDs (see Figure 5.1) were tested as chiral selectors by  $^1\text{H}$  NMR spectroscopy. Aromatic derivatized CDs exhibited exceptional enantioselectivity for ruthenium(II) tris(diimine) complexes when used as HPLC stationary phases.<sup>74</sup> The aromatic groups extend the cavity of cyclodextrin host and provide  $\pi$ - $\pi$  interaction sites. Sulfated- and sulfobutyl ether-cyclodextrins are commonly used in capillary electrophoresis (CE) and the enantiomers of several ruthenium(II) tris(diimine) complexes have been separated using them as chiral selectors.<sup>150</sup> Therefore, these particular derivatized cyclodextrins are promising candidates as chiral shift reagents for Ru complexes. In addition, the anionic derivative cyclodextrin, carboxymethyl- $\beta$ -cyclodextrin (CM- $\beta$ -CD), was also evaluated for comparison purposes.

The  $^1\text{H}$  NMR spectral changes of  $[\text{Ru}(\text{phen})_3]\text{Cl}_2$  in  $\text{D}_2\text{O}$  upon adding various cyclodextrins are shown in Figure 5.3. Generally, increasing the concentration of the host reagent promotes the formation of diastereomeric complexes and enhances the enantiomeric discrimination visible in the NMR spectra. Due to water solubility and limited availability of some derivatized cyclodextrins, the concentrations of CDs are set four times as high as the concentration of the guest (1mM) (see Experimental). In Figure 5.3, proton signal splittings are clearly observed using five cyclodextrins (S- $\beta$ -CD, S- $\gamma$ -CD, SBE- $\beta$ -CD, RN- $\beta$ -CD, and SN- $\beta$ -CD). Previous studies state that the reversible exchange between the complexed and the free solute is fast on the NMR time scale and NMR proton signals are averaged between free and

complexed solutes [34, 40, 51]. This proves that differences in complexation-induced shifts (CIS) in NMR spectra result from the enantiomeric composition of the solute. Therefore signal splittings of the guest demonstrate the chiral recognition capability of the host.

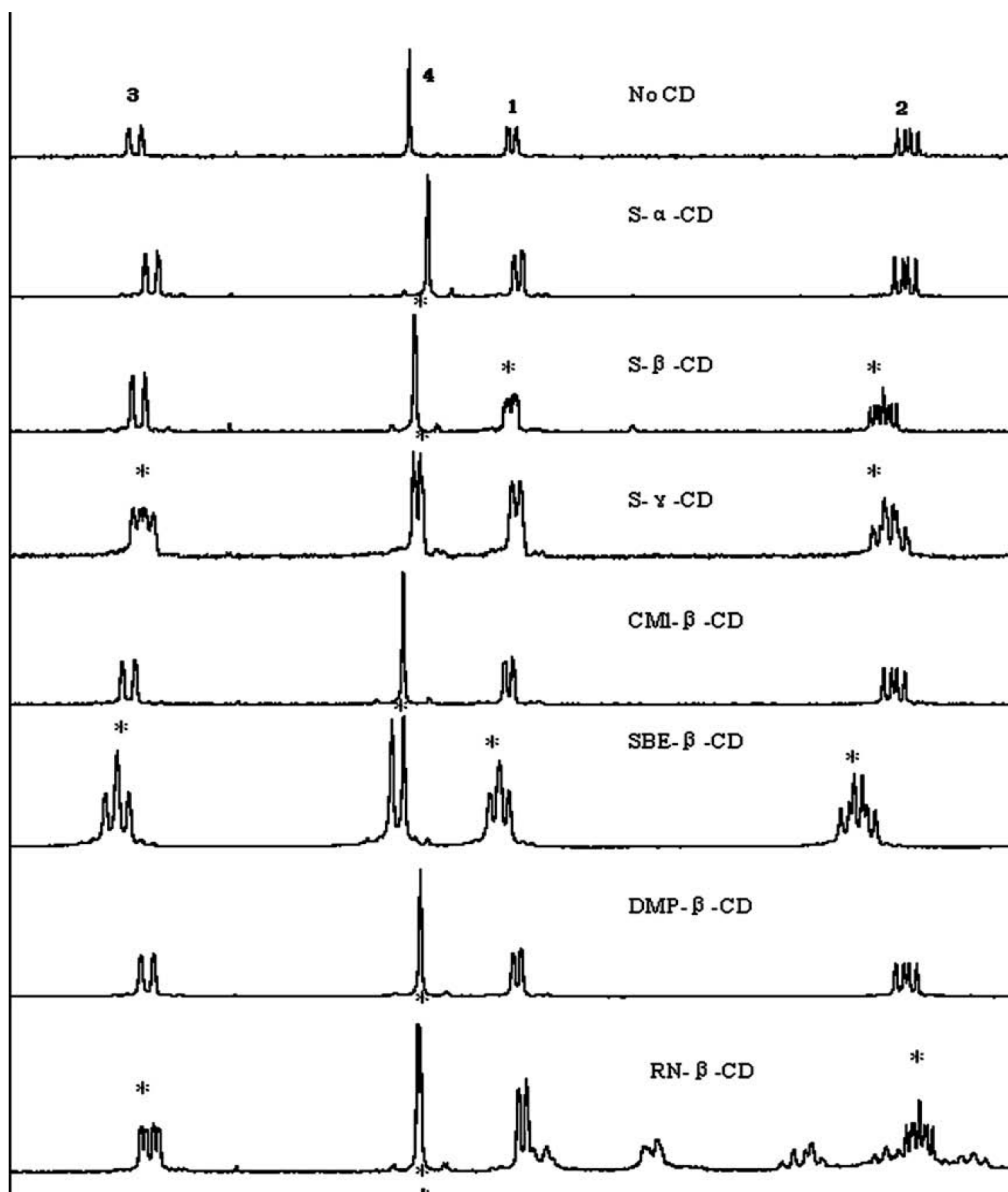


Figure 5.3.  $^1\text{H}$  NMR spectra of racemic  $[\text{Ru}(\text{phen})_3]\text{Cl}_2$  (2 mM) without and with various cyclodextrins (8 mM) in  $\text{D}_2\text{O}$ . Numbering on top spectrum indicates proton assignment as indicated in Figure 3. \* stands for non-equivalent complexation-induced shift (CIS).

Figure 5.3 shows that five CDs cause clear non-equivalent CISs and provide chiral discrimination. In the case of SBE- $\beta$ -CD, all four protons of  $[\text{Ru}(\text{phen})_3]^{2+}$  provide split signals, while signals for three of the protons are separated into a pair of peaks for the other four derivatized cyclodextrins. Many NMR studies of chiral selectors have shown that protons closer to the binding site show greater enantiomeric differences in their CISs.<sup>159, 163</sup> It should be noted that the singlet signal (H4) of  $[\text{Ru}(\text{phen})_3]^{2+}$  was split by five different derivatized cyclodextrins, and it is the only proton signal that splits in all cases. H4 is positioned furthest away from the metal core and is likely to be in close proximity to the cyclodextrin host when the complex is formed.

The magnitude of CISs of  $[\text{Ru}(\text{phen})_3]^{2+}$  should also be considered. Sulfated  $\alpha$ -CD causes higher magnetic-field shifts in most of the signals of  $[\text{Ru}(\text{phen})_3]\text{Cl}_2$ , but no differences in the CIS were observed. Compared to sulfated  $\beta$ -CD and  $\gamma$ -CD, the CISs for H1, H3 and H4 by sulfated  $\alpha$ -CD are greater. This result indicates that stronger complexation-induced shift does not necessarily produce enantioselectivity. Small upfield shifts are observed for the proton signals of  $[\text{Ru}(\text{phen})_3]^{2+}$  upon addition of RN- or SN- $\beta$ -CD. This is probably due to  $\pi$ - $\pi$  interactions.

### 5.3.2 Screening of CDs toward various Ru complexes

In order to study the capability of CDs to induce enantioselective proton NMR shifts, it is necessary to gather further examples by testing more Ru(II) complexes. Similar studies were carried out for  $[\text{Ru}(\text{bpy})_3]^{2+}$ ,  $[\text{Ru}(\text{phen})_2\text{nitrophen}]^{2+}$ ,  $[\text{Ru}(\text{phen})_2\text{aminophen}]^{2+}$ , and  $[\text{Ru}(\text{phen})_2\text{phen diamine}]^{2+}$ . For each guest, eight cyclodextrins were tested as host complexes. The concentrations of the Ru complexes and the CDs were fixed at 1 mM and 4 mM, respectively. The non-equivalent CISs of five Ru complexes are summarized in Table 1, which provides comparative data for the enantiomeric discrimination in the NMR spectra.

The five Ru(II) complexes are similar in structure and all contain three bidentate diimine ligands (bpy or phen).  $[\text{Ru}(\text{phen})_3]^{2+}$  and  $[\text{Ru}(\text{bpy})_3]^{2+}$  have the highest symmetry ( $D_3$  point group)

and therefore the simplest NMR spectra. The chemical shifts in these spectra are readily assigned and differences in the CISs caused by enantiomers are conveniently determined (data shown in Table 5.2). However, the other complexes have lower symmetry ( $C_1$  for **3** and **4**;  $C_2$  for **5**) and considerably more complex NMR spectra which make reliable quantitative analysis difficult at best, therefore only qualitative results are shown in Table 5.1.

Table 5.1 Complexation-induced chemical shifts (CIS) of Ru(II) polypyridyl complexes with various cyclodextrins

|  | S- $\alpha$ -<br>CD | S- $\beta$ -<br>CD | S- $\gamma$ -<br>CD | CM-<br>$\beta$ -CD | SBE-<br>$\beta$ -CD | DMP-<br>$\beta$ -CD | RN- $\beta$ -<br>CD | SN- $\beta$ -<br>CD |
|--|---------------------|--------------------|---------------------|--------------------|---------------------|---------------------|---------------------|---------------------|
| [Ru(phen) <sub>3</sub> ]Cl <sub>2</sub> <sup>1</sup> | - <sup>2</sup>      | + <sup>3</sup>     | +                   | -                  | +                   | -                   | +                   | +                   |
| [Ru(bpy) <sub>3</sub> ]Cl <sub>2</sub>               | -                   | -                  | +                   | -                  | +                   | -                   | +                   | +                   |
| [Ru(phen) <sub>2</sub> nitrophen]Cl <sub>2</sub>     | ppt <sup>4</sup>    | +                  | ppt                 | -                  | +                   | -                   | +                   | +                   |
| [Ru(phen) <sub>2</sub> aminophen]Cl <sub>2</sub>     | ppt                 | ppt                | ppt                 | -                  | +                   | -                   | +                   | +                   |
| [Ru(phen) <sub>2</sub> phendiamine]Cl <sub>2</sub>   | ppt                 | ppt                | ppt                 | -                  | +                   | -                   | +                   | +                   |

Note: (1) All Ru(II) complexes used are racemates. (2) “-” represents that non-equivalent CIS was not observed. (3) “+” represents that non-equivalent CIS was observed. (4) “ppt” indicates a precipitate formed (see Discussion).

SBE- $\beta$ -CD, RN- $\beta$ -CD, and SN- $\beta$ -CD are the most powerful chiral selectors and show enantioselective CISs for all five ruthenium complexes. The use of sulfated cyclodextrins (S-CDs) results in the formation of a precipitate. In approximately half of the cases (S-CDs), the amount of the precipitate is so large that good NMR spectra are unavailable. In cases where enough amount of Ru complex remained in solution, non-equivalent CIS are observed in three of the Ru(II) complexes and this is only with the larger  $\beta$  and  $\gamma$ -CDs (see Table 5.1). HPLC analysis of the supernatants using Cyclobond RN column<sup>74</sup> shows that the supernatant is still racemic composition and the precipitation by sulfated-CDs is not enantioselective. The other two cyclodextrins, CM- $\beta$ -CD and DMP- $\beta$ -CD, did not show chiral discrimination toward any of the Ru complexes. Overall, these results clearly indicate that anionic and aromatic neutral

cyclodextrins can discriminate between enantiomers of Ru(II) trisdiimine complexes and that the nature of the CD derivative is of crucial importance.

Table 5.2 Differences in CISs (complexation-induced shifts) due to enantiomeric composition of Ru(II) complexes

| Ru complex                              | H position (ppm)* | Difference in CISs (Hz) |         |           |          |          |
|---|-------------------|-------------------------|---------|-----------|----------|----------|
|   |                   | S-β-CD                  | S-γ- CD | SBE-β- CD | RN-β- CD | SN-β- CD |
| [Ru(phen) <sub>3</sub> ]Cl <sub>2</sub> | 1 (7.9518)        | 2.3                     |         | 6.0       |          | 5.7      |
|   | 2 (7.4438)        | 3.2                     | 2.3     | 8.2       | 3.2      |          |
|   | 3 (8.4355)        |                         | 4.6     | 7.6       | 3.2      | 4.1      |
|   | 4 (8.0837)        | 0.9                     | 4.6     | 7.8       | 1.8      | 3.2      |
| [Ru(bpy) <sub>3</sub> ]Cl <sub>2</sub>  | 1 (8.3847)        |                         |         |           | 2.8      |          |
|   | 2 (7.8964)        |                         |         | 4.1       |          |          |
|   | 3 (7.2171)        |                         | 3.2     | 5.7       |          | 2.3      |
|   | 4 (7.6820)        |                         |         |           |          |          |

Note: Blank represents that CISs of enantiomers are the same. \*: All the chemical shifts of protons of Ru(II) complexes are obtained in free solution without CDs.

As seen in Table 5.2, differences in the magnitude of the CISs are observed for guests **1** and **2**, which, in part, reflect the chiral recognition capability of the hosts. SBE-β-CD shows the largest differences in CISs of any CD tested. We attribute this to the electrostatic effects between the cationic Ru(II) complexes and the anionic CD. Electrostatic effects are well known to play important roles in the enantioselective complexation of host-guest pairs.<sup>115, 156, 159</sup> The larger difference in CISs observed for the SBE- derivatives over the S-derivatives suggests the ability of the charged substituents in a sulfobutylether group to wrap around the host gives a better discrimination between the guest enantiomers. As stated earlier the carboxymethyl derivatives do not show any non-equivalent CIS for any Ru(II) complex examined, revealing that charge alone is not always enough to ensure enantiodiscrimination.

In fact, electrostatics is not an absolute requirement for chiral discrimination. Kano et al.<sup>115</sup> reported that chiral recognition of [Ru(phen)<sub>3</sub>]<sup>2+</sup> was observed by neutral 2,3,6-tri-O-methyl-α-CD, but not 2,3,6-tri-O-methyl-β-CD in <sup>1</sup>H NMR measurements. They explained this by a smaller cavity size of TMe-α-CD. In our work, proton signals of [Ru(phen)<sub>3</sub>]<sup>2+</sup> show distinct splittings in the presence of RN- or SN-β-CD. This is the first time that a significant difference in complexation-induced shifts (CISs) using neutral aromatic CDs has been observed. Here,

weaker intermolecular interactions (such as  $\pi$ - $\pi$  interaction) combine to contribute significantly to chiral discrimination. Interestingly, the differences in CISs for SN- $\beta$ -CD are always larger than those for RN- $\beta$ -CD. These two CDs are diastereomeric with both having cyclodextrins of the same chirality and appended naphthylethyl groups with either R or S absolute stereochemistry. Larger differences in CISs for SN- $\beta$ -CD show a higher enantiomeric discrimination for the [SN- $\beta$ -CD/Ru(II)trisdiimine] host-guest complex over that with the RN derivative and imply a better steric fit in the host-guest complex. Overall, the anionic SBE- $\beta$ -CD is a more effective chiral selector for cationic Ru guests than neutral CDs but the secondary steric effects apparent in the SN- and RN- $\beta$ -CDs may be useful in the design of improved chiral selectors. For example, sulfonation of the naphthyl or ethyl groups on a SN- $\beta$ -CD would be a logical step towards higher enantioselectivity.

It is important to note that four CDs exhibit chiral recognition toward  $[\text{Ru}(\text{bpy})_3]^{2+}$ , while five CDs cause clear non-equivalent CISs for  $[\text{Ru}(\text{phen})_3]^{2+}$ . Furthermore, differences in CISs of  $[\text{Ru}(\text{bpy})_3]^{2+}$  are normally smaller than the values for  $[\text{Ru}(\text{phen})_3]^{2+}$  (data shown in Table 5.2). This indicates that CDs provide a greater ability to differentiate enantiomers of  $[\text{Ru}(\text{phen})_3]^{2+}$  than those of  $[\text{Ru}(\text{bpy})_3]^{2+}$ .

### 5.3.3 Stoichiometry and binding constant

In host-guest chemistry, NMR works as an excellent spectroscopic tool to provide information involving the complexation stoichiometry and the strength of complexation.<sup>157, 160, 161</sup> In this work, the host-guest stoichiometry was investigated by the method of continuous variations (Job's plot). The complexation between SBE- $\beta$ -CD and  $[\text{Ru}(\text{phen})_3]^{2+}$  was studied because the largest differences of CISs were observed in this case (shown in Table 5.2). Pure  $\Delta$ - and  $\Lambda$ - $[\text{Ru}(\text{phen})_3]^{2+}$  were used as guests in separate studies to evaluate stoichiometry. The mole fraction of the guest was varied in the range of 0.10-0.80 with the total concentration of SBE- $\beta$ -CD and  $[\text{Ru}(\text{phen})_3]^{2+}$  fixed at 5 mM. The Job's plot is shown in Figure 5.4. The curves of

different protons show a maximum corresponding to a molar fraction of 0.5 and the data fit a 1:1 host-guest complex.

The binding constants ( $K_a$ ) were determined from NMR titration experiments (Scott's method). It should be noted that the derivatized cyclodextrins used in our work are somewhat heterogeneous mixtures of closely related components with different substitution degrees and different positions (i.e., homologues and isomers).<sup>155</sup> Therefore, the calculated binding constant ( $K_a$ ) is not an absolutely accurate thermodynamic value, but rather a weighted average for the host mixture. Nevertheless, these apparent values provide useful information when comparing one relative to the other. The Scott plots of H2 of  $\Delta$ - and  $\Lambda$ -[Ru(phen)<sub>3</sub>]<sup>2+</sup> with added SBE- $\beta$ -CD are shown in Figure 5.5. Good linearity is obtained and the correlation coefficients ( $r^2$ ) are greater than 0.97. From Scott curves,  $K_a$  and  $\Delta\delta_s$  can be determined (see Experimental).  $K_a$  and  $\Delta\delta_s$  of  $\Delta$ - and  $\Lambda$ -[Ru(phen)<sub>3</sub>]<sup>2+</sup> are  $318\text{M}^{-1}$ , 58.5Hz, and  $416\text{M}^{-1}$ , 66.2Hz, respectively. CE experiments showed that  $\Lambda$ -[Ru(phen)<sub>3</sub>]<sup>2+</sup> migrated after  $\Delta$ -[Ru(phen)<sub>3</sub>]<sup>2+</sup> when using SBE- $\beta$ -CD as the chiral selector and stronger association interaction was observed in  $\Lambda$ -[Ru(phen)<sub>3</sub>]<sup>2+</sup>-CD

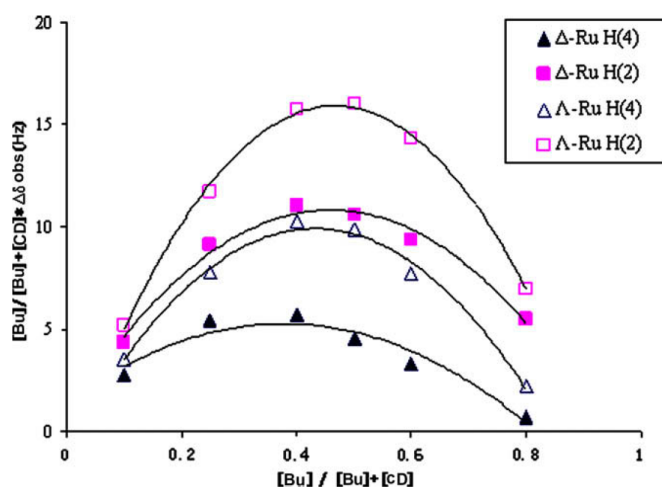


Figure 5.4 Job plots of  $\Delta$ -[Ru(phen)<sub>3</sub>]<sup>2+</sup> and  $\Lambda$ -[Ru(phen)<sub>3</sub>]<sup>2+</sup> in solution with SBE- $\beta$ -CD.  $\Delta\delta_{\text{obs}}$  is the difference of the guest chemical shifts between the free form (without CD) and the complexation form (with CD).

pair.<sup>150</sup> This is consistent with our binding constant results. The ratio of binding constants ( $\alpha$ ) of two enantiomers is a measure of enantioselectivity. For  $[\text{Ru}(\text{phen})_3]^{2+}$  enantiomers, SBE- $\beta$ -CD produced an  $\alpha=1.32$ . Proton signal splitting in NMR spectra is due to different binding of  $[\text{Ru}(\text{phen})_3]^{2+}$  enantiomers with SBE- $\beta$ -CD.

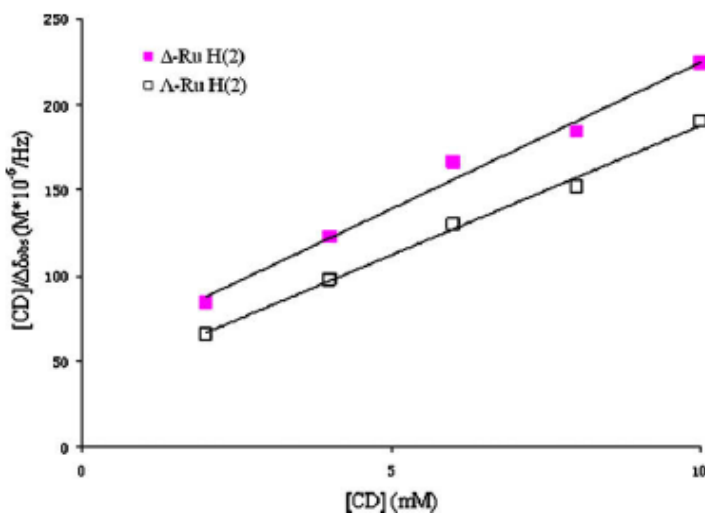


Figure 5.5 Scott plots of  $\Delta$ - $[\text{Ru}(\text{phen})_3]\text{Cl}_2$  and  $\Lambda$ - $[\text{Ru}(\text{phen})_3]\text{Cl}_2$  in solution with SBE- $\beta$ -CD. Note:  $\Delta\delta_{\text{obs}}$  is the difference of the guest chemical shifts between the free form (without CD) and the complexation form (with CD).

#### 5.3.4 Correlation of NMR with CE and LC

In a CE separation process, the guest-host association takes place in a free solution condition, which is similar to the environment of NMR experiments. Therefore, reliable correlations between these two techniques are expected. Our group reported enantioseparations of Ru(II) tris(diimine) using CE and micellar capillary electrophoresis (MCE) methods.<sup>150</sup> The separation data of four complexes ( $[\text{Ru}(\text{phen})_3]^{2+}$ ,  $[\text{Ru}(\text{bpy})_3]^{2+}$ ,  $[\text{Ru}(\text{phen})_2\text{nitrophen}]^{2+}$ ,  $[\text{Ru}(\text{phen})_2\text{aminophen}]^{2+}$ ) are compared since  $[\text{Ru}(\text{phen})_2\text{phenyldiamine}]^{2+}$  was not tested in the CE analysis.<sup>150</sup> In CE experiments, sulfated- $\gamma$ -CD and SBE- $\beta$ -CD are powerful chiral selectors and selectivity was observed for all four

complexes, while sulfated- $\alpha$ -CD does not separate enantiomers of any Ru complex. These results correlate well with the NMR data (Table 5.1). Using capillary zone electrophoresis (CZE), sulfated- $\beta$ -CD and CM- $\beta$ -CD separated  $[\text{Ru}(\text{bpy})_3]^{2+}$  and  $[\text{Ru}(\text{phen})_2\text{nitrophen}]^{2+}$  enantiomers, respectively, even though nonequivalent CISs are not observed in the  $^1\text{H}$  NMR spectra. This discrepancy may be explained by the differences in solution composition between the two techniques or that the CE technique is simply more sensitive to the weak complexation involved in these cases.

We had previously shown that enantiomers of several Ru(II)trisdiimine complexes could be separated by HPLC using a Cyclobond RN column as the chiral stationary phase (CSP).<sup>74</sup> Here the RN- $\beta$ -CD is covalently linked to silica gel via a linker function. Enantioselectivity was also observed using Cyclobond SN CSP although oddly enough the resolution ( $R_s = 0.7$ ) was less than that for the Cyclobond RN column ( $R_s = 2.4$ ) when separating  $\square\Delta$ - and  $\Lambda$ - $[\text{Ru}(\text{phen})_3]^{2+}$ . Also the retention of the Ru complex was greater on the SN column. This indicates that it is not the overall strength of binding that is the most important for enantioselectivity, but rather it is the difference in binding of the enantiomers that is crucial. Overall, these results show good agreement with the NMR non-equivalent CISs data (Table 5.1). Table 5.1 indicates that RN- $\beta$ -CD and SN- $\beta$ -CD show chiral discrimination to all five Ru complexes. These results prove that good correlations exist between NMR and separative methods, such as CE and LC. However, the data also reveal that the greater the CIS in the host-guest complex as determined by NMR does not always translate to better resolving ability when applied to chromatographic techniques. Nonetheless, NMR can clearly be used as a quick screening method for the enantiodiscrimination ability of cyclodextrin-based chiral selectors and can cautiously be applied towards the selection of appropriate chiral selectors in CE and LC runs.

#### 5.4 Conclusions

A number of derivatized CDs have been screened as chiral selectors for the widely-studied Ru(II) trisdiimine class of compounds by  $^1\text{H}$  NMR spectroscopy. In particular, SBE- $\beta$ -CD, RN- $\beta$ -CD, and SN- $\beta$ -CD show chiral discrimination toward all five Ru complexes, which indicate that aromatic and anionic derivatizing groups are beneficial for chiral recognition. These findings are consistent with expectations for binding the lipophilic, aromatic, divalent Ru(II)trisdiimine cations. Highly symmetric Ru(II) complexes show the most easily interpreted complexation in solution with non-equivalent complexation-induced shifts observed for the  $\Delta$  and  $\Lambda$  enantiomers in the proton NMR. Binding studies revealed a 1:1 host-guest complex stoichiometry for SBE- $\beta$ -CD and  $[\text{Ru}(\text{phen})_3]^{2+}$  and tighter binding for the  $\Lambda$ - $[\text{Ru}(\text{phen})_3]^{2+}$  enantiomer. Comparisons of the magnitude of the CIS in the NMR data obtained for CDs with Ru(II)trisdiimine complexes with those obtained by separative methods (resolution by LC and CE using CDs) show some correlation excepting that increased binding between the CD and the Ru complex (as inferred by the magnitude of the CIS) is not always beneficial for the most efficient separative methodology.

## CHAPTER 6

### DEVELOPMENT OF NEW LC CHIRAL STATIONARY PHASES BASED ON RUTHENIUM TRIS(DIIMINE) COMPLEXES

Enantiopure ruthenium(II) *tris*(diimine) complexes have been covalently bonded to silica and evaluated as chiral stationary phases for LC. Three binding chemistries were tested and the CSP synthesized by reductive amination of the aldehyde-functionalized silica provided the largest enantioselectivity. The Ru complex-bonded CSP showed selectivity toward a variety of racemic compounds. Circular dichroism (CD) detection was used to confirm the enantiomeric separations. This CSP worked especially well for the enantiomeric separation of binaphthyl type compounds in the normal phase mode and appeared to be selective for acidic compounds in the polar organic mode. Effects of mobile phase composition on the enantioseparations were also studied.

#### 6.1 Introduction

Enantiomeric separation has been an important topic for several decades. Among various chiral separation methods, LC with chiral stationary phases (CSPs) has been dominant due to its good reproducibility, wide selectivity, easy operation, and ability to do preparative and semipreparative separations.<sup>28, 29, 37, 57, 128, 166-168</sup> CSPs are produced by immobilizing pure enantiomers (chiral selectors) to solid support (silica) via chemical bonding or physical absorption. Although a large number of papers related to the development of CSPs have been published, only a few types of CSPs dominate the field of LC enantiomeric separations. However, researchers continue to investigate new types of chiral stationary phases, in hopes of finding a more universal stationary phase or a more specific stationary phase, which is especially powerful for selected groups of compounds.

One type of chiral selector that has not received much attention in LC is that of transition metal complexes.<sup>169-173</sup> The helical chirality of the enantiomers of ruthenium *tris*(diimine) complexes is shown schematically in Figure 6.1. The earliest study involving a metal-ligand complex as a stationary phase showed that the  $\Delta$ - and  $\Lambda$ -enantiomers of a metal chelate complex were absorbed on a clay support in stereoregular manners and similar behavior was observed between “enantiomers” of different types, such as  $\Delta$ -[Ni(phen)<sub>3</sub>]<sup>2+</sup> and  $\Lambda$ -[Ru(phen)<sub>3</sub>]<sup>2+</sup>.<sup>172</sup> Yamagishi<sup>171</sup> reported that a column of  $\Lambda$ -[Ru(phen)<sub>3</sub>]<sup>2+</sup> absorbed onto montmorillonite gave “optical resolution” of tris(chelated) and bis(chelated) metal complexes. Later, the same group extended the applicability of this column to chiral aromatic compounds, by showing separation of 2,3-diphenylpyrazine and binaphthyl enantiomers.<sup>170</sup> Also, they used spherically shaped synthetic hectorite instead of montmorillonite in order to improve the column efficiency.<sup>173</sup> However, all the reported columns were prepared by simply absorbing the metal complexes onto the clay and some mobile phases had to be avoided so as to prevent desorption of the chiral selectors from the clay.

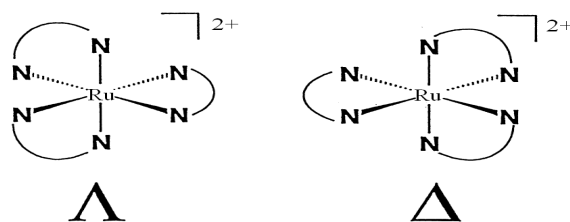


Figure 6.1 Mirror image relationship of Ru(II) *tris*(diimine)

To our knowledge, the CSPs based on Ru complexes which are covalently linked to the support have not been reported. In the present work, we have attached chiral, non-racemic Ru *tris*(diimine) complexes to high surface area silica gel in an attempt to improve the performance of this class of CSPs. Three different chemistries linking the Ru complex to 5- $\mu$ m spherical silica gel were studied in order to improve the chiral selector loading. The CSP prepared via an amination reaction between aldehyde-functionalized silica and the peripheral amino group of

Rutrisphenanthroline complex gave the best performance. The column was then evaluated as a chiral stationary phase for HPLC by injecting 155 racemic analytes. Three operation modes (normal phase mode, polar organic mode, and reversed phase mode) were tested. Effects of mobile phase compositions on the separations were studied.

## 6.2 Experiment

### 6.2.1 Chemicals

Anhydrous N, N-dimethylformamide (DMF), anhydrous toluene, 3-(triethoxysilyl)propyl isocyanate, 1,6-diisocyanatohexane, sodium periodate, sodium cyanoborohydride, sodium monophosphate, phosphoric acid, ammonium nitrate, ammonium chloride, and most racemic analytes used in this study were purchased from Sigma-Aldrich (Milwaukee, WI, USA). Acetonitrile, 2-propanol, n-heptane, ethanol, and methanol of HPLC grade were obtained from EMD (Gibbstown, NJ). Tetramethylammonium nitrate (TMAN), ammonium trifluoroacetate, ammonium nitrate, ammonium chloride, and ammonium acetate were purchased from Sigma-Aldrich (St. Louis, MO). Water was obtained from Millipore (Billerica, MA). Kromasil silica (5 $\mu$ m spherical diameter, 100 Å and 200 Å pore size) was obtained from Supelco (Bellefonte, PA).

### 6.2.2 Synthesis of $[Ru(phen)_2aminophen](PF_6)_2$ and $[Ru(phen)_2phendiamine](PF_6)_2$

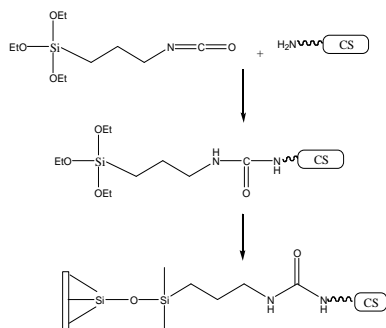
The compounds: 5-nitro-1,10-phenanthroline,<sup>118</sup>  $Ru(phen)_2Cl_2$ ,<sup>119, 120</sup>  $[Ru(phen)_2phendione]Cl_2$  (phendione = 1,10-phenanthroline-5,6-dione),<sup>122</sup> and  $[Ru(phen)_2nitrophen](PF_6)_2$  were prepared as previously reported.<sup>74</sup>

Racemates of  $[Ru(phen)_2nitrophen](PF_6)_2$  and  $[Ru(phen)_2phendione](PF_6)_2$  were converted to chloride salts by metatheses, and resolved as reported.<sup>74</sup>  $[Ru(phen)_2nitrophen]Cl_2$  was reduced to  $[Ru(phen)_2(aminophen)]Cl_2$  (aminophen=5-amino-1,10-phenanthroline), described in Ref.<sup>74</sup>.  $[Ru(phen)_2(phendiamine)]Cl_2$  (phendiamine=5,6-diamino-1,10-phenanthroline) was prepared according to Ref.<sup>174</sup>.

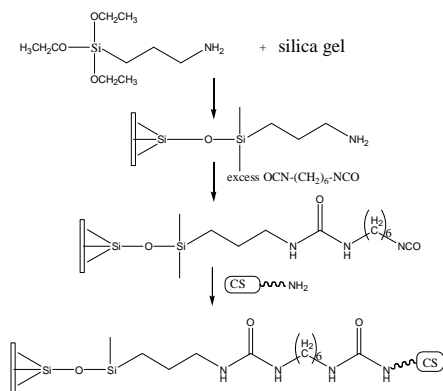
### 6.2.3 Preparation of Ru complex-bonded chiral stationary phases

Three different linkage strategies for chemically attaching Ru tris(diimine) complex to 5 $\mu$ m-diameter silica gel were conducted and the synthetic schemes of three binding methods are shown in Figure 6.2.

Binding method 1



Binding method 2



Binding method 3

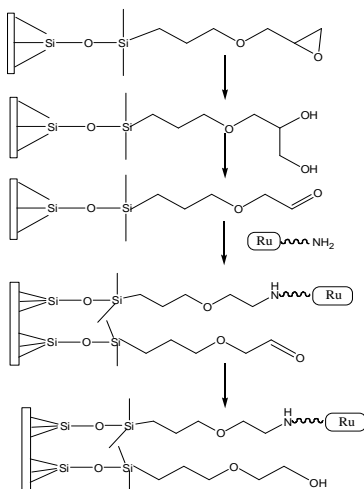


Figure 6.2 Schemes of three synthetic methods of Ru complex-based CSPs

The first binding method<sup>29, 57</sup> involved reacting Ru complex with excess 3-(triethoxysilyl)propyl isocyanate in anhydrous DMF at 90 °C for five hours. Then the product was added to dry silica gel and heated at 105 °C overnight. The mixture was cooled, filtered and washed as indicated previously. The second approach involved three steps and was analogous to those reported previously for antibiotic stationary phases.<sup>57</sup> 3-Aminopropyl-triethoxysilane was added to silica-toluene slurry dropwise after the silica was dewatered using Dean-Stack trap. The mixture was refluxed for 4h and then cooled, filtered, and washed with toluene, methanol, and acetone. 1,6-Diisocyanatohexane was added to dry amino-silica toluene slurry while kept in an ice bath. Then the slurry mixture was heated to 70°C for 4h. The excess reactant was removed by vacuum filtration and the solid product was washed with anhydrous toluene. Then the Ru-complex in pyridine was added and the mixture was heated to 70°C and allowed to react for overnight. Finally the product was filtered, washed and dried. In the third linkage chemistry, the diol-silica was prepared according the literature.<sup>175</sup> The diol groups were oxidized in 60 mM sodium periodate in water/methanol (4:1) at room temperature. Then the aldehyde-silica was filtered and dried. Ru complex was added to the resulting aldehyde-silica in anhydrous methanol and refluxed overnight. Finally, the remaining aldehyde moieties were reduced by sodium cyanoborohydride (NaCNBH<sub>3</sub>) in phosphate buffer (pH=3).<sup>176</sup> The elemental analysis results are shown in Table 1 (See 6.3.1 Results and Discussion session). Then the CSP was slurry packed into 25cmx0.46cm (i.d.) stainless steel column.

#### *6.2.4 Column evaluation*

The first chromatographic system was an HP (Agilent Technologies, Palo Alto, CA, USA) 1050 system, which consists of a UV VWD detector, an autosampler, a quaternary pump and Chemstation software. The second HPLC system was composed of a pump (Shimadzu, LC-6A) and a circular dichroism detector (Jasco, CD-2095 plus). For the LC analysis, the injection volume, the flow rate, and the detection wavelength are 5 µL, 1mL/min, and 254 nm, respectively. Separations were carried out at room temperature (~22 oC) if not specified. The

mobile phase was degassed by ultrasonication under vacuum for 5 min. The analytes were dissolved in ethanol, or the appropriate mobile phases. Each sample was analyzed in duplicate. In the normal phase mode, heptane/ethanol was used as the mobile phase. The mobile phase of the polar organic mode was composed of acetonitrile/methanol and a small amount of salt. Water/acetonitrile was used as the mobile phase in the reversed phase mode.

### 6.3 Results and Discussion

#### 6.3.1 Evaluation of binding chemistries

Normally, bonded chiral stationary phases are more stable and robust than coated ones, because the absorbed chiral selectors may be soluble in some solvents and can be removed by the mobile phases employed to affect the separation. The objective of this work is to synthesize the first LC CSP in which a chiral Ru complex was covalently bonded to a modern silica gel support.

The initial step was to compare the performances of different Ru complexes as chiral selectors. Two Ru *tris*(diimine) complexes with amino groups were selected:  $[\text{Ru}(\text{phen})_2(\text{aminophen})](\text{PF}_6)_2$  and  $[\text{Ru}(\text{phen})_2(\text{phendiamine})](\text{PF}_6)_2$  (structures shown in Figure 6.3).

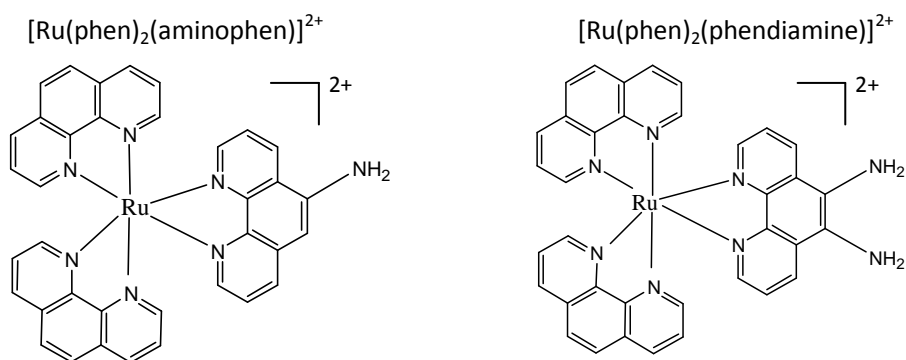


Figure 6.3 Structures of two Ru *tris*(diimine) complexes as chiral selectors

It was found that amino groups of these compounds were poorer nucleophiles than typical aliphatic amines due to the electron withdrawing nature of  $\text{Ru}^{2+}$ , and the fact that they are attached to an aromatic ring system. Therefore, nucleophilic coupling reactions that are commonly used to immobilize other chiral selectors to the surface of silica gel<sup>29, 57</sup> tend to be more difficult for these metal complexes.  $\Lambda$ -[Ru(phen)<sub>2</sub>aminophen](PF<sub>6</sub>)<sub>2</sub> and  $\Lambda$ -[Ru(phen)<sub>2</sub>phendiamine](PF<sub>6</sub>)<sub>2</sub> were chemically bonded to silica gel using the same binding method (binding method 1 in Figure 6.2). The carbon percentage of the final products is 4% for [Ru(phen)<sub>2</sub>aminophen](PF<sub>6</sub>)<sub>2</sub>-bonded silica, and 7% for [Ru(phen)<sub>2</sub>phendiamine](PF<sub>6</sub>)<sub>2</sub>-bonded silica, respectively. This indicates that replacing [Ru(phen)<sub>2</sub>aminophen](PF<sub>6</sub>)<sub>2</sub> with [Ru(phen)<sub>2</sub>phendiamine](PF<sub>6</sub>)<sub>2</sub> effectively improved the chiral selector loading. The enantiomeric performances of these two CSPs were evaluated by HPLC using the same experimental conditions. The chromatograms of cis-4,5-diphenyl-2-oxazolidinone separated on the [Ru(phen)<sub>2</sub>aminophen](PF<sub>6</sub>)<sub>2</sub>-bonded CSP and the [Ru(phen)<sub>2</sub>phendiamine](PF<sub>6</sub>)<sub>2</sub>-bonded CSP are shown in Figure 6.4.

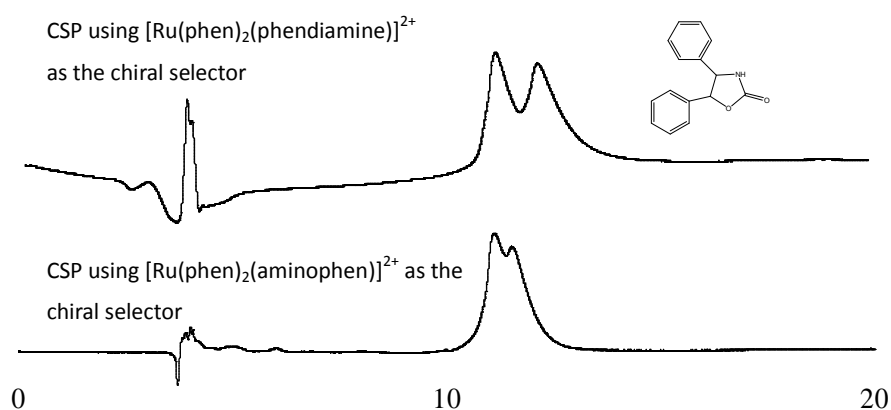


Figure 6.4 Comparison between two CSPs using  $\Lambda$ -[Ru(phen)<sub>2</sub>(aminophen)]<sup>2+</sup> and  $\Lambda$ -[Ru(phen)<sub>2</sub>(phendiamine)]<sup>2+</sup> as the chiral selectors. The analyte and mobile phase is cis-4,5-Diphenyl-2-oxazolidinone, and 95%water/5%acetonitrile, respectively.

It is evident that the CSP using  $\Lambda$ -[Ru(phen)<sub>2</sub>(phendiamine)]<sup>2+</sup> provided higher selectivity and resolution, although similar retention was observed on these two columns. Both elemental analysis and chromatographic results show that [Ru(phen)<sub>2</sub>(phendiamine)]<sup>2+</sup> is more suitable for preparing stationary phases, providing higher chiral selector loading and better enantioselectivity. Therefore, [Ru(phen)<sub>2</sub>(phendiamine)]<sup>2+</sup> was selected to study further binding chemistries. In addition, the surface area of silica gel plays an important role in synthesis. Replacing 200Å silica (pore size, surface area is ~180m<sup>2</sup>/g) with 100Å silica (pore size, surface area is ~450m<sup>2</sup>/g) significantly improved the carbon loading from 3% to 7% using the same Ru complex. Therefore, 100Å silica was used for subsequent studies.

Special attention was paid to the chemical binding procedures in order to obtain stationary phases with good chiral selector loading. To determine the best immobilization process, reactions were carried out using three different methods (Figure 6.2), named isocyanate binding (Method **1**), diisocyanate binding (Method **2**) and aldehyde binding (Method **3**), which are commonly used to prepare macrocyclic glycopeptide and cyclodextrin CSPs.<sup>29, 57</sup> Small scale reactions were conducted due to limited availability of enantiopure Ru complex. The elemental analyses of three products are shown in Table 6.1.

Table 6.1 Elemental analysis results of Ru complex-silica products synthesized by three different methods

| Description                  | C%   | H%  | N%  |
|------------------------------|------|-----|-----|
| Method <b>1</b> isocyanate   | 7.2  | 1.2 | 1.5 |
| Method <b>2</b> diisocyanate | 13.5 | 2.2 | 4.5 |
| Method <b>3</b> aldehyde     | 9.2  | 1.6 | 0.4 |

Also, comparison of the color of the final products allows a qualitative comparison of the binding methods, since these Ru complexes have a pronounced orange color. Diisocyanate binding chemistry (method **2**) gave a product with the highest carbon loading (13.5%), but the

color of the final product was the lightest. This is explained by the fact that the high percentage of carbon originates mainly from the large quantity of the diisocyanate linkage present. Comparing isocyanate binding (method **1**) and aldehyde binding (method **3**), visual observation shows the darkness of products is similar and carbon percent of method **3** is higher than method **1** (9.2% versus 7.2%, shown in Table 6.1). These two methods were then utilized to provide sufficient media to pack into 25cm columns (i.e., 3.5 grams of each, respectively), which were evaluated using the same analytes and mobile phases. The chromatograms of 1,1'-bi-2-naphthol separated on the CSPs prepared via isocyanate and aldehyde binding methods are shown in Figure 6.5. The enantioselectivity of the analyte separated on the CSP that utilized the aldehyde-binding is greater than that achieved on isocyanate-bound CSP.

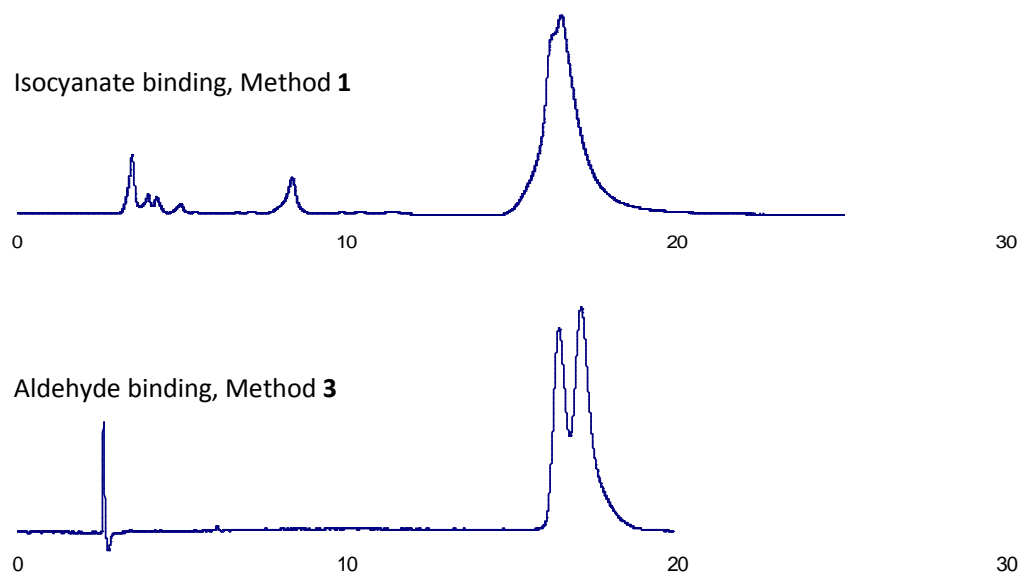


Figure 6.5 Comparison between two binding methods. The chromatograms were obtained on the CSPs prepared via isocyanate binding (method **1** in Figure 2) and aldehyde binding (method **3** in Figure 2), respectively. The chiral selectors ( $[\text{Ru}(\text{phen})_2(\text{phen diamine})]^{2+}$ ) and silica (pore size: 100Å) used are the same for two CSPs. The analyte and mobile phase is 1,1'-bi-2-naphthol and 80%heptane/20%ethanol, respectively.

### 6.3.2 Evaluation of the CSP prepared via aldehyde binding method

In this study, the best CSP was obtained by binding  $[\text{Ru}(\text{phen})_2(\text{phendiamine})]^{2+}$  to 100Å silica via aldehyde binding chemistry.

A set of 155 chiral compounds with a wide variety of functionalities was used to test this Ru complex-bonded CSP. Three operation modes (normal phase, polar organic mode, and reversed phase) were studied. It should be noted that acidic compounds with –COOH group are not eluted with heptane/ethanol, or acetonitrile/water, due to strong charge-charge interaction with the Ru complex-bonded stationary phase. It was also observed that salts (such as ammonium nitrate) are necessary to elute these acidic compounds in the polar organic mode. The other compounds without acidic groups did not give retention in the polar organic mode. Therefore, 35 acidic compounds were studied only in the polar organic mode and the other 120 compounds were injected in the normal phase and reversed phase modes. Table 6.2 lists the chromatographic data for all compounds separated in three chromatographic modes. The chromatographic data include retention factor ( $k_1'$ ), selectivity ( $\alpha$ ), and resolution ( $R_s$ ). Examples of optimized separations in all three modes are shown in Figure 6.6.

Overall, seventeen racemic compounds were separated on the best Ru complex-based CSP using three mobile phase modes mentioned above. The polar organic mode appeared to produce more successful separations than the other two modes. In the polar organic mode, eight compounds are separated, compared to five compounds separated in the normal phase, and four in the reversed phase, respectively. Four compounds are baseline resolved ( $R_s \geq 1.5$ ) and thirteen were partially separated ( $0.4 < R_s < 1.5$ ). Although the enantioseparation capability of Ru complex-based CSP is relatively limited, Ru-CSP is selectively effective for acidic compounds, considering 8 racemic analytes were separated out of 35 tested.

A closer examination of the data reveals some interesting facts. Ru complex bonded stationary phase appears to be multimodal in that they can be used in normal phase, polar

organic, and reversed-phase modes. The CSP was not irreversibly altered when changing from one mobile phase mode to another. Previous papers <sup>74, 138, 139</sup> also indicate that the stereochemistry at these ruthenium centers is very robust and these compounds are not easily racemized or decomposed in ordinary protic or aprotic solvents.

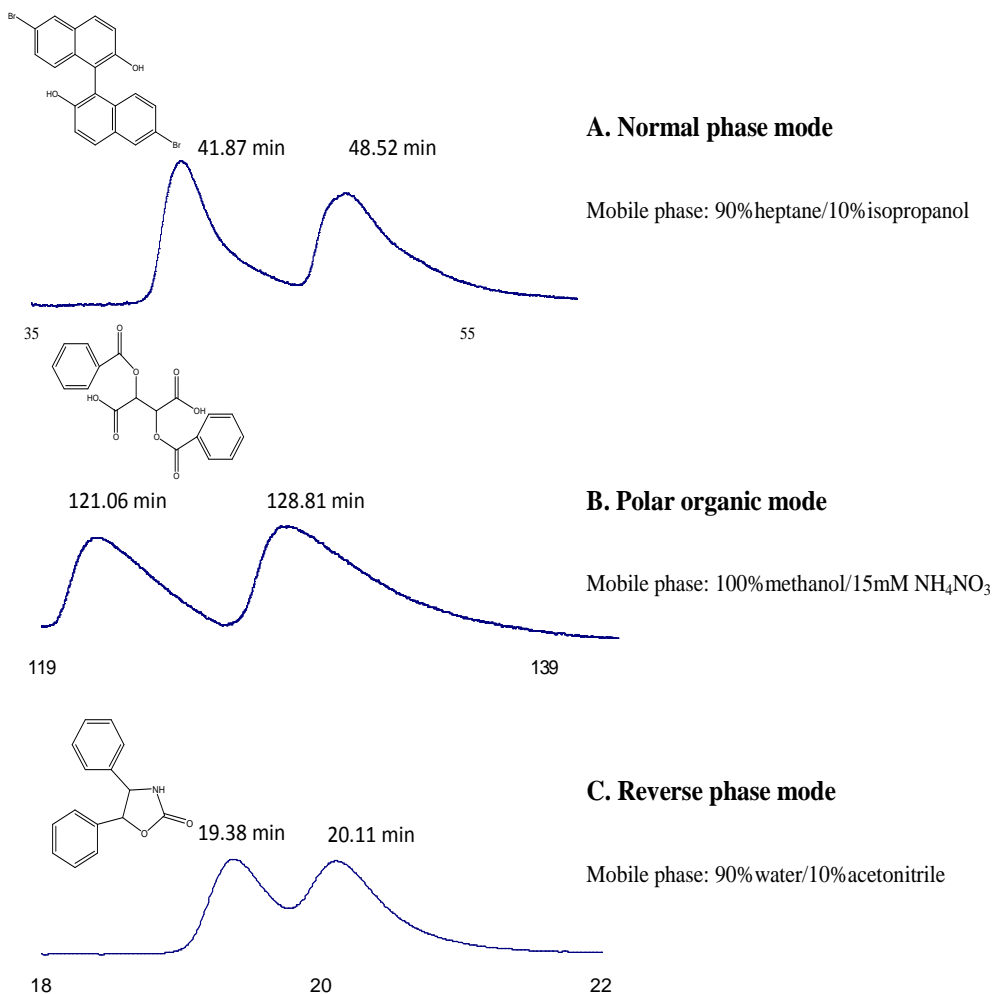


Figure 6.6 Optimized separations in three operation modes. Chromatographic data: (a)  $k_1'$ =14.26,  $\alpha$ =1.11,  $R_s$ =1.5; (b)  $k_1'$ =17.34,  $\alpha$ =1.07,  $R_s$ =1.5 (flow rate=0.5mL/min); (c)  $k_1'$ =3.70,  $\alpha$ =1.05,  $R_s$ =0.9 (flow rate=0.8mL/min).

Table 6.2 Chromatographic data of enantiomers resolved by the Ru complex-based CSP

| Mode           | No. | Analyte name  | k <sub>1'</sub> | α    | R <sub>s</sub> | Mobile phase   |
|----------------|-----|---|-----------------|------|----------------|----------------|
| Normal phase   | 1   | 6,6'-Dibromo-1,1'-bi-2-naphthol                                     | 11.69           | 1.17 | 1.5            | A              |
|                | 2   | 1,1'-Bi-2-naphthol  | 23.70           | 1.08 | 1.5            | B              |
|                | 3   | (3a(R,S)-cis)-(±)-3,3a,8,8a-Tetrahydro-2H-indeno[1,2-d]oxazol-2-one | 2.72            | 1.08 | 0.6            | C              |
|                | 4   | 2-(4-Biphenyl)-5-phenyloxazole                                      | 1.22            | 1.02 | 0.5            | B              |
|                | 5   | 4-Phenyl-1,3-dioxane  | 0.92            | 1.03 | 0.6            | D              |
| Polar organic  | 6   | 2,3-Dibenzoyl-DL-tartaric acid                                      | 17.34           | 1.07 | 1.5            | E <sup>a</sup> |
|                | 7   | O,O'-di-p-toluoyl-DL-tartaric acid                                  | 15.49           | 1.07 | 1.5            | E <sup>a</sup> |
|                | 8   | 3-nitrophenylboronic acid tartaric acid ester                       | 5.41            | 1.28 | 1.4            | F              |
|                | 9   | 2-(4-chloro-2-methylphenoxy)propionic acid                          | 3.14            | 1.03 | 0.6            | F              |
|                | 10  | (R/S)-(-/+)-1.1'-Binaphthyl-2,2'-diyl hydrogenphosphate             | 4.57            | 1.02 | 0.6            | F              |
|                | 11  | N-(3,5-Dinitrobenzoyl)-DL-phenylglycine                             | 2.14            | 1.02 | 0.5            | F              |
|                | 12  | trans-4-Cotininecarboxylic acid                                     | 1.28            | 1.05 | 0.6            | F              |
|                | 13  | 2-Phenoxypropionic acid   | 1.56            | 1.02 | 0.5            | F              |
| Reversed phase | 14  | cis-4,5-Diphenyl-2-oxazolidinone                                    | 3.70            | 1.05 | 0.9            | G <sup>b</sup> |
|                | 15  | 2,3-Dihydro-7a-methyl-3-phenylpyrrolo[2,1-b]oxazol-5(7aH)-one       | 3.74            | 1.04 | 0.6            | H <sup>b</sup> |
|                | 16  | 4-Methyl-5-phenyl-2-oxazolidinone                                   | 2.48            | 1.03 | 0.6            | H <sup>b</sup> |
|                | 17  | (3a(R,S)-cis)-(±)-3,3a,8,8a-Tetrahydro-2H-indeno[1,2-d]oxazol-2-one | 2.36            | 1.02 | 0.5            | H <sup>b</sup> |

Note: (a) The flow rate and the column temperature are 0.5 mL/min and 0 °C in order to improve the resolution; (b) The flow rate is 0.8 mL/min to avoid high pressure (>300bar), which could damage silica support. The mobile phase compositions are (A) 90%heptane/10%isopropanol; (B) 95%heptane/5%isopropanol; (C) 80%heptane/20%ethanol; (D) 60%heptane/40%ethanol; (E) 100%methanol/15mM NH<sub>4</sub>NO<sub>3</sub>; (F) 100%methanol/12.5mM NH<sub>4</sub>NO<sub>3</sub>; (G) 90%water/10%acetonitrile; (H) 98%water/2%acetonitrile.

The Ru complex-bonded CSP provides the best resolution for compounds of binaphthyl types in the normal phase mode. This indicates that different retention mechanisms may be involved in different mobile phase modes. In the normal phase mode where the non-polar solvents are used as the mobile phase,  $\pi$ - $\pi$  interactions can play an important role in the chiral recognition process. The phenanthroline ring linked to  $\text{Ru}^{2+}$  is very electron deficient and  $\pi$ - $\pi$  interactions are strong when it associates with  $\pi$ -basic compounds, such as 1,1'-bi-2-naphthol. Also, the carbamate linker provides additional sites for dipolar interactions. The helical chirality of Ru complex possibly provides a good fit with those analytes of helical chirality (such as binaphthyl compounds). Steric interaction may be important as well. These results are in agreement with previous reports on the  $[\text{Ru}(\text{phen})_3]^{2+}$ -clay column, which was shown to separate 1,1'-bi-2-naphthol.<sup>170</sup>

In the polar organic mode, the dominant interactions between the analyte and CSP usually involve some combination of hydrogen bonding, electrostatic, and dipolar interactions. The fact that Ru complex column shows enantioselectivity toward acidic compounds demonstrates that electrostatic interaction between positively-charged Ru complex and negatively-charged acidic analyte plays an important role in chiral recognition. In addition, electrostatic interactions between a solute and the stationary phase may be associated with a slow adsorption-desorption process, giving rise to broad and more poorly-defined peaks.

In addition, the circular dichroism detector was applied to test the compounds with appropriate retentions ( $1 < k' < 6$ ) in the normal phase and reversed phase. A positive-negative signal split in the circular dichroism chromatogram was observed in many cases (shown in Figure 6.7), where only one single peak was obtained in the UV chromatograms. This occurred when there was chiral recognition between the CSP and racemic analyte, but only moderate enantioselectivity and low efficiency. It is found that the Ru-complex CSP shows enantioselectivity to a wide variety of compounds when using CD detection. All the compounds showing selectivity in normal phase and reversed phase are listed in Table 6.3. In summary, 47

compounds were slightly separated in the reversed phase conditions, compared to 22 in the normal phase mode. Considering its broader selectivity, the reversed phase mode is more successful than the normal phase mode.

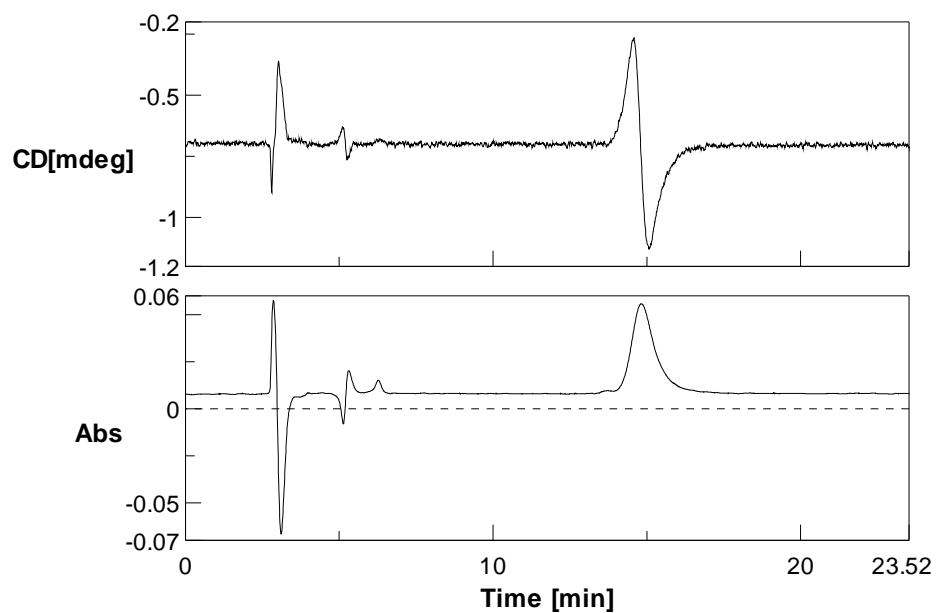


Figure 6.7 UV and CD chromatograms of the analyte retained on the Ru-complex column. The analyte is 4-(4-methoxy-phenyl)-6-methyl-2-thioxo-1,2,3,4-tetrahydro-pyrimidine-5-carboxylic acid allyl ester. The mobile phase and wavelength is 80%heptane/20%ethanol and 254 nm, respectively.

Table 6.3 Enantioselectivity of compounds observed by the circular dichroism (CD) detector

| Normal phase |                   | Reversed phase |                   |     |                   |
|--------------|-------------------|----------------|-------------------|-----|-------------------|
| No.          | Analyte structure | No.            | Analyte structure | No. | Analyte structure |
| 1            |                   | 1              |                   | 25  |                   |
| 2            |                   | 2              |                   | 26  |                   |
| 3            |                   | 3              |                   | 27  |                   |
| 4            |                   | 4              |                   | 28  |                   |
| 5            |                   | 5              |                   | 29  |                   |
| 6            |                   | 6              |                   | 30  |                   |
| 7            |                   | 7              |                   | 31  |                   |
| 8            |                   | 8              |                   | 32  |                   |
| 9            |                   | 9              |                   | 33  |                   |
| 10           |                   | 10             |                   | 34  |                   |
| 11           |                   | 11             |                   | 35  |                   |

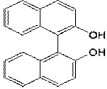
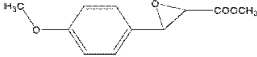
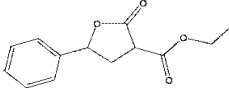
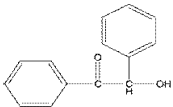
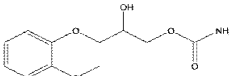
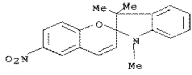
(Continued)

Table 6.3 continued

| Normal phase |                   | Reversed phase |                   |     |                   |
|--------------|-------------------|----------------|-------------------|-----|-------------------|
| No.          | Analyte structure | No.            | Analyte structure | No. | Analyte structure |
| 12           |                   | 12             |                   | 36  |                   |
| 13           |                   | 13             |                   | 37  |                   |
| 14           |                   | 14             |                   | 38  |                   |
| 15           |                   | 15             |                   | 39  |                   |
| 16           |                   | 16             |                   | 40  |                   |
| 17           |                   | 17             |                   | 41  |                   |
| 18           |                   | 18             |                   | 42  |                   |
| 19           |                   | 19             |                   | 43  |                   |
| 20           |                   | 20             |                   | 44  |                   |
| 21           |                   | 21             |                   | 45  |                   |

(Continued)

Table 6.3 continued

| Normal phase |   | Reversed phase |   |     |   |
|--------------|---|----------------|---|-----|---|
| No.          | Analyte structure   | No.            | Analyte structure   | No. | Analyte structure   |
| 22           |  | 22             |  | 46  |  |
|              |   | 23             |  | 47  |  |
|              |   | 24             |  |     |   |

### 6.3.3 Effect of mobile phase composition and temperature on enantioseparation

In order to optimize enantioseparation on Ru complex-bonded stationary phase, effects of mobile phase compositions have been studied. In the normal phase mode, the concentration and nature of the alcohol modifier in the mobile phase affect the retention and selectivity of analyte.<sup>79, 177</sup> Figure 6.8 shows effects of varying alcohol types. Five different alcohols were studied when the volume percentage of alcohols remained the same. Increasing alkyl chain length of primary and secondary alcohols enhances the retention, illustrated by comparison of ethanol, 1-propanol and 1-butanol, or comparison of isopropanol and 2-butanol. Using five alcohols, the enantioselectivities are different, ranging between 1.10-1.21. The concentration of the alcohol modifier also affects enantioseparation greatly (results shown in Figure 6.9). The retention factor of the analyte increased from 1.60 to 16.59, when reducing ethanol percentage from 40% to 5%. The improvement in enantioresolution resulted from much longer retention, because selectivity remained unchanged.

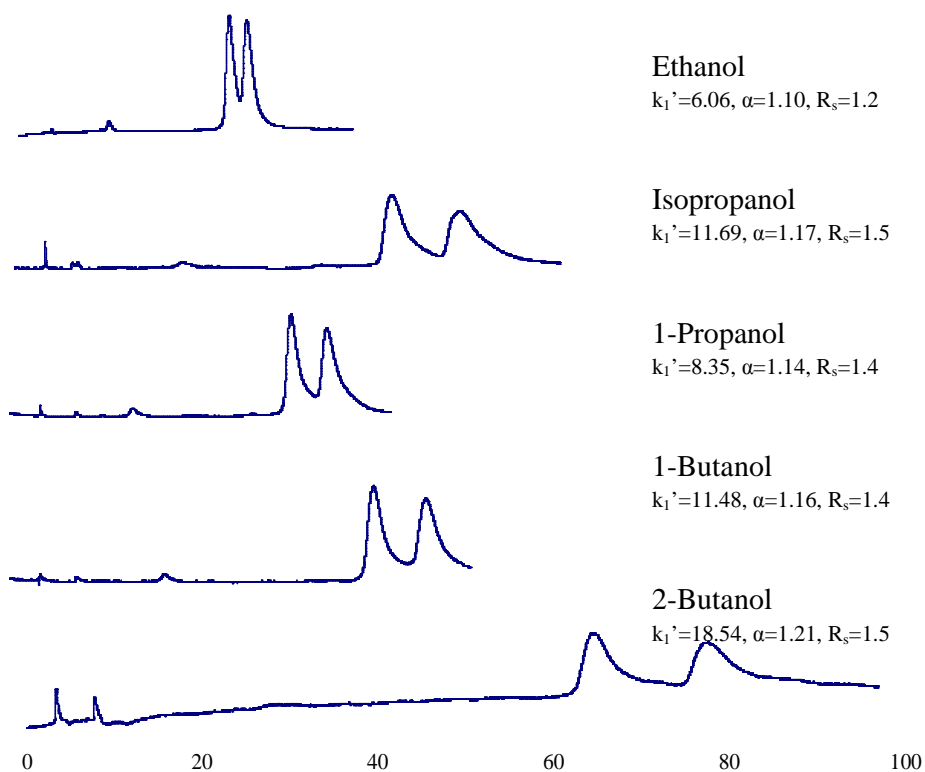


Figure 6.8 Effect of nature of alcohol on enantioseparations of 6,6'-dibromo-1,1'-bi-2-naphthol in the normal phase mode. The mobile phase is composed of 90%heptane/10%alcohol and all the other chromatographic conditions are kept the same.

In the polar organic mode, additives, such as acetic acid, triethylamine, and ammonium nitrate are often added. These additives in the mobile phase can usually shorten the retention time and improve chromatographic efficiency. In these studies, additives were necessary to elute acidic compounds by competing with analyte for strong binding sites. Different salts were tested as additives, while the salt concentration remained the same (12.5 mM). The chromatographic results are listed in Table 6.4 and it is evident that the type of salt additive affects retention and resolution significantly. The highest selectivity and resolution were obtained with the mobile phase containing ammonium nitrate. Furthermore, increasing the salt

concentration was found to decrease retention (data not shown), which is a trend usually observed in the polar organic mode on other chiral stationary phases.

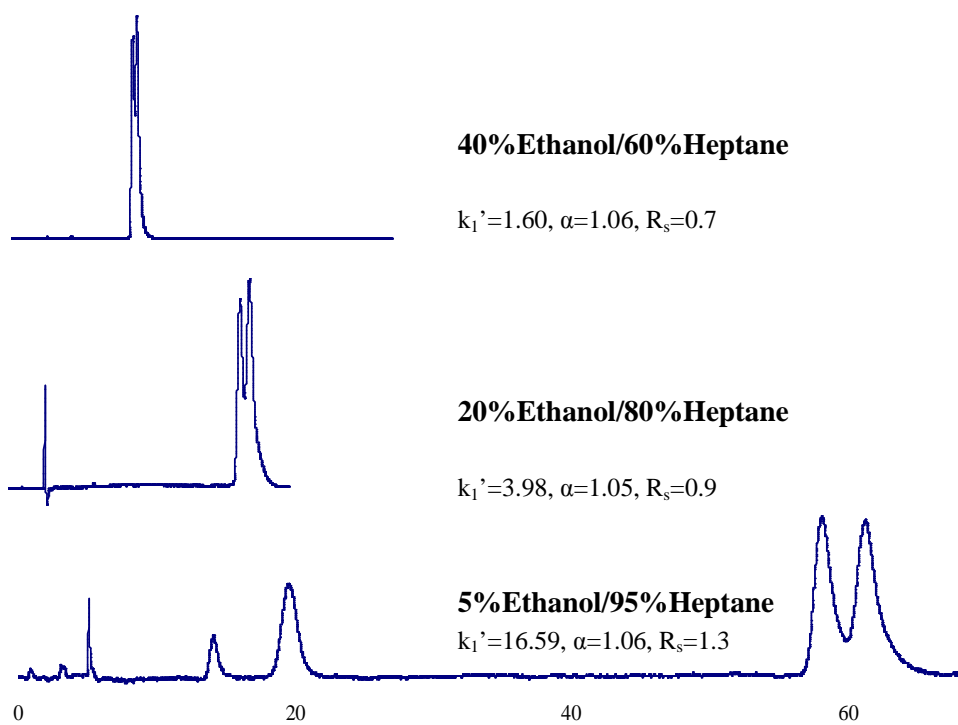


Figure 6.9 Effect of concentration of alcohol. The analyte and mobile phase are 6,6'-dibromo-1,1'-bi-2-naphthol.

In order to study the effect of temperature on enantioseparation of Ru complex-bonded CSP, a study of varying temperature between 0 °C– 30 °C was carried out. Chromatograms at three specific temperatures are shown in Figure 6.10. When increasing temperature, enantioresolution decreases due to lower retention and selectivity. Resolution of chiral separation is often improved by lowering the column temperature.



#### 6.4 Conclusions

Silica gel-based Ru complex-bonded chiral stationary phases have been developed for the first time. The best Ru-complex column was obtained using a reductive amination binding reaction and high surface area silica. Extensive liquid chromatographic studies with UV and CD detectors show Ru complex-bonded CSP provide enantioselectivity toward a wide variety of compounds, in particular, compounds with acidic groups. While the Ru complex-bonded CSP did not have high efficiency, the bonded phase is likely more robust than its coated predecessors. The development of the first transition metal complex-bonded chiral stationary phases and chromatographic studies provide insight concerning chiral stationary phase bonding strategies.

## CHAPTER 7

### DEVELOPMENT OF NEW HPLC CHIRAL STATIONARY PHASES BASED ON NATIVE AND DERIVATIZED CYCLOFRUCTANS

An unusual class of chiral selectors, cyclofructans, is introduced for the first time as bonded chiral stationary phases. Compared to native cyclofructans (CFs), which have rather limited capabilities as chiral selectors, aliphatic- and aromatic-functionalized CF6s possess unique and very different enantiomeric selectivities. Indeed, they are shown to separate a very broad range of racemic compounds. In particular, aliphatic-derivatized CF6s with a low substitution degree baseline separate all tested chiral primary amines. It appears that partial derivatization on the CF6 molecule disrupts the molecular internal hydrogen bonding, thereby making the core of the molecule more accessible. In contrast, highly aromatic-functionalized CF6 stationary phases lose most enantioselective capabilities toward primary amines, however they gain broad selectivity for most other types of analytes. This class of stationary phases also demonstrates high “loadability” and therefore has great potential for preparative separations. The variations in enantiomeric selectivity often can be correlated with distinct structural features of the selector. The separations occur predominantly in the presence of organic solvents.

#### 7.1 Introduction

Enantiomeric separations have attracted great attention in the past few decades. Early enantioselective LC work in the 1980's provided the impetus for the 1992 FDA policy statement on the development of stereoisomeric drugs.<sup>1</sup> This was because the facile analysis and preparation of many pharmaceutically active enantiomers became possible for the first time. Such broadly applicable techniques were essential for pharmacokinetic and pharmacodynamic studies, development, quality control and sometimes production of enantiomeric drugs. HPLC with chiral stationary phases (CSPs) is far and away the most powerful and widely used

technique for solvent-based enantiomeric separations at both analytical and preparative scales. Supercritical fluid separations are increasing in importance, particularly for preparative separations.

Currently, over a hundred CSPs have been reported, and these CSPs are made by coating or bonding the chiral selectors, usually to silica gel supports. Interestingly, only a few types/classes of CSPs dominate the field of enantiomeric separations, for example, polysaccharide-based CSPs,<sup>3-12</sup> macrocyclic antibiotic CSPs,<sup>17-27</sup> and  $\pi$  complex CSPs.<sup>39-42</sup> Researchers continue to make great efforts to develop new HPLC CSPs, which could make a substantial impact on enantiomeric separations. It has been stated that today, in order for any new CSPs to have an impact, they must fulfill one or more of the following requirements:<sup>178</sup> (a) broader applicability than existing CSPs; (b) superior separations for specific groups of compounds; or (c) fill an important unfulfilled separation niche. In the present paper, a unique class of CSPs based on cyclofructan (CF) is introduced, and is shown to have the potential to satisfy all of the above-mentioned requirements.

Cyclofructans (CFs) are one of a relatively small group of macrocyclic oligosaccharides.<sup>179, 180</sup> Cyclodextrins are perhaps the best known member of this class of molecules.<sup>28, 29</sup> However, as will be shown, cyclofructans are quite different in both their structure and behavior. Cyclofructans consist of six or more  $\beta$ -(2 $\rightarrow$ 1) linked D-fructofuranose units (see Figure 7.1). Common abbreviations for these compounds are CF6, CF7, CF8, etc, which indicate the number of fructose units in the macrocyclic ring. Cyclofructans were first reported by Kawamura and Uchiyama in 1989.<sup>179</sup>

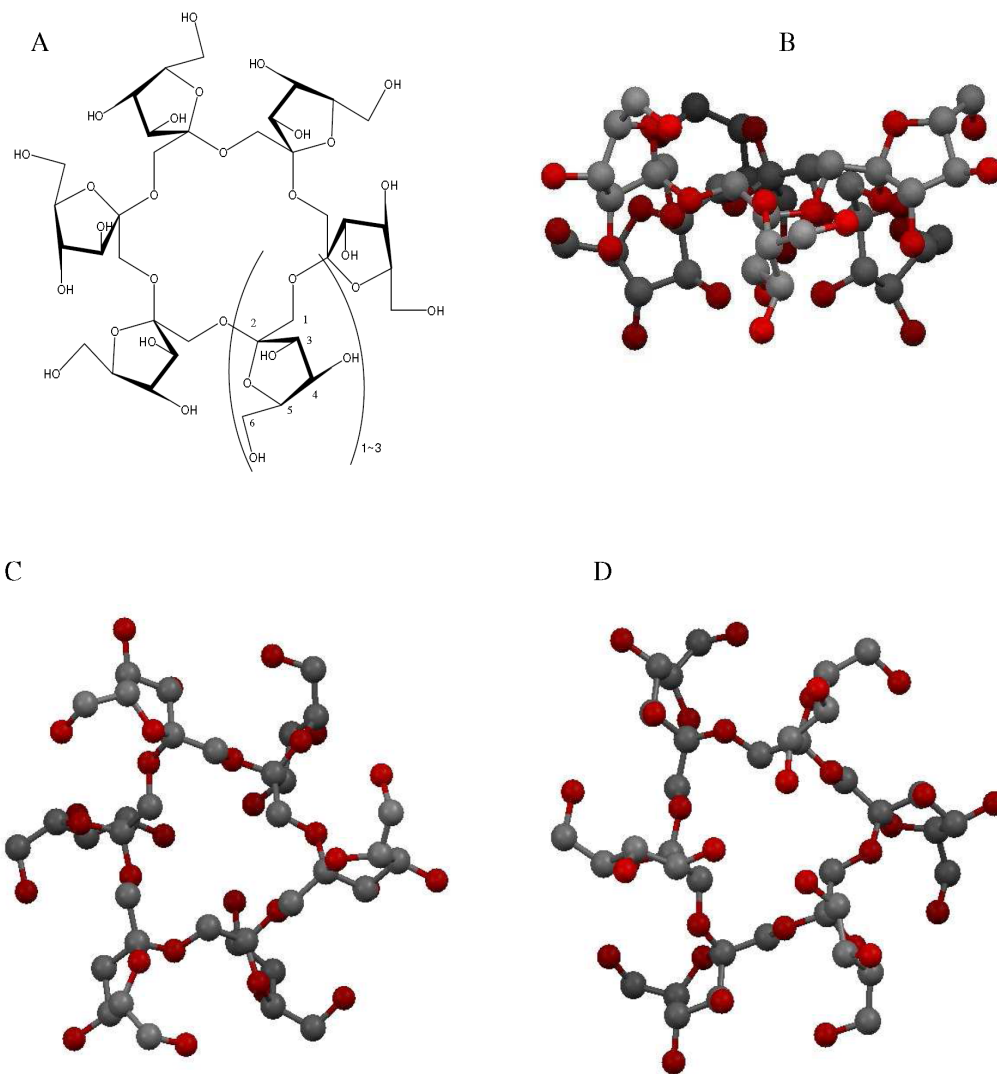


Figure 7.1 Structure of cyclofructan. (A) Molecular structure of CF6, CF7 and CF8; (B-D) Crystal structure of CF6: B. side view; C. hydrophobic side up; D. hydrophilic side up. Color scheme: oxygen atoms are red and carbons are black. Hydrogens are not shown.

Since then, cyclofructans have been used in a variety of applications mostly as additives to consumer products, such as moderators of food and drink bitterness and astringency,<sup>181-183</sup> browning prevention agent,<sup>184</sup> ink formulation agent,<sup>185</sup> lubricants<sup>186</sup> and so on. In addition, cyclofructans have been shown to have cryoprotective effects,<sup>187</sup> and complexing abilities toward metal ions.<sup>188</sup> However, to date and to our knowledge, there have been no published reports on HPLC enantiomeric separations using either native cyclofructan or derivatized cyclofructans as chiral selectors.

In the present work, we described the unique structure of CF6, synthesis of CF6-based CSPs, chiral separation mechanistic considerations, their chromatographic performance in terms of enantiomeric separations, and the pronounced effect of certain derivatization approaches on CF6 structure and selectivity.

## 7.2 Experimental Section

### *7.2.1 Materials*

Cyclofructans (CFs) can be produced either by fermentation of inulin via any of five microorganisms (for example, *Bacillus circulans* OKUMZ 31B and *B. circulans* MCI-2554),<sup>179, 189-195</sup> or incubation of inulin with the active enzyme cyclinulo-oligosaccharide fructanotransferase (CFTase).<sup>180</sup> Also, the CFTase gene has been isolated, and its sequence has been determined and incorporated into common baker's yeast.<sup>180, 192</sup> Therefore, mass-produced CFs could be available at low cost. CF6, and a mixture of CF7 (80%) + CF6 (20%) were generously donated by Mari Yasuda at Mitsubishi Chemical Group (Tokyo, Japan). Different types of silica (all of 5 $\mu$ m spherical diameters) were utilized. They include Daiso silica of 5 $\mu$ m spherical diameter (300 Å pore size, 107 m<sup>2</sup>/g surface area; 200 Å, 170 m<sup>2</sup>/g; 120 Å, 324 m<sup>2</sup>/g; 100 Å, 440 m<sup>2</sup>/g), and Kromasil silica (300 Å, 116 m<sup>2</sup>/g; 200 Å, 213 m<sup>2</sup>/g; 100 Å, 305 m<sup>2</sup>/g). Anhydrous N,N-dimethylformamide (DMF), anhydrous toluene, anhydrous pyridine, acetic acid (AA), triethylamine (TEA), trifluoroacetic acid (TFA), butylamine, sodium hydride, 3-(triethoxysilyl)propyl isocyanate, 1,6-diisocyanatohexane, (3-aminopropyl)triethoxysilane, 3-

glycidoxypropyltrimethoxy silane, and all of 81 racemic analytes tested in this study were purchased from Sigma-Aldrich (Milwaukee, WI, USA). All isocyanate and isothiocyanate derivatization reagents were also obtained from Sigma-Aldrich. They include methyl isocyanate, ethyl isocyanate, isopropyl isocyanate, *tert*-butyl isocyanate, methyl isothiocyanate, 3,5-dimethylphenyl isocyanate, 3,5-dichlorophenyl isocyanate, *p*-tolyl isocyanate, 4-chlorophenyl isocyanate, 3,5-bis(trifluoromethyl)phenyl isocyanate, R-1-(1-naphthyl)ethyl isocyanate, S-1-(1-naphthyl)ethyl isocyanate, S- $\alpha$ -methylbenzyl isocyanate. 1-Chloro-3,5-dinitrobenzene, and 4-chloro-2,6-dinitrobenzotrifluoride were obtained from Alfa Aesar (Ward Hill, MA, USA). Acetonitrile (ACN), 2-propanol (IPA), *n*-heptane, ethanol (ETOH), and methanol (MEOH) of HPLC grade were obtained from EMD (Gibbstown, NJ, USA). Water was obtained from Millipore (Billerica, MA, USA).

#### 7.2.2 Synthesis of CF-based CSPs

Native or derivatized cyclofructan were bonded to silica support by a variety of different methods. Native CF6 is used as an example to describe the procedures for the three binding chemistries tested. In the first method, silica (3 g) was dried at 110 °C for 3 h. Anhydrous toluene was added and any residual water was removed using a Dean-Stark trap for 3h. The mixture was cooled down <40 °C and 1mL of (3-aminopropyl)triethoxysilane was added dropwise to the 3 g silica-toluene slurry. Next the mixture was refluxed for 4 h and then cooled, filtered, washed and dried to obtain amino-functionalized silica (3.3 g). Then, 2 mL of 1,6-diisocyanatohexane was added to the dry amino-silica toluene slurry, which was kept in an ice bath. Next, the slurry mixture was heated to 70°C for 4h. The excess reactant was removed by vacuum filtration and the solid product was washed with anhydrous toluene twice. Lastly, 1 g of dried cyclofructan dissolved in 20 mL of pyridine was added and the mixture was heated to 70°C and allowed to react for 15 h. Finally 3.7 g of product was obtained.

The second binding chemistry also forms the carbamate linker. Cyclofructan (1g) was dissolved in 40 mL of anhydrous pyridine. To this solution, 0.7 mL of 3-(triethoxysilyl)propyl

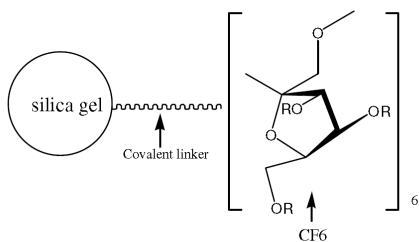
isocyanate was added dropwise under dry argon atmosphere protection. And the mixture was heated at 90 °C for 5h. Next, residual water was removed from silica gel (3g) using a Dean-Stark trap and 150 mL of anhydrous toluene. After the two mixtures were cooled to room temperature, the cyclofructan reaction mixture was added to the silica-toluene slurry and heated at 105 °C overnight. The final mixture was cooled and washed. After drying in vacuum overnight, 3.4 g of product was obtained.

The third binding chemistry forms an ether linkage. Epoxy-functionalized silica was synthesized as previously described.<sup>57</sup> First, CF6 (1g) was dissolved in 30 mL of anhydrous DMF. Then, 0.2 g NaH was added to the solution under dry argon protection and stirred for 10 min. Unreacted NaH was removed by vacuum filtration. Lastly, dry epoxy-functionalized silica (3.3 g) was added to the filtrate, and the mixture was heated at 140 °C for 3 h and subsequently cooled down to room temperature. After filtration and drying, 3.5 g of product was obtained.

Syntheses of derivatized cyclofructan chiral stationary phases (CSPs) have been conducted in a variety of ways. For example, native cyclofructan can be chemically bonded to silica, then derivatized; or cyclofructan can be first partially derivatized, then bonded to silica. Figure 7.2 shows the diagram of covalently-bonded CF6 and the structures of the aliphatic and aromatic derivatization groups used in this study. All derivatization groups were bonded to CF6 via a carbamate or a thiocarbamate linkage, with the exception of dinitrophenyl and dinitrophenyl-trifluoromethyl groups, which are attached to CF6 via an ether linkage.<sup>154</sup> Table 7.1 shows elemental analysis data for the native CF6-CSP, partially-derivatized methyl carbamate-CF6 CSP, and completely-derivatized R-naphthylethyl carbamate-CF6 CSP.

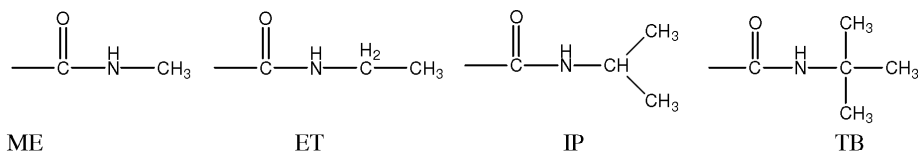
After the cyclofructan derivative is bonded to the support, it can be further derivatized to achieve more complete coverage, or to have two different derivative groups on the cyclofructan ( $\pi$ -acid and  $\pi$ -basic groups).

(A) CSP based on chemically-bonded CF6



R=H or derivatization group

(B) Aliphatic derivatization groups



(C) Aromatic derivatization groups

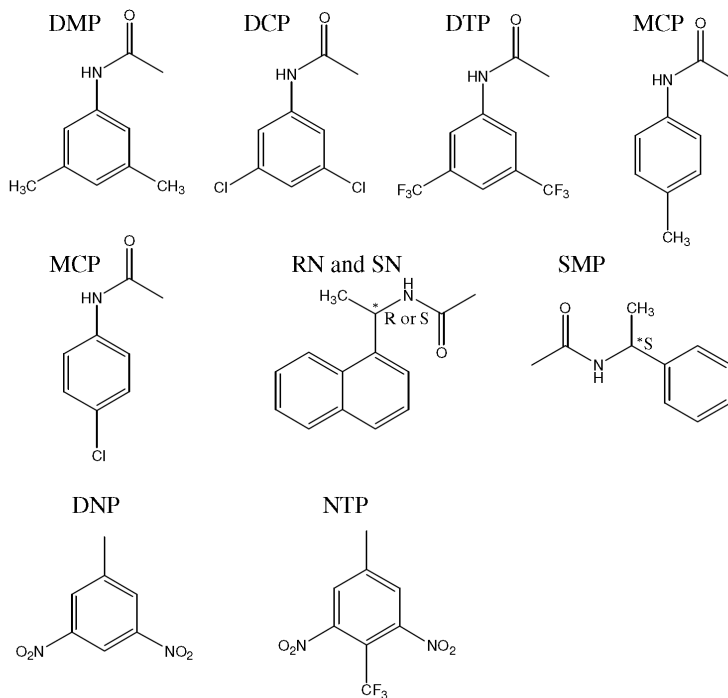


Figure 7.2 Scheme of chemically-bonded CF6 stationary phase and derivatized-CF6 CSPs and chemical structure of all derivatizing groups.

Table 7.1 Elemental analysis results of three representative CF6-based stationary phases

| Chiral selector               | Degree of substitution | C%    | H%   | N%   |
|-------------------------------|------------------------|-------|------|------|
| Native CF6                    | 0                      | 10.19 | 1.78 | 0.41 |
| Methyl carbamate CF6          | Low <sup>a</sup>       | 12.02 | 1.90 | 1.01 |
| R-naphthylethyl carbamate CF6 | Very high <sup>b</sup> | 19.11 | 2.52 | 1.57 |

<sup>a</sup> DS ~ 6. <sup>b</sup> Complete derivatization (DS=18).

### 7.2.3 HPLC method

The HPLC column packing system is composed of an air driven fluid pump (HASKEL, DSTV-122), an air compressor, a pressure regulator, a low pressure gauge, two high pressure gauges (10000 psi and 6000 psi), a slurry chamber, check valves and tubings. The CSP was slurry packed into a 25cmx0.46cm (i.d.) stainless steel column.

The HPLC system was an Agilent 1100 system (Agilent Technologies, Palo Alto, CA, USA), which consists of a diode array detector, an autosampler, a binary pump and Chemstation software. All chiral analytes were dissolved in ethanol, methanol or appropriate mobile phases. For the LC analysis, the injection volume and the flow rate were 5  $\mu$ L and 1mL/min, respectively. Separations were carried out at room temperature (~20 °C) if not specified. The mobile phase was degassed by ultrasonication under vacuum for 5 min. Each sample was analyzed in duplicate. Three operation modes (normal phase mode, polar organic mode, and reversed phase mode) were tested. In normal phase mode, heptane with ethanol or isopropanol was used as the mobile phase. In some cases, TFA was used as an additive. The mobile phase of the polar organic mode was composed of acetonitrile/methanol and small amounts of acetic acid and triethylamine. Water/acetonitrile or acetonitrile/acetate buffer (20 mM, pH=4.1) was used as the mobile phase in the reversed phase mode. A Berger SFC unit was used, equipped with an FCM1200 flow control module, a TCM 2100 thermal column

module, a dual pump control module, and a column selection valve. The flow rate was 4mL/min. The co-solvent was composed of methanol:ethanol:isopropanol=1:1:1 and 0.2% DEA (diethylamine). The gradient mobile phase composition was: 5% co-solvent hold during 0-0.6 min, 5-60% during 0.6-4.3 min, 60% hold during 4.3-6.3 min, 60%-5% during 6.3-6.9min, 5% hold during 6.9-7.9 min.

For the calculations of chromatographic data,  $t_0$  was determined by the peak of the refractive index change due to the sample solvent, or determined by injecting 1,3,5-tri-*tert*-butylbenzene in the normal phase mode. The molecular structure modeling program is ACD/3D viewer freeware.

### 7.3 Results And Discussion

#### *7.3.1 Structure and properties of cyclofructans*

Cyclofructans consist of six or more D-fructofuranose units (Figure 7.1) and each fructofuranose unit contains four stereogenic centers and three hydroxyl groups. Their central skeleton has the same structure as the respective crown ethers. Table 7.2 gives relevant physico-chemical data for CF6, CF7 and CF8. It indicates that the “cavity” inner diameter (i.e., distance between opposing oxygen atoms in the molecular core) increase significantly from 2.3 Å for CF6 to 4.1 Å for CF8.<sup>195</sup> And the macrocycle outer diameter of CF6-CF8 demonstrates the same trend. However, the macrocycle heights are all quite similar.

Table 7.2 Physical properties of cyclofructans 6-8

| Macrocycle | M.W.    | Melting Point (°C)                           | $[\alpha]_D^{20}$ (°) in H <sub>2</sub> O | Cavity i.d. (Å) <sup>c</sup> | Macrocycle o.d. (Å) <sup>c</sup> | Macrocycle Height (Å) <sup>c</sup> |
|------------|---------|--|---|------------------------------|----------------------------------|------------------------------------|
| <b>CF6</b> | 972.84  | 210-219 <sup>a</sup><br>231-233 <sup>b</sup> | -64.6 <sup>b</sup><br>-63.5 <sup>d</sup>  | 2.3                          | 14.6                             | 8.7-9.4                            |
| <b>CF7</b> | 1134.98 | 215-222 <sup>a</sup>                         | -59.1 <sup>d</sup>                        | 4.1                          | 15.9                             | 8.5-8.9                            |
| <b>CF8</b> | 1297.12 | N/A  | N/A                                       | 4.7                          | 16.1                             | 8.5-9.2                            |

<sup>a</sup>Melts and decomposes in this range; <sup>b</sup>Values taken from Ref. 28; <sup>c</sup>Values estimated from Ref. 46. Estimates accounting for van der Waals radii. <sup>d</sup>Measured in our lab.

Among cyclofructans, CF6 has attracted the most attention due to its availability in pure form and its highly defined geometry. The crystal structure of CF6 (shown in Figure 7.1B-D) reveals that six fructofuranose rings are arranged in spiral fashion around the crown ether skeleton, either up or down towards the mean plane of the crown ether.<sup>193, 194</sup> Six 3-position hydroxyl groups alternate to point towards or away from the molecular center, and three oxygen atoms pointing inside (oxygen atoms in the molecular center of Figure 7.1D) are very close to each other (~3 Å). As a result, access to the 18-crown-6 core on one side of the macrocycle is blocked by the hydrogen bonding between these hydroxyl groups<sup>194</sup> (Figure 7.1D). This side of the macrocycle is relatively hydrophilic as the result of the directionality of all its hydroxyl groups (Figure 7.1D). The other side of CF6 appears to be more hydrophobic, resulting from the methylene groups of -O-C-CH<sub>2</sub>-O- around the central indentation (Figure 7.1C). A computational lipophilicity pattern of CF6 also confirms that CF6 shows a clear “front/back” regionalization of hydrophilic and hydrophobic surfaces.<sup>195</sup> Both the crystal structure and computational modeling studies demonstrate that CF6 appears to have considerable additional internal hydrogen bonding. The fact that three 3-OH groups completely cover one side of the 18-crown-6 ring and the skeleton crown oxygens are almost folded inside the molecule, makes CF6 very different from other 18-crown-6 ether based chiral selectors. It is worth emphasizing that CF6-8 do not possess central hydrophobic cavities, as do cyclodextrins.<sup>28, 29</sup> Consequently, hydrophobic inclusion complexation, which plays an important role in the association of organic molecules with cyclodextrins, does not seem to be relevant for cyclofructans.

For the above-mentioned structural reasons, native CF6 appears to have limited capabilities to form either hydrophobic inclusion complexes or ion/crown ether inclusion complexes. In order to investigate whether or not CF6 provides any chiral recognition capabilities, we synthesized the covalently bonded native-CF6 stationary phase. We also conducted extensive CE experiments investigating CF6 as a chiral run buffer additive. The native CF6-based column was evaluated by injecting a set of 81 analytes with a wide variety of

functionalities, including amines, carboxylic acids, and alcohols. This CSP based on native CF6 only partially separated enantiomers of a few primary amines (Figure 7.3A top) and two binaphthyl compounds [i.e., 1,1'-bi(2-naphthyl diacetate), and 1,1'-bi-2-naphthol bis(trifluoromethanesulfonate)]. It appeared that none of them were baseline separated due to a combination of marginal selectivity, inefficient separations often coupled with poor peak shapes and often long retention. For all of other analytes, the CF6-CSP exhibited negligible enantioselectivity. Furthermore no enantiomeric separations were obtained with native CF6 in CE.

### *7.3.2 Initial observations on the effects of derivatization of cyclofructan 6*

The hypothesis that extensive intramolecular hydrogen bonding in CF6 (see Fig. 7.1D) and its compact configuration has detrimental effects on its enantioselective separation ability could be tested if one could disrupt its internal hydrogen bonding and allow the structure to “relax” or open somewhat. One way to do this is to block a few of the crucial hydrogen bonding groups within the CF6 structure. Interestingly, when CF6 CSPs were made with either aliphatic or aromatic substituted-CF6s (with a low degree of hydroxyl group substitution), they exhibited tremendous enantioselectivity toward chiral primary amines (see Figure 7.3A). Molecular modeling was performed for the derivatized CF6 (Figure 7.4A) and helps to explain the improved enantiomeric resolution toward primary amines. In this simplest case, it is supposed that initial derivatization with the methyl substituent (ME) occurs with the 6-OH groups. Figure 7.4A shows a side view of the molecular model of ME-carbamate CF6, obtained with ACD/3D viewer freeware program. It suggests that the CF6 intramolecular hydrogen bonding is disrupted after partial derivatization, causing a “relaxation” of the molecular structure. This may expose the crown ether core and/or other previously inaccessible hydrogen bonding sites of the CF6. Substitution of a few of the hydroxyl groups, especially with larger derivatization groups can increase the steric bulk, which can be beneficial for improving peak efficiency (as will be discussed). However, further increases in the substitution degree on the CF6 molecule (Figure

7.3B) results in significantly worse capabilities for separating primary amines. Enantioselectivity for all primary amines was completely lost on the RN-CSP with complete substitution. The reason for this becomes apparent from the structure of CF6 with 18 RN groups (Figure 7.4B), which shows the RN groups are positioned up or down, thus enlarging the depth of the molecule and again sterically blocking the molecular core. The conversion of all hydroxyl groups to carbamate groups also removes all hydrogen bonding donor groups and most oxygens are buried deep inside the molecule. Thus, having many bulky functional groups can sterically hinder the chiral recognition of primary amines. Also, it is found that aliphatic- and aromatic-functionalized CF6 CSPs provide different capabilities for separating primary amines. Figure 7.5 shows one example, comparing methyl, isopropyl and RN derivatized-CF6 stationary phases of the same substitution degree. The IP- and ME-derivatized columns gave higher enantioselectivity and resolution for tryptophanol. A noticeable improvement in peak efficiency was observed on these aliphatic-functionalized columns. The aliphatic-functionalized CF6 stationary phases separate primary amines more effectively, providing higher selectivity and/or higher efficiency. These results demonstrate that the size of the derivatizing group also plays an important role in the separation of primary amines. Although aliphatic-functionalized CF6 stationary phases with a low substitution degree were highly successful for the separations of primary amines, they show poor capabilities for separating most other analytes.

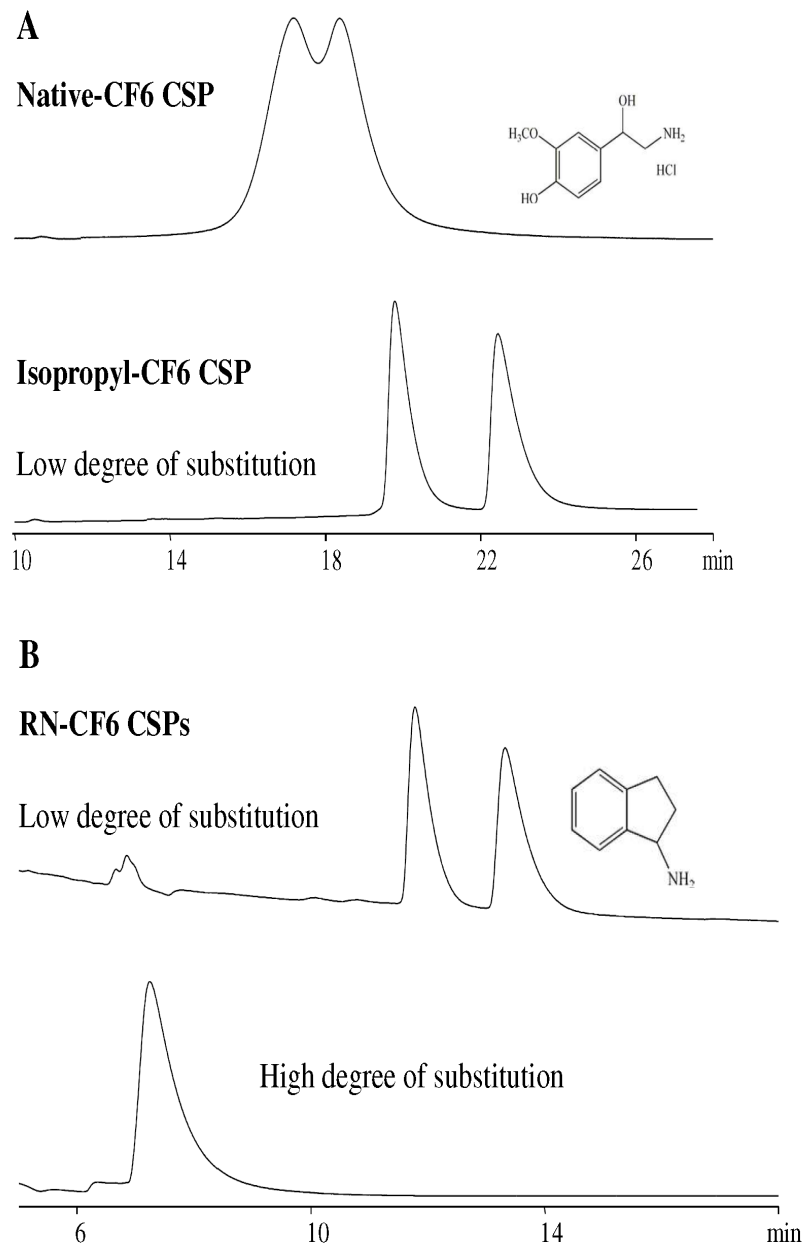
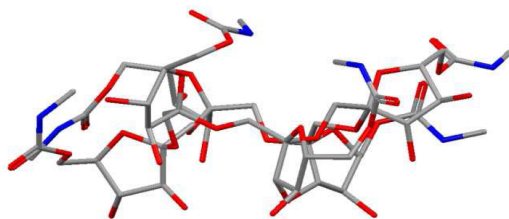


Figure 7.3 Separation of primary amines on derivatized-CF6 stationary phases with different substitution degrees. Analytes and mobile phases are: (A) normetanephrine hydrochloride, 75ACN/25MEOH/0.3AA/0.2TEA (top), 60ACN/40MEOH/0.3AA/0.2TEA (bottom); (B) 1-aminoindan, 60ACN/40MEOH/0.3AA/0.2TEA (top and bottom).

(A) Low degree of hydroxyl substitution with a small aliphatic group



(B) High degree of hydroxyl substitution with a bulky aromatic groups

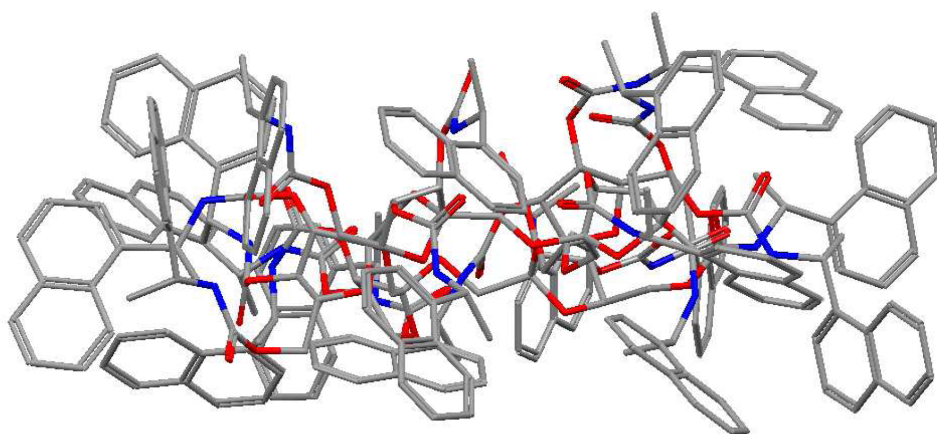


Figure 7.4 Edge view of CF6 derivatized with (A) six methyl carbamate groups and (B) eighteen R-naphthylethyl carbamate groups. The color coding is: oxygen atoms are red, carbon atoms are black and nitrogen atoms are blue. Hydrogen atoms are not shown. Compare these edge views with that of native cyclodextrins in Figure 1B.

Aromatic-functionalization of a native chiral selector is a common strategy used to develop new chiral stationary phases, such as dimethylphenyl and dichlorophenyl substitution of amylose and cellulose,<sup>3-12</sup> and dimethylphenyl and naphthylethyl substitution of  $\beta$ -cyclodextrin.<sup>30-34</sup> Compared to native chiral selectors, the aromatic derivatized-types provide improved enantioseparation capabilities and separate a wider range of analytes. Therefore it was logical to synthesize aromatic-functionalized CF6 stationary phases with a higher substitution degree. Evaluations of these stationary phases show that highly aromatic-functionalized CSPs negate the previously found almost universal selectivity for chiral primary amines. However, there was a dramatic enhancement in enantiomeric selectivity for most other

types of compounds. Figure 7.6 illustrates the enhanced selectivity provided by the RN-carbamate CF6 stationary phase. N-(3,5-dinitrobenzoyl)-DL-leucine was successfully separated ( $\alpha=1.91$ ,  $R_s=4.4$ ) by the RN-CF6 column, while no separation was observed on the CF6-CSP. The aromatic-functionalized CF6 CSPs provide ample opportunities for multiple hydrogen bonding interactions,  $\pi$ - $\pi$  interaction, and dipole-dipole interaction, aided by steric interactions to obtain effective chiral recognition.

It appears from these initial results, that cyclofructan can be functionalized in such ways as to provide two completely different types of chiral selectors which separate enantiomers via two different mechanisms. The minimally functionalized CF6 (with smaller aliphatic moieties) has a relaxed structure that exposes its crown ether core and additional hydroxyl groups. This allows for interactions with and separation of chiral primary amines in organic solvents for the first time. More highly aromatic derivatized CF6 has a sterically crowded structure (Fig 7.4B) that hinders access to its molecular core, but provides other ample interaction sites about its periphery. It is these sites that provide chiral recognition for a broad range of compounds. In the following sections more detailed examination and optimization of these two functionalized cyclofructan formats are discussed.

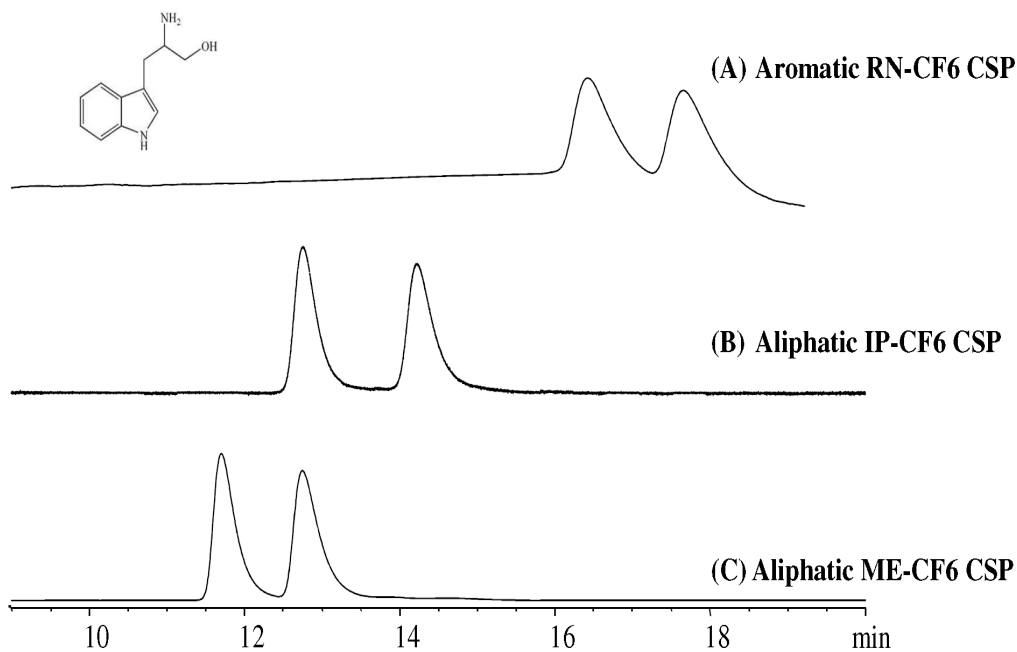


Figure 7.5 Comparison between aromatic- and aliphatic-derivatized-CF6 CSPs. The analyte is DL-tryptophan. The chromatographic data and mobile phases are: (A)  $k_1=4.66$ ,  $\alpha=1.12$ ,  $R_s=1.4$ , 75ACN/25MEOH/0.3AA/0.2TEA; (B)  $k_1=3.39$ ,  $\alpha=1.15$ ,  $R_s=2.7$ , 60ACN/40MEOH/0.3AA/0.2TEA; (C)  $k_1=3.03$ ,  $\alpha=1.12$ ,  $R_s=1.7$ , 60ACN/40MEOH/0.3AA/0.2TEA.

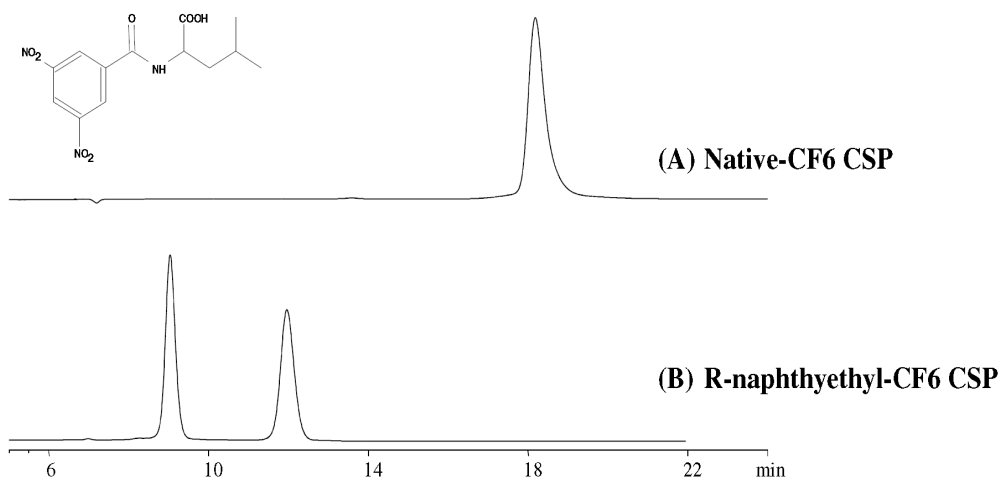


Figure 7.6 Comparison between native- and aromatic-functionalized CF6 chiral columns. The analyte is N-(3,5-dinitrobenzoyl)-DL-leucine. Mobile phases: (A) 90heptane/10ETOH/0.1TFA; (B) 70heptane/30ETOH/0.1TFA.

### 7.3.3 Cyclofructan CSPs based on aliphatic-functionalized CF6

Initial studies (*supra vide*) showed that aliphatic-CF6 CSPs provide excellent enantiomeric separation abilities for primary amines, so it was necessary to conduct more comprehensive studies on these aliphatic-functionalized stationary phases. Aliquots of CF6 were respectively derivatized with four different aliphatic moieties: methyl (ME), ethyl (ET), isopropyl (IP), and *tert*-butyl (TB) groups. Among them, IP- and ME-functionalized CF6 appeared to give the best enantiomeric separations of primary amines. Representative chromatographic data are shown in Table 7.3. For comparison, data generated on the aromatic RN-CF6 CSP with a low substitution degree also are included. The IP CSP gave the highest selectivity toward nine primary amines, while slightly higher selectivity was obtained on the methyl-derivatized CF6 column for two of the compounds. However, in those two cases, the IP-CSP gave better or the same resolution, due to its higher efficiency. In most cases the aromatic derivatized RN-CSP gave the poorest enantioselectivities and resolutions. Compared to all other columns (Figure 7.2), the isopropyl-derivatized CF6 CSP provided higher selectivity and/or higher efficiency, and it produced baseline separations of all racemic primary amines tested.

Furthermore, thiocarbamate linkages between CF6 and various functional groups also were tested using the analogous isothiocyanate derivatization reagent. A comparison of the separations obtained from CF6 after derivatization with methyl isocyanate versus methyl isothiocyanate is shown in Figure 7.7. The methyl-functionalized CSP based on the carbamate linkage produced significantly higher selectivity and resolution.

For primary amines, enantioresolution was observed in both the polar organic mode and normal phase mode (shown in Figure 7.8). While operating under normal phase conditions, both acidic additives (trifluoroacetic acid) and basic additives (butylamine) were tested. In this instance, the acidic modifier is thought to act to maintain an ion-pair. Fronting asymmetric wide peaks were always observed in the normal phase mode with an acidic additive, due to strong

interactions between basic analyte and the weakly acidic silica-based stationary phase. The selectivity of primary amines on the CF6 column was lost in most cases when using a butylamine additive, although symmetric peaks were observed (data not shown). The effect of butylamine in decreasing the retention and selectivity can be attributed to the fact that this basic additive simply competes with basic analytes for the primary interaction sites on the chiral stationary phase. In the polar organic mode, better resolution ( $R_s=1.6$ ) was observed due to good selectivity ( $\alpha=1.16$ ) and highest efficiency (symmetric sharp peaks). However, higher enantioselectivity ( $\alpha=1.25$ ) often was obtained in the normal phase mode. This trend is true for all tested primary amines: better resolution was obtained in the polar organic mode. All primary amines were baseline separated using the same or similar mobile phase compositions, which streamlines the method development process. In addition, the polar organic mode offers other advantages, for example, short analysis times, low back-pressure, and better analyte solubility in the mobile phase. In order to evaluate the effects of acidic and basic additives in the polar organic mode on the separation of primary amines, different types and amounts of basic additives were investigated and the results are shown in Table 7.4. The highest enantioselectivity was obtained using the combination of triethylamine and acetic acid as additives. Also, the ratio of acidic/basic additives has been optimized and it was determined that addition of 0.3% acetic acid/0.2% triethylamine commonly results in highest selectivity.

The most important feature of the derivatized-CF6 CSPs is their extremely high success rate for separating primary amines. Indeed, 100% of the tested primary amines were baseline separated. Currently, the most effective CSPs available for separating racemic primary amines are synthetic chiral crown ether-based stationary phases.<sup>197-201</sup> However, their applications are intrinsically restricted to primary amines, with the partial exception of 18-crown-6 tetracarboxylic acid. Furthermore, strong acidic, aqueous mobile phases are always necessary to protonate and separate these primary amines. The derivatized CF6-based CSPs differ significantly from all other crown ether-based ones, in that they work best in polar organic and normal phase

solvents for separating primary amines, and their applications are not always limited to primary amines.

Table 7.3 Chromatographic data of primary amines separated on derivatized-CF6 CSPs

| #  | Compound name                             | CSP <sup>a</sup> | k <sub>1</sub> | α    | Rs  | Mobile phase <sup>b</sup> |
|----|---|------------------|----------------|------|-----|---------------------------|
| 1  | trans-1-Amino-2-indanol                   | IP               | 2.85           | 1.31 | 3.9 | 60A40M0.3AA0.2T           |
|    |   | ME               | 2.44           | 1.28 | 3.5 | 60A40M0.3AA0.2T           |
|    |   | RN-L             | 1.43           | 1.23 | 1.6 | 60A40M0.3AA0.2T           |
| 2  | cis-1-Amino-2-indanol                     | IP               | 2.69           | 1.12 | 1.6 | 60A40M0.3AA0.2T           |
|    |   | ME               | 2.47           | 1.10 | 1.5 | 60A40M0.3AA0.2T           |
|    |   | RN-L             | 3.00           | 1.07 | 0.8 | 75A25M0.3AA0.2T           |
| 3  | Normetanephrine hydrochloride             | IP               | 5.83           | 1.16 | 2.6 | 60A40M0.3AA0.2T           |
|    |   | RN-L             | 2.84           | 1.15 | 1.6 | 60A40M0.3AA0.2T           |
|    |   | ME               | 5.24           | 1.14 | 2.0 | 60A40M0.3AA0.2T           |
| 4  | DL-Octopamine hydrochloride               | IP               | 6.09           | 1.14 | 2.1 | 60A40M0.3AA0.2T           |
|    |   | ME               | 5.46           | 1.12 | 1.8 | 60A40M0.3AA0.2T           |
|    |   | RN-L             | 2.74           | 1.10 | 1.5 | 60A40M0.3AA0.2T           |
| 5  | Phenylpropanolamine hydrochloride         | IP               | 3.64           | 1.13 | 2.2 | 60A40M0.3AA0.2T           |
|    |   | RN-L             | 1.81           | 1.13 | 1.6 | 60A40M0.3AA0.2T           |
|    |   | ME               | 3.17           | 1.11 | 1.9 | 60A40M0.3AA0.2T           |
| 6  | 1-Aminoindan                              | IP               | 3.90           | 1.17 | 3.1 | 60A40M0.3AA0.3T           |
|    |   | RN-L             | 3.21           | 1.17 | 2.1 | 60A40M0.3AA0.2T           |
|    |   | ME               | 3.37           | 1.15 | 2.7 | 60A40M0.3AA0.2T           |
| 7  | 1,1-Diphenyl-2-aminopropane               | IP               | 1.12           | 1.09 | 1.5 | 60A40M0.3AA0.2T           |
|    |   | RN-L             | 3.31           | 1.07 | 1.5 | 85A15M0.3AA0.2T           |
|    |   | ME               | 1.94           | 1.07 | 1.3 | 75A25M0.3AA0.2T           |
| 8  | 2-Amino-1-(4-nitrophenyl)-1,3-propanediol | ME               | 2.40           | 1.18 | 1.9 | 60A40M0.3AA0.2T           |
|    |   | IP               | 2.16           | 1.15 | 2.3 | 60A40M0.3AA0.2T           |
|    |   | RN-L             | 6.74           | 1.14 | 1.7 | 85A15M0.3AA0.2T           |
| 9  | α-Methylbenzylamine                       | ME               | 3.07           | 1.17 | 1.5 | 60A40M0.3AA0.2T           |
|    |   | IP               | 2.77           | 1.15 | 1.5 | 60A40M0.3AA0.2T           |
|    |   | RN-L             | 8.12           | 1.09 | 0.8 | 85A15M0.3AA0.2T           |
| 10 | DL-Tryptophanol                           | IP               | 3.39           | 1.15 | 2.7 | 60A40M0.3AA0.2T           |
|    |   | ME               | 3.03           | 1.12 | 1.7 | 60A40M0.3AA0.2T           |
|    |   | RN-L             | 4.66           | 1.12 | 1.4 | 75A25M0.3AA0.2T           |
| 11 | 1,2,2-Triphenylethylamine                 | IP               | 1.14           | 1.16 | 1.6 | 75A25M0.3AA0.2T           |
|    |   | ME               | 0.48           | 1.07 | 0.6 | 75A25M0.3AA0.2T           |

<sup>a</sup>Abbreviations: ME, methyl carbamate-CF6 CSP; IP, isopropyl carbamate-CF6 CSP; RN-L, R-naphthylethyl carbamate-CF6 CSP with a low substitution degree. <sup>b</sup>Abbreviations of mobile phases: A: acetonitrile; M: methanol; AA: acetic acid; T: triethylamine.

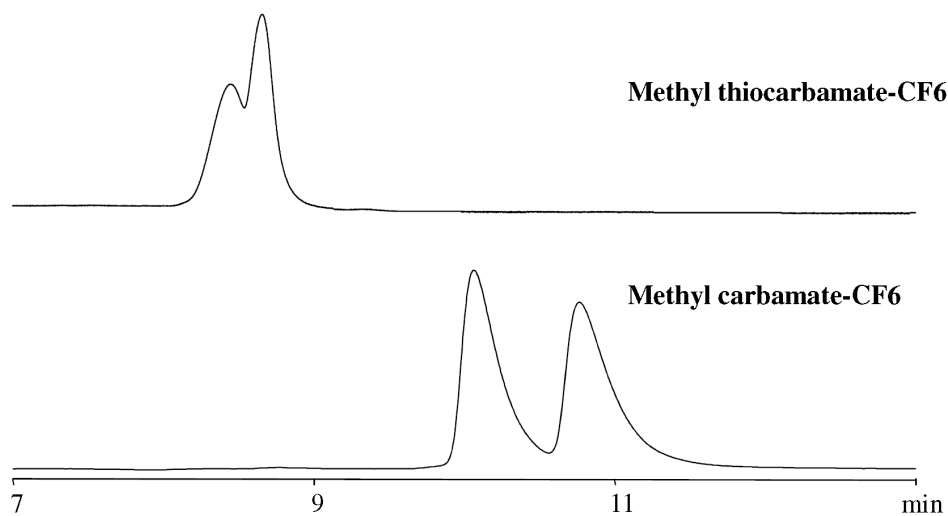


Figure 7.7 Comparison between methyl carbamate- and methyl thiocarbamate-CF6 CSPs. The analyte and mobile phase are *cis*-1-amino-2-indanol, and 60ACN/40MEOH/0.3AA/0.2TEA, respectively.

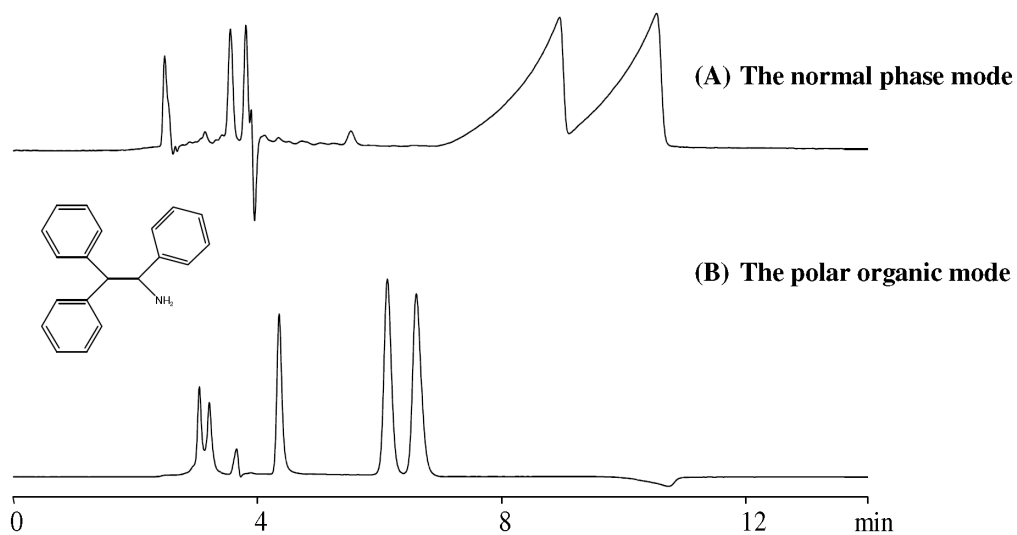


Figure 7.8 Separation of 1,2,2-triphenylethylamine on the IP-CF6 column. The chromatographic data and mobile phases are: (A)  $k_1=2.09$ ,  $\alpha=1.25$ ,  $R_s=1.4$ , 70heptane/30ETOH/0.1TFA; (B)  $k_1=1.14$ ,  $\alpha=1.16$ ,  $R_s=1.6$ , 75ACN/25MEOH/0.3AA/0.2TEA.

Table 7.4 Additive effect of separation of ( $\pm$ ) trans-1-amino-2-indanol (primary amine type) in the polar organic mode on the IP-CF6 column

|   |                | $k_1$ | $\alpha$ | $R_s$ |
|---|----------------|-------|----------|-------|
| Change basic additive type <sup>a</sup>   | triethylamine  | 2.85  | 1.31     | 4.0   |
|   | trimethylamine | 3.36  | 1.29     | 5.3   |
|   | ethanolamine   | 1.97  | 1.14     | 2.6   |
|   | diethylamine   | 3.67  | 1.29     | 1.6   |
| Change additive amount ratio <sup>b</sup> | 0.30AA/0.20TEA | 2.85  | 1.31     | 4.0   |
|   | 0.20AA/0.30TEA | 2.69  | 1.24     | 3.9   |
|   | 0.25AA/0.25TEA | 3.24  | 1.27     | 4.4   |

<sup>a</sup>The mobile phase is composed of 60%acetonitrile/40%methanol/0.3%acetic acid (equals 52mM) /14 mM basic additive. <sup>b</sup>Volume percentage.

#### 7.3.4 Cyclofructan CSPs based on aromatic-functionalized CF6

Ten different CSPs were made which consisted of silica bonded cyclofructan, highly functionalized with ten different aromatic moieties (See Fig. 7.2). Their respective chromatographic performances were evaluated by injecting all 70 probe molecules (non primary amine types). Among these ten aromatic derivatized-CF6 CSPs, four CSPs appeared to produce superior results. They are: 3,5-dimethylphenyl (DMP), 3,5-dichlorophenyl (DCP), R-1-(1-naphthyl)ethyl (RN), and S- $\alpha$ -methylbenzyl (SMP). The chromatographic data of the 70 probe analytes on these four columns are listed in Table 5. If one analyte is separated on more than one columns, the results are listed in descending order of selectivity. If the IP-functionalized CSP showed an enantioseparation, the data also was included for comparison purposes. Chromatograms of four representative separations under optimized conditions are shown in Figure 7.9. In summary, 40 analytes out of 70 were separated, including 35 baseline ( $R_s \geq 1.5$ ) and 5 partial resolution ( $0.3 < R_s < 1.5$ ). Table 7.5 clearly demonstrates the aromatic derivatized-CF6 columns show excellent enantioselectivity toward various types of analytes, including acids, secondary amines, tertiary amines, alcohols, and others. Although they are not universally effective for all of the tested enantiomers, the variety of compounds separated by derivatized-CF6 was encouraging.

Table 7.5 Chromatographic data of other compounds separated on six derivatized-CF6 stationary phases in optimized conditions

| #                                    | Compound name  | CSP <sup>a</sup> | k <sub>1</sub> | $\alpha$ | Rs  | Mobile phase <sup>b</sup> |
|--------------------------------------|--|------------------|----------------|----------|-----|---------------------------|
| <b>Acids</b>                         |  |                  |                |          |     |                           |
| 1                                    | O-Acetylmandelic acid  | IP               | 11.00          | 1.04     | 1.2 | 98H2E0.1TFA               |
|                                      |  | SMP              | 9.86           | 1.04     | 0.9 | 98H2E0.1TFA               |
| 2                                    | 2,3-Dibenzoyl-DL-tartaric acid                                     | IP               | 5.93           | 1.08     | 1.0 | 99A1M0.3AA0.2T            |
|                                      |  | RN               | 7.74           | 1.04     | 1.2 | 99.8A0.2M0.3AA0.2T        |
| 3                                    | Ketorolac  | IP               | 8.30           | 1.03     | 0.9 | 95H5E0.1TFA               |
|                                      |  | SMP              | 4.77           | 1.03     | 0.6 | 90H10E0.1TFA              |
|                                      |  | RN               | 4.65           | 1.03     | 0.6 | 90H10E0.1TFA              |
| 4                                    | Phenethylsulfamic acid   | IP               | 3.24           | 1.14     | 2.6 | 60A40M0.3AA0.2T           |
|                                      |  | SMP              | 3.18           | 1.13     | 0.8 | 70H30E0.1TFA              |
|                                      |  | RN               | 5.90           | 1.10     | 1.3 | 80A20M0.3AA0.2T           |
|                                      |  | DMP              | 2.03           | 1.10     | 0.6 | 70H30E/0.1TFA             |
| 5                                    | 1-Methyl-6,7-dihydroxy-1,2,3,4-tetrahydroisoquinoline hydrobromide | RN               | 8.87           | 1.16     | 1.6 | 70H30E0.1TFA              |
|                                      |  | SMP              | 7.19           | 1.14     | 2.2 | 70H30E0.1TFA              |
|                                      |  | IP               | 2.74           | 1.11     | 1.8 | 60A40M0.3AA0.2T           |
|                                      |  | DMP              | 4.12           | 1.07     | 1.2 | 70H30E0.1TFA              |
| <b>Secondary and tertiary amines</b> |  |                  |                |          |     |                           |
| 1                                    | Bis-[(R/S)-1-phenylethyl]amine HCl                                 | RN               | 4.04           | 1.16     | 2.5 | 90H10E0.1TFA              |
|                                      |  | SMP              | 7.07           | 1.13     | 1.5 | 98H2E0.1TFA               |
| 2                                    | Bendroflumethiazide  | RN               | 5.50           | 1.16     | 2.3 | 70H30E0.1TFA              |
|                                      |  | SMP              | 4.27           | 1.03     | 0.5 | 70H30E0.1TFA              |
| 3                                    | Tröger's base  | DMP              | 0.95           | 1.59     | 5.7 | 70H30E                    |
|                                      |  | RN               | 0.96           | 1.53     | 4.2 | 70H30E                    |
|                                      |  | DCP              | 1.25           | 1.28     | 2.0 | 80H20E                    |
|                                      |  | SMP              | 0.94           | 1.19     | 1.5 | 80H20E                    |
|                                      |  | IP               | 0.62           | 1.11     | 0.9 | 80H20E                    |
| 4                                    | Orphenadrine citrate salt  | DCP              | 8.28           | 1.51     | 3.0 | 80H20E                    |
| 5                                    | Diperodon hydrochloride  | DCP              | 2.89           | 1.21     | 1.2 | 80H20E                    |
|                                      |  | SMP              | 10.36          | 1.06     | 0.7 | 70H30E0.1TFA              |
| <b>Amino acid derivatives</b>        |  |                  |                |          |     |                           |
| 1                                    | N-(3,5-dinitrobenzoyl)-DL-leucine                                  | RN               | 0.80           | 1.91     | 4.4 | 50H50E0.1TFA              |
|                                      |  | DMP              | 5.54           | 1.12     | 2.3 | 90H10E0.1TFA              |
|                                      |  | SMP              | 1.85           | 1.11     | 1.5 | 80H20E0.1TFA              |
|                                      |  | DCP              | 7.45           | 1.06     | 0.6 | 80H20E0.1TFA              |
| 2                                    | N-(3,5-Dinitrobenzoyl)-DL-phenylglycine                            | RN               | 7.22           | 1.12     | 1.8 | 70H30E0.1TFA              |
|                                      |  | DMP              | 11.01          | 1.08     | 1.5 | 90H10E0.1TFA              |
|                                      |  | SMP              | 10.80          | 1.05     | 1.1 | 90H10E0.1TFA              |
| 3                                    | Carbobenzyloxy-alanine   | SMP              | 3.83           | 1.10     | 1.6 | 90H10E0.1TFA              |
|                                      |  | DCP              | 6.49           | 1.06     | 1.3 | 95H5E0.1TFA               |
| 4                                    | N-Benzoyl-DL-phenylalanine   | SMP              | 4.49           | 1.19     | 3.2 | 90H10E0.1TFA              |

Table 7.5-continued

|                 |   |     |       |      |     |               |
|-----------------|---|-----|-------|------|-----|---------------|
|                 | $\beta$ -naphthyl ester                                     | DMP | 4.00  | 1.10 | 1.7 | 90H10I0.1TFA  |
|                 |   | IP  | 6.19  | 1.08 | 1.5 | 95H5E0.1TFA   |
|                 |   | RN  | 10.25 | 1.06 | 0.6 | 95H5E0.1TFA   |
|                 |   | DCP | 3.63  | 1.05 | 0.7 | 90H10I0.1TFA  |
| 5               | 3,5-Dinitrobenzoyl-tryptophan methyl ester                  | RN  | 3.99  | 1.17 | 2.2 | 50H50E0.1TFA  |
|                 |   | SMP | 2.76  | 1.10 | 1.5 | 70H30E0.1TFA  |
|                 |   | DMP | 5.19  | 1.09 | 1.5 | 80H20E0.1TFA  |
| 6               | N-2,4-Dinitrophenyl-DL-norleucine                           | DMP | 5.54  | 1.10 | 1.7 | 95H5I0.1TFA   |
|                 |   | RN  | 10.91 | 1.07 | 1.3 | 95H5E0.1TFA   |
| 7               | Dansyl-norleucine cyclohexylammonium salt                   | SMP | 6.95  | 1.07 | 1.4 | 90H10E0.1TFA  |
|                 |   | DMP | 15.05 | 1.05 | 1.2 | 95H5E0.1TFA   |
|                 |   | IP  | 6.93  | 1.04 | 0.8 | 90H10E0.1TFA  |
| <b>Alcohols</b> |   |     |       |      |     |               |
| 1               | $\alpha$ -Methyl-9-anthracenemethanol                       | RN  | 5.05  | 1.08 | 1.7 | 98H2I0.1TFA   |
|                 |   | DMP | 7.61  | 1.03 | 0.7 | 99H1I0.1TFA   |
|                 |   | SMP | 5.18  | 1.02 | 0.5 | 98H2E0.1TFA   |
| 2               | Benzoin   | DMP | 5.91  | 1.07 | 1.5 | 99H1I0.1TFA   |
|                 |   | SMP | 4.89  | 1.05 | 1.3 | 98H2E0.1TFA   |
|                 |   | RN  | 6.22  | 1.04 | 0.8 | 98H2E0.1TFA   |
| 3               | N,N'-Dibenzyl-tartramide                                    | DMP | 18.03 | 1.10 | 1.5 | 95H5I0.1TFA   |
|                 |   | DCP | 3.34  | 1.10 | 1.2 | 80H20E0.1TFA  |
|                 |   | RN  | 11.30 | 1.06 | 1.3 | 90H10E0.1TFA  |
|                 |   | SMP | 9.26  | 1.05 | 0.8 | 90H10E0.1TFA  |
| 4               | furoin  | IP  | 9.91  | 1.03 | 1.3 | 95H5E0.1TFA   |
|                 |   | DMP | 9.98  | 1.03 | 0.6 | 98H2E0.1TFA   |
|                 |   | SMP | 5.64  | 1.02 | 0.5 | 90H10E/0.1TFA |
| 5               | Cromakalim  | DMP | 16.00 | 1.05 | 1.5 | 95H5E0.1TFA   |
|                 |   | DCP | 8.69  | 1.05 | 1.1 | 90H10E0.1TFA  |
|                 |   | RN  | 8.84  | 1.02 | 0.4 | 90H10E0.1TFA  |
| <b>Others</b>   |   |     |       |      |     |               |
| 1               | 1,1'-Bi(2-naphthyl diacetate)                               | IP  | 0.40  | 1.35 | 2.9 | 70H30E        |
|                 |   | DMP | 0.74  | 1.21 | 1.7 | 70H30E        |
|                 |   | SMP | 0.77  | 1.17 | 1.9 | 70H30E        |
|                 |   | RN  | 1.79  | 1.11 | 1.6 | 90H10E0.1TFA  |
|                 |   | DCP | 1.15  | 1.08 | 1.1 | 90H10E0.1TFA  |
| 2               | 5,5',6,6',7,7',8,8'-Octahydro(1,1'-binaphthalene)-2,2'-diol | DMP | 5.47  | 1.18 | 2.8 | 99H1I0.1TFA   |
|                 |   | RN  | 5.34  | 1.11 | 1.9 | 98H2E0.1TFA   |
|                 |   | SMP | 4.47  | 1.09 | 1.5 | 98H2E0.1TFA   |
| 3               | 2,2'-Diamino-1,1'-binaphthalene                             | DMP | 1.43  | 1.45 | 5.3 | 70H30E        |
|                 |   | DCP | 1.77  | 1.22 | 2.0 | 80H20E        |
|                 |   | SMP | 1.91  | 1.20 | 3.1 | 70H30E        |
|                 |   | RN  | 2.31  | 1.18 | 2.8 | 70H30E        |
|                 |   | IP  | 2.15  | 1.16 | 3.0 | 80H20E        |
| 4               | 6,6'-Dibromo-1,1'-bi-2-naphthol                             | DMP | 0.74  | 1.58 | 4.7 | 70H30E        |

Table 7.5-continued

|    |   |     |       |      |     |               |
|----|---|-----|-------|------|-----|---------------|
|    |   | DCP | 2.13  | 1.24 | 5.0 | 90H10E        |
|    |   | SMP | 0.93  | 1.19 | 2.1 | 70H30E        |
|    |   | RN  | 1.17  | 1.15 | 1.5 | 70H30E        |
|    |   | IP  | 3.63  | 1.07 | 1.5 | 90H10E        |
| 5  | Althiazide  | RN  | 2.83  | 1.16 | 1.9 | 50H50E0.1TFA  |
|    |   | DMP | 8.80  | 1.04 | 0.7 | 80H20E0.1TFA  |
|    |   | IP  | 8.29  | 1.02 | 0.8 | 70H30E0.1TFA  |
|    |   | SMP | 7.10  | 1.02 | 0.5 | 70H30E/0.1TFA |
| 6  | 1,1'-Bi-2-naphthol<br>bis(trifluoromethanesulfonate)                          | SMP | 3.84  | 1.17 | 2.0 | 100H          |
|    |   | IP  | 1.17  | 1.08 | 1.5 | 100H          |
|    |   | RN  | 6.13  | 1.08 | 1.3 | 100H          |
| 7  | cis-4,5-Diphenyl-2-oxazolidinone  | DMP | 5.41  | 1.09 | 1.6 | 90H10I0.1TFA  |
|    |   | RN  | 6.82  | 1.04 | 0.8 | 90H10I0.1TFA  |
| 8  | 2,3-Dihydro-7a-methyl-3-<br>phenylpyrrolo[2,1-b]oxazol-5(7aH)-<br>one         | RN  | 3.20  | 1.12 | 1.9 | 85H15I0.1TFA  |
|    |   | DMP | 5.13  | 1.05 | 1.1 | 98H2E0.1TFA   |
|    |   | SMP | 2.46  | 1.03 | 0.7 | 98H2E0.1TFA   |
|    |   | DCP | 2.67  | 1.02 | 0.6 | 90H10E0.1TFA  |
| 9  | Ethyl 11-cyano-9,10-dihydro-endo-<br>9,10-ethanoanthracene-11-<br>carboxylate | SMP | 1.44  | 1.13 | 2.0 | 90H10I0.1TFA  |
|    |   | RN  | 3.21  | 1.08 | 1.5 | 98H2E0.1TFA   |
|    |   | IP  | 1.42  | 1.08 | 1.5 | 95H5E0.1TFA   |
|    |   | DMP | 2.07  | 1.03 | 0.5 | 98H2E0.1TFA   |
| 10 | Lormetazepam  | SMP | 3.87  | 1.08 | 1.5 | 80H20E0.1TFA  |
|    |   | IP  | 8.46  | 1.06 | 1.5 | 90H10E0.1TFA  |
|    |   | RN  | 5.02  | 1.04 | 0.7 | 80H20E0.1TFA  |
| 11 | 3a,4,5,6-Tetrahydro-succininido[3,4-b]<br>acenaphthen-10-one                  | SMP | 2.36  | 1.13 | 2.2 | 70H30E0.1TFA  |
|    |   | IP  | 2.14  | 1.12 | 1.9 | 70H30E0.1TFA  |
|    |   | RN  | 3.25  | 1.10 | 1.5 | 70H30E0.1TFA  |
|    |   | DMP | 7.35  | 1.08 | 1.5 | 90H10E0.1TFA  |
| 12 | 3-(alpha-Acetyl-4-chlorobenzyl)-4-<br>hydroxycoumarin                         | DMP | 5.35  | 1.17 | 2.0 | 90H10I0.1TFA  |
|    |   | SMP | 5.16  | 1.14 | 2.2 | 90H10E0.1TFA  |
|    |   | RN  | 15.94 | 1.10 | 1.6 | 95H5E0.1TFA   |
|    |   | DCP | 4.65  | 1.10 | 1.4 | 90H10E0.1TFA  |
|    |   | IP  | 4.61  | 1.09 | 1.5 | 90H10E0.1TFA  |
| 13 | Warfarin  | DMP | 9.87  | 1.10 | 1.6 | 95H5I0.1TFA   |
|    |   | SMP | 7.19  | 1.08 | 0.9 | 90H10I0.1TFA  |
|    |   | DCP | 4.98  | 1.07 | 0.8 | 90H10E0.1TFA  |
|    |   | RN  | 11.94 | 1.05 | 1.2 | 95H5E0.1TFA   |
|    |   | IP  | 4.60  | 1.02 | 0.5 | 90H10E0.1TFA  |
| 14 | Fipronil  | SMP | 16.03 | 1.09 | 2.0 | 98H2E0.1TFA   |
|    |   | IP  | 2.83  | 1.08 | 1.5 | 90H10E0.1TFA  |
|    |   | RN  | 12.02 | 1.07 | 1.5 | 97H3E0.1TFA   |
|    |   | DCP | 0.55  | 1.03 | 0.4 | 80H20E        |
| 15 | trans-Stilbene oxide  | IP  | 0.62  | 1.10 | 1.3 | 100H          |
|    |   | SMP | 2.02  | 1.09 | 1.5 | 100HEP        |

Table 7.5-continued

|    |   |     |       |      |     |              |
|----|---|-----|-------|------|-----|--------------|
| 16 | Thalidomide                             | RN  | 2.75  | 1.07 | 1.0 | 100HEP       |
|    |   | SMP | 5.89  | 1.10 | 1.9 | 70H30E0.1TFA |
|    |   | DMP | 8.03  | 1.08 | 1.5 | 80H20E0.1TFA |
|    |   | DCP | 10.69 | 1.05 | 1.0 | 80H20E       |
| 17 | 3,5-Dinitrobenzoyl-2-aminoheptane       | RN  | 7.85  | 1.04 | 0.7 | 70H30E0.1TFA |
|    |   | RN  | 1.68  | 1.15 | 2.2 | 80H20E0.1TFA |
| 18 | 3,5-Dinitro-N-(1-phenylethyl)-benzamide | RN  | 1.24  | 1.92 | 8.2 | 50H50E0.1TFA |
|    |   | SMP | 0.93  | 1.14 | 1.5 | 70H30E0.1TFA |

<sup>a</sup>Abbreviations of CSPs: DMP, dimethylphenyl carbamate-CF6 CSP; DCP, dichlorophenyl carbamate-CF6 CSP; RN, R-naphthylethyl carbamate-CF6 CSP; SMP, S-methylbenzyl carbamate-CF6 CSP. IP, isopropyl carbamate-CF6 CSP; ME, methyl carbamate-CF6 CSP.

<sup>b</sup>Abbreviations of mobile phases: H: heptane; I: isopropanol; E: ethanol; A: acetonitrile; M: methanol; AA: acetic acid; T: triethylamine; TFA: trifluoroacetic acid.

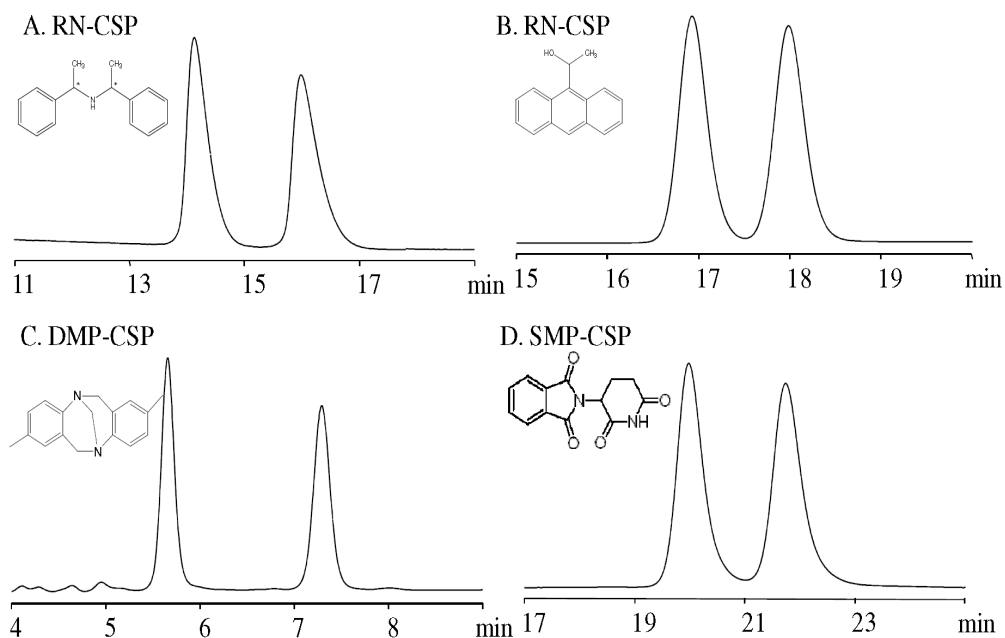


Figure 7.9 Selected chromatograms showing enantioseparations of various analytes on different derivatized-CF6 columns. The analytes and mobile phases are: (A) Bis-[(R/S)-1-phenylethyl]amine, 90H10E0.1TFA; (B) α-Methyl-9-anthracenemethanol, 98heptane/2IPA/0.1TFA; (C) Tröger's base, 70heptane/30ETOH; (D) Thalidomide, 70heptane/30ETOH/0.1TFA.

Table 7.5 clearly demonstrates that the nature of the aromatic group plays a major role in chiral recognition. The aromatic-functionalized CF6 CSPs demonstrate complementary capability of enantiomeric selectivities, in that some analytes were baseline separated on one column, while only a partial separation or no separation was observed on other aromatic functionalized CF6 columns. Figure 7.10 illustrates this complementary behavior for 3,5-dinitro-N-(1-phenylethyl)benzamide which was well separated ( $R_s=8.2$ ) on the RN-CF6 column with an extremely high selectivity ( $\alpha=1.92$ ), and also baseline separated ( $\alpha=1.14$ ,  $R_s=1.5$ ) on the SMP column. However, a single peak was observed using the DMP-CF6 and DCP-CF6 columns. The stereogenic center of 3,5-dinitro-N-(1-phenylethyl)benzamide is directly attached to a phenyl ring, which participates in  $\pi$ - $\pi$  interactions with the aromatic moieties of the derivatized CF6. Compared to DMP, both RN and SMP contain a stereogenic center, directly connected to the aromatic ring (phenyl or naphthyl), which may be beneficial for chiral recognition of this analyte.

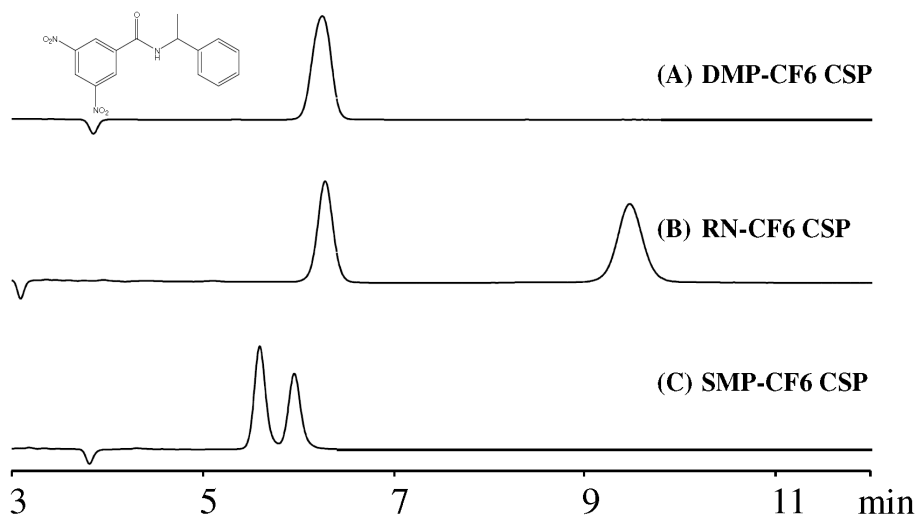


Figure 7.10 Complimentary character of the aromatic-derivatized CF6 CSPs. The analyte is 3,5-dinitro-N-(1-phenylethyl)benzamide. The CSPs and mobile phases are: (A) 3,5-dimethylphenyl carbamate-CF6 CSP, 70heptane/30ETOH/0.1TFA; (B) R-naphthylethyl carbamate-CF6 CSP, 50heptane/50ETOH/0.1TFA; (C) S- $\alpha$ -methylphenyl carbamate-CF6 CSP, 70heptane/30ETOH/0.1TFA.

One advantage for all CF6-based CSPs is their excellent stability. These columns are stable in all common organic solvents and no detrimental changes in column performance was observed after more than 1000 injections. The selection of the mobile phase is an important parameter in enantioselective chromatography. Therefore, it was necessary to compare all three operation modes (i.e., the normal phase mode, polar organic mode, and the reversed phase mode) when evaluating these CF6-based columns. Further, the effects of other experimental factors, such as alcohol modifier type in the normal phase mode, and the column temperature on the separations were studied. Such fundamental information offers guidance for method development.

For neutral and acidic compounds, better resolution was typically obtained in the normal phase mode. Figure 7.11 shows one example comparing the reversed phase mode and normal phase mode. 6,6'-Dibromo-1,1'-bi-2-naphthol is baseline separated ( $\alpha=1.58$ ,  $R_s=4.7$ ) using 70%heptane/30%ethanol, while only a tiny peak split ( $\alpha=1.03$ ,  $R_s=0.6$ ) was observed using the reversed phase mode. With the polar organic mobile phase, no retention of this analyte was obtained. Water in the reversed phase system may compete too effectively for hydrogen bonding sites on the chiral stationary phase, and thus it has a negative effect on the separation of enantiomeric compounds. It is well known that certain interactions are enhanced in less polar solvents.<sup>30, 36, 39, 202</sup> Specifically these are  $\pi$ - $\pi$ , n- $\pi$ , dipolar and hydrogen bonding interactions. Since these CSPs are effective mainly in the normal phase mode and polar organic mode, these must be the dominant associative interactions, while steric repulsion is important in all solvent systems.

In the normal phase mode, ethanol and isopropanol are commonly used as alcohol modifiers. Ordinarily, the ethanol modifier yields good enantioselectivity, better peak efficiency, and faster elution, therefore it was chosen as the primary polar organic modifier. Isopropanol also was tested for further optimization, because in some cases higher enantioselectivity is

observed using isopropanol rather than ethanol (Figure 7.12). The value of  $\alpha$  for the enantioseparation of N-benzoyl-DL-phenylalanine  $\beta$ -naphthyl ester is improved from 1.05 to 1.10, when replacing ethanol with isopropanol.

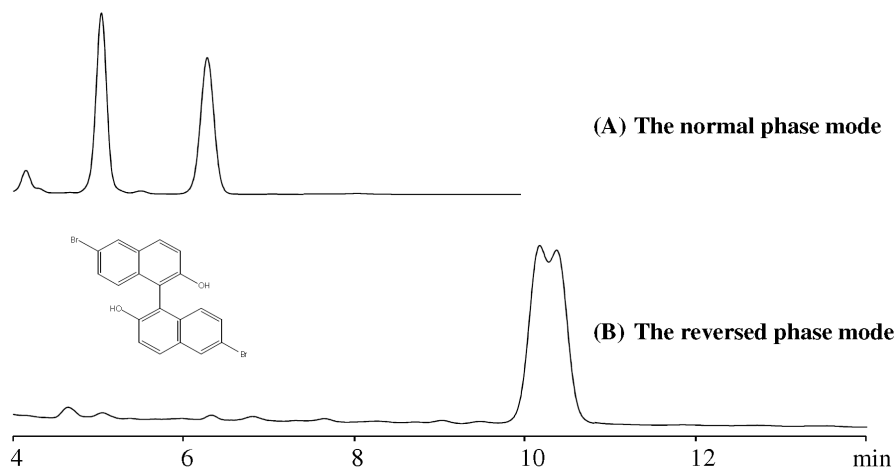


Figure 7.11 Separation of 6,6'-dibromo-1,1'-bi-2-naphthol in the normal phase mode and reversed phase mode on the DMP-CF6 column. The chromatographic data and mobile phases are: (A)  $k_1=0.74$ ,  $\alpha=1.58$ ,  $R_s=4.7$ , 70heptane/30ETOH; (B)  $k_1=2.51$ ,  $\alpha=1.03$ ,  $R_s=0.6$ , 50ACN/50water.

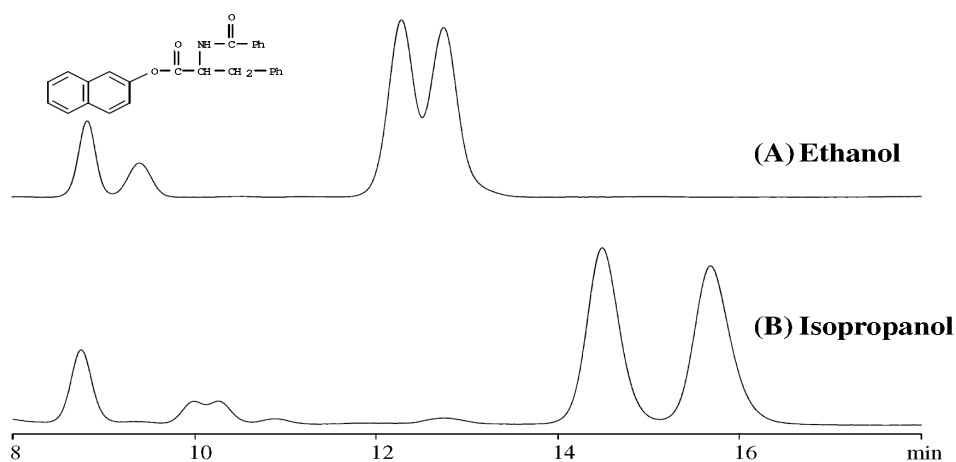


Figure 7.12 Effect of alcohol modifier on enantioseparation in the normal phase mode on the DMP-CF6 column. The mobile phase is 90heptane/10 alcohol modifier. The analyte is N-benzoyl-DL-phenylalanine  $\beta$ -naphthyl ester. The chromatographic data are: (A)  $k_1=3.23$ ,  $\alpha=1.05$ ,  $R_s=0.8$ ; (B)  $k_1=4.00$ ,  $\alpha=1.10$ ,  $R_s=1.7$ .

At lower temperatures, enantioselectivity usually increases, at the expense of efficiency. Figure 7.13 illustrates that reducing the column temperature from 20 °C to 0 °C significantly improves enantioselectivity and resolution. Therefore, lowering the column temperature is another strategy to optimize enantioseparations with these CSPs, as it is with most other CSPs.

In order to assess the potential for preparative HPLC, it is necessary to perform loading tests on any new stationary phases. Sample loading was examined by injecting N-(3,5-dinitrobenzoyl)-phenylglycine on the RN-CF6 column in the polar organic mode. Figure 7.14 shows that 4200 µg of this racemate has been baseline separated on an analytical column. It should be noted that the injection amount was limited by the solubility of the analyte in the mobile phase. It is clear that more sample could be loaded while maintaining baseline resolution. These brush-type CSPs based on derivatized-CF6 demonstrate great potential for preparative HPLC.<sup>75, 203, 204</sup> In addition, comprehensive SFC investigations of these cyclofructan-based CSPs are under way and a representative chromatogram is shown in Figure 7.15.

Most recently, we have begun to study the cyclofructan containing seven units (CF7) as a chiral selector. Preliminary studies show that the derivatized-CF7 CSP also successfully separates various types of analytes and an initial result is shown in Figure 7.16. It is worth mentioning that this analyte was only partially separated by all derivatized-CF6 columns. This demonstrates that the dimethylphenyl carbamate-CF7 likely has somewhat different enantioselectivities. This work is on-going and will be presented in a subsequent publication.

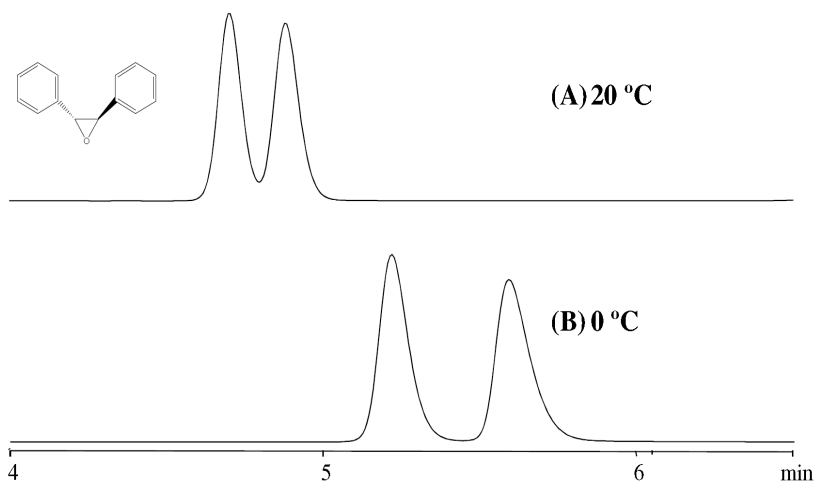


Figure 7.13 Temperature effect on separation of trans-stilbene oxide on the IP-CF6 column. The mobile phase is 100% heptane. The chromatographic data: (A)  $k_1=0.62$ ,  $\alpha=1.10$ ,  $R_s=1.3$ ; (B)  $k_1=0.80$ ,  $\alpha=1.16$ ,  $R_s=2.0$ .

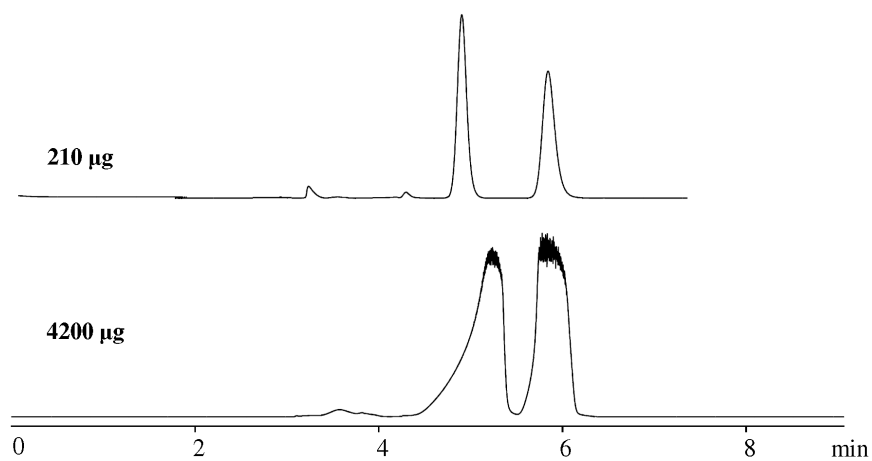


Figure 7.14 Loading test on the RN-CF6 column. The analyte is N-(3,5-dinitrobenzoyl)-DL-phenylglycine. The mobile phase is 85ACN/15MEOH/0.3AA/0.2TEA. Injection volumes are: 5µL (top) and 100µL (bottom). UV detection: 350 nm.

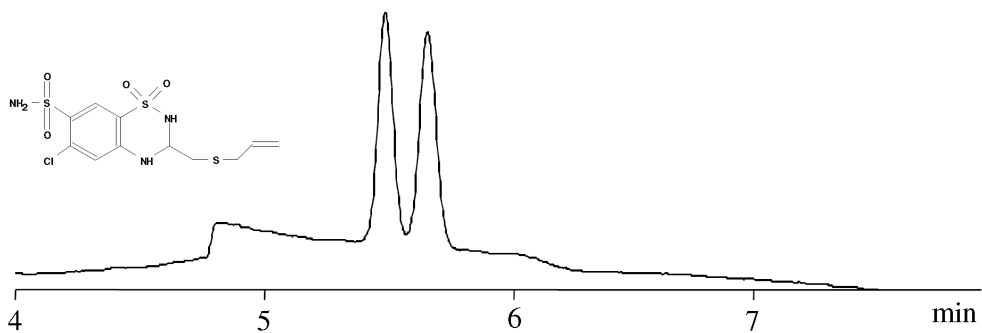


Figure 7.15 SFC chromatogram of althiazide on the RN-CF6 column. The gradient mobile phase is as described in EXPERIMENTAL SECTION.

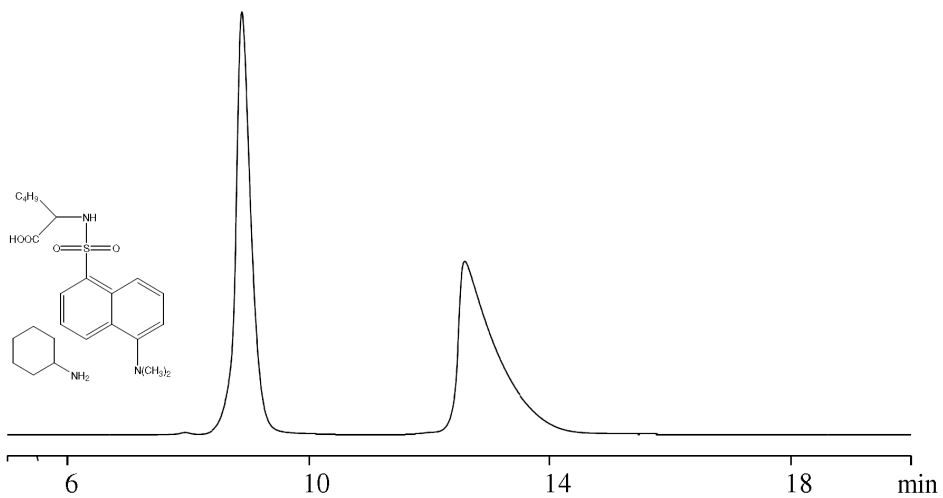


Figure 7.16 Separation of dansyl-norleucine cyclohexylammonium salt on the dimethylphenyl carbamate-CF7 CSP. The mobile phase is 80heptane/20ETOH/0.1TFA.

#### 7.4 Conclusions

Cyclofructans are a completely new class of chiral selectors. While native cyclofructan 6 has limited capabilities as a chiral selector, specific, derivatized cyclofructans appear to be exceptional chiral selectors which can be “tuned” to separate enantiomers of different types of molecules. Partial derivatization of the cyclofructan hydroxyl groups appears to disrupt internal hydrogen bonding and “relax” the structure. When “lightly” derivatized with aliphatic functionalities, CF6 becomes exceptionally adept at separating enantiomers of primary amines and does so in organic solvents and supercritical CO<sub>2</sub>. This is in contrast to all known chiral crown ether CSPs that work exclusively with aqueous acidic solvents. When CF6 is extensively functionalized with aromatic moieties, it no longer effectively separates primary amine racemates. However, it does separate a broad variety of other enantiomers. Furthermore, its preparative separation capabilities appear to be exceptional and this indicates that it is likely that multiple analytes can associate simultaneously with a single chiral selector. While this class of chiral selectors is in its infancy, it is clear that they will be further developed and play an important role in future enantiomeric separations.

## CHAPTER 8

### GENERAL CONCLUSIONS

In the first part (chapters 2-4) of this dissertation, enantiomeric separations of  $\beta$ -lactam compounds and ruthenium(II) polypyridyl complexes have been investigated using two classes of commercial chiral stationary phases. Enantioseparations of 12  $\beta$ -lactams were achieved on nine cyclodextrin-based CSPs. Among them, the dimethylphenyl carbamate-functionalized  $\beta$ -CD stationary phase was the most effective and separated 11 of 12 analytes. The dimethylated- $\beta$ -CD also produced good enantioselectivity and separated 8 analytes out of 12. The reversed phase mode was most effective, and produced the highest resolutions for all of the tested analytes. It was found that more rigid aromatic and tricyclic compounds were more easily separated. The next two chapters in this dissertation focus on separations of enantiomeric ruthenium (II) polypyridyl complexes by using two types of chiral selectors, cyclodextrins and macrocyclic antibiotics. Among five macrocyclic antibiotic columns, the Chirobiotic T2, on which the chiral selector was teicoplanin, was the most effective. With this stationary phase, all test complexes were baseline separated. Also, all tested Ru(II) complexes were eluted with the same retention order, in that the  $\Lambda$ -enantiomer eluted first. The fact that all Ru complexes were eluted in the same order also was observed on the Cyclobond RN (R-naphthylethyl carbamate- $\beta$ -CD) stationary phase, which was the best chiral selector for separating these metal complexes among the nine CD-type stationary phases. Rapid, highly efficient, baseline separations of all the tested Ru complexes were achieved on this column. Furthermore, it was more effective than the T2 column, due to higher selectivity and faster elution.

The second part (chapter 5) of this dissertation focuses on the study of enantioselective host-guest complexation between Ru(II) complexes and cyclodextrins using NMR spectroscopy. NMR technique is one of the most useful techniques to study chiral recognition mechanisms

and it allows one to investigate host-guest complexation at the molecular level. In this study, eight derivatized CDs were investigated as chiral selectors for Ru complexes by  $^1\text{H}$  NMR spectroscopy. The results demonstrate that aromatic and anionic derivatizing groups are beneficial for chiral recognition since sulfobutyl ether- $\beta$ -cyclodextrin sodium salt (SBE- $\beta$ -CD), R-naphthylethyl carbamate  $\beta$ -cyclodextrin (RN- $\beta$ -CD), and S-naphthylethyl carbamate  $\beta$ -cyclodextrin (SN- $\beta$ -CD) show chiral recognition for all five Ru complexes. Thermodynamic studies indicate that a 1:1 host-guest complex stoichiometry for SBE- $\beta$ -CD and  $[\text{Ru}(\text{phen})_3]^{2+}$  and stronger binding for the  $\Lambda$ - $[\text{Ru}(\text{phen})_3]^{2+}$  enantiomer.

The last part (chapter 6-7) focuses on development of new chiral stationary phases. Considerable effort was spent on developing new bonded chiral stationary phases. Enantiomerically pure Ru polypyridyl complexes containing amine groups were attached to the silica support for the first time. Different binding chemistries were investigated and the CSP synthesized by reductive amination of aldehyde-functionalized silica provided the best enantioselectivity. Extensive LC studies indicated that the Ru complex-bonded CSP produced better resolution toward binaphthyl type compounds in the normal phase mode and appeared to be selective for acidic compounds in the polar organic mode. This CSP appeared to be more robust than its coated types. An unusual class of chiral selectors, cyclofructans, is introduced for the first time as bonded chiral stationary phases. While native cyclofructan 6 has limited capabilities as a chiral selector, "lightly" derivatized cyclofructans appear to be exceptional chiral selectors for chiral primary amines. The reason for this can be explained by the effect of the partial derivatization of the cyclofructan hydroxyl groups appears to disrupt internal hydrogen bonding and make the molecular core more accessible. In particular, aliphatic-functionalized CF6 CSPs are most effective for separating primary amines. The isopropyl carbamate-functionalized CSP gave the best performance for separating primary amines among the fourteen derivatized-CF6 CSPs tested. It baseline separated all 11 tested racemic primary amines. It was also found that these CSPs produced better separations for primary amines in

organic solvents. This is completely different from all known chiral crown ether CSPs that are known to work exclusively with aqueous acidic solvents. When CF6 is extensively functionalized with aromatic moieties, its capability for enantioseparating chiral primary amines is lost. Interestingly, it does separate a broad variety of other enantiomers, including secondary and tertiary amines, acids, and alcohols. The best aromatic-derivatized CSPs are R-naphthylethyl, dimethylphenyl, dichlorophenyl, and S- $\alpha$ -methylbenzyl-derivatized ones. The best enantiomeric separations of non-primary amine analytes were obtained using normal phase solvents. This was due to the fact that higher selectivities and efficiencies were obtained in this mode. Furthermore, its preparative separation capabilities appeared to be exceptional.

APPENDIX A  
PUBLICATION INFORMATION OF CHAPTER 2-7

Chapter 2: A manuscript published in *Journal of Liquid Chromatography & Related Technologies*. P. Sun, C. Wang, D.W. Armstrong, 2006, 29, 1847-1860. Copyright ©2006 with permission from Taylor & Francis Group, LLC.

Chapter 3: A manuscript published in *Journal of Molecular Structure*. P. Sun, A. Krishnan, A. Yadav, F.M. MacDonnell, D.W. Armstrong, 2008, 890, 75-80. Copyright ©2008 with permission from Elsevier.

Chapter 4: A manuscript published in *Inorganic Chemistry*. P. Sun, A. Krishnan, A. Yadav, S. Singh, F.M. MacDonnell, D.W. Armstrong, 2007, 46, 10312-10320. Copyright ©2007 with permission from the American Chemical Society.

Chapter 5: A manuscript published in *Inorganica Chimica Acta*. P. Sun, F.M. MacDonnell, D.W. Armstrong, 2009, 362, 3073-3078. Copyright ©2009 with permission from Elsevier.

Chapter 6: A manuscript published in *Journal of Liquid Chromatography & Related Technologies*. P. Sun, S. Perera, F.M. MacDonnell, D.W. Armstrong, 2009, 32, 1979-2000. Copyright ©2009 with permission from Taylor & Francis Group, LLC.

Chapter 7: A manuscript published in *Analytical Chemistry*, 2009. P. Sun, C. Wang, Z.S. Breitbach, Y. Zhang, D.W. Armstrong. Copyright ©2009 with permission from the American Chemical Society.

## REFERENCES

- (1) Anonymous *chirality* **1992**, *5*, 338-341.
- (2) Armstrong, D. W., Chen, S., Chang, C., and Chang, S. *J. Liq. Chromatogr.* **1992**, *15*, 545-556.
- (3) Subramanian, G., Ed.; In *Chiral separation techniques*; WILEY-VCH Verlag GmbH & Co. KGaA: Weinheim, Germany, 2007; , pp 618.
- (4) Okamoto, Y.; Kawashima, M.; Hatada, K. *J. Chromatogr.* **1986**, *363*, 173-186.
- (5) Okamoto, Y.; Nakano, T. *Chem. Rev. (Washington, D. C.)* **1994**, *94*, 349-372.
- (6) Okamoto, Y.; Yashima, E. *Angew. Chem., Int. Ed.* **1998**, *37*, 1021-1043.
- (7) Yashima, E.; Fukaya, H.; Okamoto, Y. *J. Chromatogr., A* **1994**, *677*, 11-19.
- (8) Yashima, E.; Okamoto, Y. *Bull. Chem. Soc. Jpn.* **1995**, *68*, 3289-3307.
- (9) Yashima, E.; Yamada, M.; Kaida, Y.; Okamoto, Y. *J. Chromatogr., A* **1995**, *694*, 347-354.
- (10) Yashima, E.; Sahavattanapong, P.; Okamoto, Y. *Chirality* **1996**, *8*, 446-451.
- (11) Yashima, E.; Okamoto, Y. *Chem. Anal.* **1997**, *142*, 345-376.
- (12) Oguni, K.; Oda, H.; Ichida, A. *J. Chromatogr., A* **1995**, *694*, 91-100.
- (13) Hesse, G.; Hagel, R. *Chromatographia* **1973**, *6*, 277-280.
- (14) Okamoto, Y.; Kawashima, M.; Yamamoto, K.; Hatada, K. *Chem. Lett.* **1984**, 739-742.
- (15) Yashima, E.; Yamamoto, C.; Okamoto, Y. *J. Am. Chem. Soc.* **1996**, *118*, 4036-4048.
- (16) Kubota, T.; Yamamoto, C.; Okamoto, Y. *Chirality* **2003**, *15*, 77-82.
- (17) Armstrong, D. W.; Tang, Y.; Chen, S.; Zhou, Y.; Bagwill, C.; Chen, J. *Anal. Chem.* **1994**, *66*, 1473-1484.
- (18) Ekborg-Ott, K. H.; Kullman, J. P.; Wang, X.; Gahm, K.; He, L.; Armstrong, D. W. *Chirality* **1998**, *10*, 627-660.
- (19) Ekborg-Ott, K.; Liu, Y.; Armstrong, D. W. *Chirality* **1998**, *10*, 434-483.
- (20) Peter, A.; Torok, G.; Armstrong, D. W. *J. Chromatogr., A* **1998**, *793*, 283-296.
- (21) Karlsson, C.; Karlsson, L.; Armstrong, D. W.; Owens, P. K. *Anal. Chem.* **2000**, *72*, 4394-4401.
- (22) Berthod, A.; Valleix, A.; Tizon, V.; Leonce, E.; Caussignac, C.; Armstrong, D. W. *Anal. Chem.* **2001**, *73*, 5499-5508.
- (23) Torok, G.; Peter, A.; Armstrong, D. W.; Tourwe, D.; Toth, G.; Sapi, J. *Chirality* **2001**, *13*, 648-656.
- (24) Liu, Y.; Berthod, A.; Mitchell, C. R.; Xiao, T. L.; Zhang, B.; Armstrong, D. W. *J. Chromatogr. A* **2002**, *978*, 185-204.
- (25) Mitchell, C. R.; Armstrong, D. W.; Berthod, A. *J. Chromatogr. A* **2007**, *1166*, 70-78.
- (26) Berthod, A.; Xiao, T. L.; Liu, Y.; Jenks, W. S.; Armstrong, D. W. *J. Chromatogr. A* **2002**, *955*, 53-69.
- (27) Armstrong, D. W.; Rundlett, K.; Reid, G. L., III *Anal. Chem.* **1994**, *66*, 1690-1695.
- (28) Armstrong, D. W.; DeMond, W. *J. Chromatogr. Sci.* **1984**, *22*, 411-415.
- (29) Armstrong, D. W.; Ward, T. J.; Armstrong, R. D.; Beesley, T. E. *Science* **1986**, *232*, 1132-1135.
- (30) Armstrong, D. W.; Hilton, M.; Coffin, L. *Lc-Gc* **1991**, *9*, 646, 648-52.
- (31) Armstrong, D. W.; Chang, C. D.; Lee, S. H. *J. Chromatogr.* **1991**, *539*, 83-90.
- (32) Stalcup, A. M.; Chang, S. C.; Armstrong, D. W. *J. Chromatogr.* **1991**, *540*, 113-128.
- (33) Armstrong, D. W.; Stalcup, A. M.; Hilton, M. L.; Duncan, J. D.; Faulkner, J. R., Jr.; Chang, S. C. *Anal. Chem.* **1990**, *62*, 1610-1615.

- (34) Chang, S. C.; Reid, G. L. III.; Chen, S.; Chang, C. C.; Armstrong, D. W. *Trends Anal. Chem.* **1993**, *12*, 144-153.
- (35) Mikes, F.; Boshart, G. *J. Chromogr.* 1978, *149*, 455-464.
- (36) Pirkle, W. H.; Pochapsky, T. C. *J. Am. Chem. Soc.* **1986**, *108*, 352-354.
- (37) Pirkle, W. H.; Pochapsky, T. C. *Adv. Chromatogr.* **1987**, *27*, 73-127. (38) Pirkle, W. H.; Tsipouras, A.; Hyun, M. H.; Hart, D. J.; Lee, C. S. *J. Chromatogr.* **1986**, *358*, 377-384.
- (39) Pirkle, W. H.; Welch, C. J. *Tetrahedron: Asymmetry* **1994**, *5*, 777-780.
- (40) Maier, N. M.; Franco, P.; Lindner, W. *J. Chromatogr. A* **2001**, *906*, 3-33.
- (41) Laemmerhofer, M.; Lindner, W. *J. Chromatogr. A* **1996**, *741*, 33-48.
- (42) Gubitz, G.; Schmid, M. G., Eds.; In *Chiral separations: Methods and Protocols; Methods in Molecular Biology*; Humana Press: Totowa, NJ, 2004; Vol. 243, pp 432.
- (43) Matagne, A.; Lamotte-Brasseur, J.; Frere, J. *Biochem. J.* **1998**, *330*, 581-598.
- (44) Matagne, A.; Dubus, A.; Galleni, M.; Frere, J. *Nat. Prod. Rep.* **1999**, *16*, 1-19.
- (45) Lamotte, J.; Dive, G.; Ghuysen, J. M. *Eur. J. Med. Chem.* **1991**, *26*, 43-50.
- (46) Frere, J. *Mol. Microbiol.* **1995**, *16*, 385-395.
- (47) Yang, Y.; Wang, F.; Rochon, F. D.; Kayser, M. M. *Can. J. Chem.* **2005**, *83*, 28-36.
- (48) Ojima, I.; Lin, S. *J. Org. Chem.* **1998**, *63*, 224-225.
- (49) Ojima, I. *Acc. Chem. Res.* **1995**, *28*, 383-389.
- (50) Madan, S.; Milano, P.; Eddings, D. B.; Gawley, R. E. *J. Org. Chem.* **2005**, *70*, 3066-3071.
- (51) Agami, C.; Dechoux, L.; Hebbe, S.; Menard, C. *Tetrahedron* **2004**, *60*, 5433-5438.
- (52) Pirkle, W. H.; Spence, P. L. *Chirality* **1998**, *10*, 430-433.
- (53) Ficarra, R.; Calabro, M. L.; Tommasini, S.; Costantino, D.; Carulli, M.; Melardi, S.; Di Bella, M. R.; Casuscelli, F.; Romeo, R.; Ficarra, P. *Chromatographia* **1996**, *43*, 365-368.
- (54) Cirilli, R.; Del Giudice, M. R.; Ferretti, R.; La Torre, F. *J. Chromatogr.* , **2001**, *923*, 27-36.
- (55) Peter, A.; Arki, A.; Forro, E.; Fueloep, F.; Armstrong, D. W. *Chirality* **2005**, *17*, 193-200.
- (56) Armstrong, D. W.; DeMond, W.; Czech, B. P. *Anal. Chem.* **1985**, *57*, 481-484.
- (57) Armstrong, D. W.; Tang, Y.; Chen, S.; Zhou, Y.; Bagwill, C.; Chen, J. *Anal. Chem.* **1994**, *66*, 1473-1484.
- (58) Mitchell, C.; Desai, M.; McCulla, R.; Jenks, W.; Armstrong, D. *Chromatographia* **2002**, *56*, 127-135.
- (59) Soukup, R. J.; Rozhkov, R. V.; Larock, R. C.; Armstrong, D. W. *Chromatographia* **2005**, *61*, 219-224.
- (60) Juris, A.; Balzani, V.; Barigelletti, F.; Campagna, S.; Belser, P.; Von Zelewsky, A. *Coord. Chem. Rev.* **1988**, *84*, 85-277.
- (61) Hamelin, O.; Rimboud, M.; Pecaut, J.; Fontecave, M. *Inorg. Chem.* **2007**, *46*, 5354-5360.
- (62) Chavarot, M.; Menage, S.; Hamelin, O.; Charnay, F.; Pecaut, J.; Fontecave, M. *Inorg. Chem.* **2003**, *42*, 4810-4816.
- (63) Bodige, S.; Torres, A. S.; Maloney, D. J.; Tate, D.; Kinsel, G.; Walker, A.; MacDonnell, F. M. *J. Am. Chem. Soc.* **1997**, *119*, 10364-10369.
- (64) MacDonnell, F. M.; Kim, M.; Bodige, S. *Coord. Chem. Rev.* **1999**, *185-186*, 535-549.
- (65) Hiort, C.; Lincoln, P.; Norden, B. *J. Am. Chem. Soc.* **1993**, *115*, 3448-3454.
- (66) Pierard, F.; Kirsch-De Mesmaeker, A. *Inorg. Chem. Commun.* **2006**, *9*, 111-126.
- (67) Morgan, J. L.; Buck, D. P.; Turley, A. G.; Collins, J. G.; Keene, F. R. *JBIC, J. Biol. Inorg. Chem.* **2006**, *11*, 824-834.
- (68) Harris, J. E.; Desai, N.; Seaver, K. E.; Watson, R. T.; Kane-Maguire, N. A. P.; Wheeler, J. F. *J. Chromatogr. A* **2001**, *919*, 427-436.
- (69) Kane-Maguire, N. A. P.; Wheeler, J. F. *Coord. Chem. Rev.* **2001**, *211*, 145-162.
- (70) Schaeper, J. P.; Nelsen, L. A.; Shupe, M. A.; Herbert, B. J.; Kane-Maguire, N. A. P.; Wheeler, J. F. *Electrophoresis* **2003**, *24*, 2704-2710.
- (71) Lacour, J.; Torche-Haldimann, S.; Jodry, J. J. *Chem. Commun. (Cambridge)* **1998**, 1733-1734.
- (72) Ramsden, J. A.; Garner, C. M.; Gladysz, J. A. *Organometallics* **1991**, *10*, 1631-1633.

- (73) Wang, X.; Li, W.; Zhao, Q.; Li, Y.; Chen, L. *Anal. Sci.* **2005**, *21*, 125-128.
- (74) Sun, P.; Krishnan, A.; Yadav, A.; Singh, S.; MacDonnell, F. M.; Armstrong, D. W. *Inorg. Chem.* **2007**, *46*, 10312-10320.
- (75) Warnke, M. M.; Cotton, F. A.; Armstrong, D. W. *Chirality* **2007**, *19*, 179-183.
- (76) Gasparrini, F.; D'Acquarica, I.; Vos, J. G.; O'Connor, C. M.; Villani, C. *Tetrahedron: Asymmetry* **2000**, *11*, 3535-3541.
- (77) Armstrong, D. W.; Liu, Y.; Ekborgott, K. H. *Chirality* **1995**, *7*, 474-497.
- (78) Ward, T. J.; Farris, A. B., III *J. Chromatogr. A* **2001**, *906*, 73-89.
- (79) Ekborg-Ott, K. H.; Kullman, J. P.; Wang, X.; Gahm, K.; He, L.; Armstrong, D. W. *Chirality* **1998**, *10*, 627-660.
- (80) Peter, A.; Torok, G.; Armstrong, D. W.; Toth, G.; Tourwe, D. *J. Chromatogr. A* **2000**, *904*, 1-15.
- (81) Sztojkov-Ivanov, A.; Lazar, L.; Fulop, F.; Armstrong, D. W.; Peter, A. *Chromatographia* **2006**, *64*, 89-94.
- (82) Wang, A. X.; Lee, J. T.; Beesley, T. E. *Lc-Gc* **2000**, *18*, 626-628, 630, 632, 634, 636, 638-639.
- (83) Svensson, L. A.; Karlsson, K.; Karlsson, A.; Vessman, J. *Chirality* **1998**, *10*, 273-280.
- (84) Brandt, W. W.; Dwyer, F. P.; Gyarfas, E. C. *Chem. Rev.* **1954**, *54*, 959-1017.
- (85) Hoffman, M. Z.; Bolletta, F.; Moggi, L.; Hug, G. L. *J. Phys. Chem. Ref. Data* **1989**, *18*, 219-543.
- (86) Hamelin, O.; Pecaut, J.; Fontecave, M. *Chem. --Eur. J.* **2004**, *10*, 2548-2554.
- (87) Metcalfe, C.; Thomas, J. A. *Chem. Soc. Rev.* **2003**, *32*, 215-224.
- (88) Barton, J. K.; Basile, L. A.; Danishefsky, A.; Alexandrescu, A. *Proc. Natl. Acad. Sci. U. S. A.* **1984**, *81*, 1961-1965.
- (89) Satyanarayana, S.; Dabrowiak, J. C.; Chaires, J. B. *Biochemistry* **1993**, *32*, 2573-2584.
- (90) Caspar, R.; Musatkina, L.; Tatosyan, A.; Amouri, H.; Gruselle, M.; Guyard-Duhayon, C.; Duval, R.; Cordier, C. *Inorg. Chem.* **2004**, *43*, 7986-7993.
- (91) Janaratne, T. K.; Yadav, A.; Onger, F.; MacDonnell, F. M. *Inorg. Chem.* **2007**, *46*, 3420-3422.
- (92) MacDonnell, F. M.; Ali, M. D. M.; Kim, M. *Comments Inorg. Chem.* **2000**, *22*, 203-225.
- (93) MacDonnell, F. M.; Bodige, S. *Inorg. Chem.* **1996**, *35*, 5758-5759.
- (94) Hua, X.; von Zelewsky, A. *Inorg. Chem.* **1995**, *34*, 5791-5797.
- (95) Hua, X.; Von Zelewsky, A. *Inorg. Chem.* **1991**, *30*, 3796-3798.
- (96) Tzalis, D.; Tor, Y. *Chem. Commun. (Cambridge)* **1996**, 1043-1044.
- (97) Tzalis, D.; Tor, Y. *J. Am. Chem. Soc.* **1997**, *119*, 852-853.
- (98) Warnmark, K.; Baxter, P. N. W.; Lehn, J. *Chem. Commun. (Cambridge)* **1998**, 993-994.
- (99) Warnmark, K.; Heyke, O.; Thomas, J. A.; Lehn, J. *Chem. Commun. (Cambridge)* **1996**, 2603-2604.
- (100) Rutherford, T. J.; Keene, F. R. *J. Chem. Soc. Dalton Trans.* **1998**, 1155-1162.
- (101) Rutherford, T. J.; Quagliotto, M. G.; Keene, F. R. *Inorg. Chem.* **1995**, *34*, 3857-3858.
- (102) Patterson, B. T.; Keene, F. R. *Inorg. Chem.* **1998**, *37*, 645-650.
- (103) Rutherford, T. J.; Keene, F. R. *Inorg. Chem.* **1997**, *36*, 3580-3581.
- (104) Keene, F. R. *Chem. Soc. Rev.* **1998**, *27*, 185-194.
- (105) Smith, J. A.; Keene, F. R. *Chem. Commun. (Cambridge, U. K.)* **2006**, 2583-2585.
- (106) Monchaud, D.; Lacour, J.; Coudret, C.; Frayssé, S. *J. Organomet. Chem.* **2001**, *624*, 388-391.
- (107) Gruselle, M.; Thouvenot, R.; Caspar, R.; Boubekour, K.; Amouri, H.; Ivanov, M.; Tonsuaadu, K. *Mendeleev Commun.* **2004**, 282-283.
- (108) Herbert, B. J.; Carpenter, H. E.; Kane-Maguire, N. A. P.; Wheeler, J. F. *Anal. Chim. Acta* **2004**, *514*, 27-35.
- (109) Martin, S. E.; Maggie Connatser, R.; Kane-Maguire, N. A. P.; Wheeler, J. F. *Anal. Chim. Acta* **2001**, *445*, 21-27.

- (110) Shelton, C. M.; Seaver, K. E.; Wheeler, J. F.; Kane-Maguire, N. A. P. *Inorg. Chem.* **1997**, *36*, 1532-1533.
- (111) MacDonnell, F. M.; Kim, M.; Wouters, K. L.; Konduri, R. *Coord. Chem. Rev.* **2003**, *242*, 47-58.
- (112) Browne, W. R.; O'Connor, C. M.; Villani, C.; Vos, J. G. *Inorg. Chem.* **2001**, *40*, 5461-5464.
- (113) Armstrong, D. W.; Li, W.; Chang, C. D.; Pitha, J. *Anal. Chem.* **1990**, *62*, 914-923.
- (114) Armstrong, D. W.; Zukowski, J. *J. Chromatogr. A* **1994**, *666*, 445-448.
- (115) Kano, K.; Hasegawa, H. *J. Am. Chem. Soc.* **2001**, *123*, 10616-10627.
- (116) Kano, K.; Hasegawa, H. *Chem. Lett.* **2000**, 698-699.
- (117) Torres, A. S.; Maloney, D. J.; Tate, D.; Saad, Y.; MacDonnell, F. M. *Inorg. Chim. Acta* **1999**, *293*, 37-43.
- (118) Smith, G. F.; Cagle, F. W., Jr. *J. Org. Chem.* **1947**, *12*, 781-784.
- (119) Sullivan, B. P.; Salmon, D. J.; Meyer, T. J. *Inorg. Chem.* **1978**, *17*, 3334-3341.
- (120) Lay, P. A.; Sargeson, A. M.; Taube, H. *Inorg. Synth.* **1986**, *24*, 291-299.
- (121) Burstall, F. H. *J. Chem. Soc.* **1936**, 173-175.
- (122) Goss, C. A.; Abruna, H. D. *Inorg. Chem.* **1985**, *24*, 4263-4267.
- (123) Bosnich, B.; Dwyer, F. P. *Aust. J. Chem.* **1966**, *19*, 2229-2233.
- (124) Broomhead, J. A.; Young, C. G. *Inorg. Synth.* **1982**, *21*, 127-128.
- (125) Kim, M.; Konduri, R.; Ye, H.; MacDonnell, F. M.; Puntoriero, F.; Serroni, S.; Campagna, S.; Holder, T.; Kinsel, G.; Rajeshwar, K. *Inorg. Chem.* **2002**, *41*, 2471-2476.
- (126) Marcovich, D.; Tapscott, R. E. *J. Am. Chem. Soc.* **1980**, *102*, 5712-5717.
- (127) Henderson, G. G.; Ewing, A. R. *J. Chem. Soc., Trans.* **1895**, *67*, 102-108.
- (128) Stalcup, A. M.; Chang, S. C.; Armstrong, D. W. *J. Chromatogr.* **1991**, *540*, 113-128.
- (129) Berthod, A.; Chang, S. C.; Armstrong, D. W. *Anal. Chem.* **1992**, *64*, 395-404.
- (130) Morgan, O.; Wang, S.; Bae, S.; Morgan, R. J.; Baker, A. D.; Streckas, T. C.; Engel, R. J. *Chem. Soc., Dalton Trans.* **1997**, 3773-3776.
- (131) Dwyer, F. P.; Gyarfas, E. C. *J. Proc. R. Soc. N. S. W.* **1950**, *83*, 232-234.
- (132) Dwyer, F. P.; Gyarfas, E. C. *J. Proc. R. Soc. N. S. W.* **1950**, *83*, 263-265.
- (133) Dwyer, F. P.; Gyarfas, E. C. *Nature (London, U. K.)* **1949**, *163*, 918.
- (134) Watson, R. T.; Jackson, Joseph L. Jr.; Harper, J. D.; Kane-Maguire, K. A.; Kane-Maguire, L. A. P.; Kane-Maguire, N. A. P. *Inorg. Chim. Acta* **1996**, *249*, 5-7.
- (135) Tapscott, R. E.; Belford, R. L.; Paul, I. C. *Coord. Chem. Rev.* **1969**, *4*, 323-359.
- (136) Zalkin, A.; Templeton, D. H.; Ueki, T. *Inorg. Chem.* **1973**, *12*, 1641-1646.
- (137) Maloney, D. J.; MacDonnell, F. M. *Acta Crystallogr., Sect. C: Cryst. Struct. Commun.* **1997**, *C53*, 705-707.
- (138) Kim, M.; MacDonnell, F. M.; Gimon-Kinsel, M. E.; Du Bois, T.; Asgharian, N.; Griener, J. C. *Angew. Chem., Int. Ed.* **2000**, *39*, 615-619.
- (139) Gillard, R. D.; Hill, R. E. E. *J. Chem. Soc., Dalton Trans.* **1974**, 1217-1236.
- (140) Porter, G. B.; Sparks, R. H. *J. Photochem.* **1980**, *13*, 123-131.
- (141) Caspar, J. V.; Kober, E. M.; Sullivan, B. P.; Meyer, T. J. *J. Am. Chem. Soc.* **1982**, *104*, 630-632.
- (142) Caspar, J. V.; Meyer, T. J. *J. Am. Chem. Soc.* **1983**, *105*, 5583-5590.
- (143) Erkkila, K. E.; Odom, D. T.; Barton, J. K. *Chem. Rev.* **1999**, *99*, 2777-2795.
- (144) Corradini, R.; Sforza, S.; Tedeschi, T.; Marchelli, R. *Chirality* **2007**, *19*, 269-294.
- (145) Durham, B.; Caspar, J. V.; Nagle, J. K.; Meyer, T. J. *J. Am. Chem. Soc.* **1982**, *104*, 4803-4810.
- (146) Van Houten, J.; Watts, R. J. *Inorg. Chem.* **1978**, *17*, 3381-3385.
- (147) Anderson, P. A.; Deacon, G. B.; Haarmann, K. H.; Keene, F. R.; Meyer, T. J.; Reitsma, D. A.; Skelton, B. W.; Strouse, G. F.; Thomas, N. C.; et al. *Inorg. Chem.* **1995**, *34*, 6145-6157.
- (148) Mimassi, L.; Guyard-Duhayon, C.; Rager, M. N.; Amouri, H. *Inorg. Chem.* **2004**, *43*, 6644-6649.
- (149) Berthod, A.; Li, W.; Armstrong, D. W. *Anal. Chem.* **1992**, *64*, 873-879.

- (150) Jiang, C.; Tong, M.; Armstrong, D. W.; Perera, S.; Bao, Y.; Macdonnell, F. M. *Chirality* **2009**, *21*, 208-217.
- (151) Lin, X.; Zhu, C.; Hao, A. *Anal. Chim. Acta* **2004**, *517*, 95-101.
- (152) Garcia-Ruiz, C.; Crego, A. L.; Marina, M. L. *Electrophoresis* **2003**, *24*, 2657-2664.
- (153) Cucinotta, V.; Giuffrida, A.; Grasso, G.; Maccarrone, G.; Messina, M.; Vecchio, G. *J. Chromatogr. A* **2007**, *1155*, 172-179.
- (154) Zhong, Q.; He, L.; Beesley, T. E.; Trahanovsky, W. S.; Sun, P.; Wang, C.; Armstrong, D. W. *J. Chromatogr. A* **2006**, *1115*, 19-45.
- (155) Armstrong, D. W.; Stalcup, A. M.; Hilton, M. L.; Duncan, J. D.; Faulkner, J. R., Jr.; Chang, S. C. *Anal. Chem.* **1990**, *62*, 1610-1615.
- (156) Owens, P. K.; Fell, A. F.; Coleman, M. W.; Berridge, J. C. *J. Chromatogr. A* **1998**, *797*, 149-164.
- (157) Endresz, G.; Chankvetadze, B.; Bergenthal, D.; Blaschke, G. *J. Chromatogr. A* **1996**, *732*, 133-142.
- (158) Wenzel, T. J.; Amonoo, E. P.; Shariff, S. S.; Aniagyei, S. E. *Tetrahedron: Asymmetry* **2003**, *14*, 3099-3104.
- (159) Kano, K.; Hasegawa, H.; Miyamura, M. *Chirality* **2001**, *13*, 474-482.
- (160) Chankvetadze, B.; Schulte, G.; Bergenthal, D.; Blaschke, G. *J. Chromatogr. A* **1998**, *798*, 315-323.
- (161) Chankvetadze, B.; Endresz, G.; Schulte, G.; Bergenthal, D.; Blaschke, G. *J. Chromatogr. A* **1996**, *732*, 143-150.
- (162) Chankvetadze, B.; Endresz, G.; Bergenthal, D.; Blaschke, G. *J. Chromatogr. A* **1995**, *717*, 245-253.
- (163) Holzgrabe, U.; Mallwitz, H.; Branch, S. K.; Jefferies, T. M.; Wiese, M. *Chirality* **1997**, *9*, 211-219.
- (164) Dodziuk, H.; Kozminski, W.; Ejchart, A. *Chirality* **2004**, *16*, 90-105.
- (165) Uccello-Barretta, G.; Chiavacci, C.; Bertucci, C.; Salvadori, P. *Carbohydr. Res.* **1993**, *243*, 1-10.
- (166) Hinze, W. L.; Riehl, T. E.; Armstrong, D. W.; DeMond, W.; Alak, A.; Ward, T. *Anal. Chem.* **1985**, *57*, 237-242.
- (167) Okamoto, Y.; Aburatani, R.; Hatano, K.; Hatada, K. *J. Liq. Chromatogr.* **1988**, *11*, 2147-2163.
- (168) Okamoto, Y.; Kawashima, M.; Hatada, K. *J. Am. Chem. Soc.* **1984**, *106*, 5357-5359.
- (169) Yamagishi, A. *J. Chromatogr.* **1985**, *319*, 299-310.
- (170) Yamagishi, A. *J. Am. Chem. Soc.* **1985**, *107*, 732-734.
- (171) Yamagishi, A. *J. Chromatogr.* **1983**, *262*, 41-60.
- (172) Yamagishi, A.; Soma, M. *J. Am. Chem. Soc.* **1981**, *103*, 4640-4642.
- (173) Nakamura, Y.; Yamagishi, A.; Matumoto, S.; Tohkubo, K.; Ohtu, Y.; Yamaguchi, M. *J. Chromatogr.* **1989**, *482*, 165-173.
- (174) Bodige, S.; MacDonnell, F. M. *Tetrahedron Lett.* **1997**, *38*, 8159-8160.
- (175) Nilsson, K.; Larsson, P. O. *Anal. Biochem.* **1983**, *134*, 60-72.
- (176) Svensson, L. A.; Karlsson, K. *J. Microcolumn Sep.* **1995**, *7*, 231-237.
- (177) Ming, Y.; Zhao, L.; Zhang, H.; Shi, Y.; Li, Y. *Chromatographia* **2006**, *64*, 273-280.
- (178) Wang, C.; Armstrong, D. W.; Risley, D. S. *Anal. Chem.* **2007**, *79*, 8125-8135.
- (179) Kawamura, M.; Uchiyama, T.; Kuramoto, T.; Tamura, Y.; Mizutani, K. *Carbohydr. Res.* **1989**, *192*, 83-90.
- (180) Kawamura, M.; Uchiyama, T. *Carbohydr. Res.* **1994**, *260*, 297-304.
- (181) Mori, H.; Nishioka, M.; Nanjo, F. Patent Application Country: Application: JP; Patent Country: JP Patent 2006067895, 2006.
- (182) Mori, H.; Nishioka, M.; Nanjo, F. Patent Application Country: Application: JP; Patent Country: JP Patent 2006067895, 2006.

- (183) Nishioka, M.; Mori, H.; Nanjo, F. Patent Application Country: Application: JP; Patent Country: JP Patent 2004337132, 2004.
- (184) Mori, H.; Nishioka, M.; Nanjo, F. Patent Application Country: Application: JP; Patent Country: JP Patent 2006067894, 2006.
- (185) Fang, Y.; Ferrie, A. M. US Patent 2005048684, 2005.
- (186) Yokoyama, H.; Ikeuchi, H.; Teranishi, Y.; Murayama, H.; Sano, K.; Sawada, K. Patent Application Country: Application: GB; Patent Country: GB; Priority Application Country: JP Patent 2282147, 1995.
- (187) Ozaki, K.; Hayashi, M. *Int. J. Pharmacuetics* **1998**, *160*, 219-227.
- (188) Reijenga, J. C.; Verheggen, T. P. E. M.; Chiari, M. *J. Chromatogr. A* **1999**, *838*, 111-119.
- (189) Kida, T.; Inoue, Y.; Zhang, W.; Nakatsuji, Y.; Ikeda, I. *Bull. Chem. Soc. Jpn.* **1998**, *71*, 1201-1205.
- (190) Kushibe, S.; Sashida, R.; Morimoto, Y. *Biosci. , Biotechnol. , Biochem.* **1994**, *58*, 1136-1138.
- (191) Kushibe, S.; Mitsui, K.; Yamagishi, M.; Yamada, K.; Morimoto, Y. *Biosci Biotechnol Biochem* **1995**, *59*, 31-34.
- (192) Kanai, T.; Ueki, N.; Kawaguchi, T.; Teranishi, Y.; Atomi, H.; Tomorbaatar, C.; Ueda, M.; Tanaka, A. *Appl. Environ. Microbiol.* **1997**, *63*, 4956-4960.
- (193) Sawada, M.; Tanaka, T.; Takai, Y. *Chem. Lett.* **1990**, 2011-2014.
- (194) Sawada, M.; Tanaka, T.; Takai, Y.; Hanafusa, T.; Taniguchi, T.; Kawamura, M.; Uchiyama, T. *Carbohydr. Res.* **1991**, *217*, 7-17.
- (195) Immel, S.; Schmitt, G. E.; Lichtenthaler, F. W. *Carbohydr. Res.* **1998**, *313*, 91-105.
- (196) Tamura, K.; Mizutani, K.; Kuramoto, T.; Uchiyama, T.; Kawamura, M. Patent Application Country: Application: JP; Patent Country: JP Patent 02252701, 1990.
- (197) Walbroehl, Y.; Wagner, J. *J. Chromatogr. A* **1994**, *680*, 253-261.
- (198) Nishi, H.; Nakamura, K.; Nakai, H.; Sato, T. *J. Chromatogr. A* **1997**, *757*, 225-235.
- (199) Kuhn, R. *Electrophoresis* **1999**, *20*, 2605-2613.
- (200) Lakatos, S.; Fetter, J.; Bertha, F.; Huszthy, P.; Toth, T.; Farkas, V.; Orosz, G.; Hollosi, M. *Tetrahedron* **2007**, *64*, 1012-1022.
- (201) Hilton, M.; Armstrong, D. W. *J. Liq. Chromatogr.* **1991**, *14*, 9-28.
- (202) Pirkle, W. H.; Pochapsky, T. C. *Chem. Rev.* **1989**, *89*, 347-362.
- (203) Zhang, T.; Schaeffer, M.; Franco, P. *J. Chromatogr. A* **2005**, *1083*, 96-101.
- (204) Miller, L.; Orihuela, C.; Fronek, R.; Murphy, J. *J. Chromatogr. A* **1999**, *865*, 211-226.

## BIOGRAPHICAL INFORMATION

Ping Sun obtained her Bachelor of Science from Fudan University in 2001. She then went to Tsinghua University and earned her Master of Science in 2004 working on applications of HPLC-ESI-MS. Then she joined Dr. Daniel W. Armstrong's group and received her Doctor of Philosophy from the University of Texas at Arlington in December 2009. Her research focused on development of new chiral selectors for liquid chromatography.